LIBRARY & INFORMATICS
NIST(CSIR) TRIVANDRUM
G1595

# STUDIES ON CLAY (KAOLINITE) POLYMER COMPOSITES

THESIS
SUBMITTED TO
THE UNIVERSITY OF KERALA
IN PARTIAL FULFILMENT
OF THE REQUIREMENTS
FOR THE DEGREE OF
DOCTOR OF PHILOSOPHY IN PHYSICS

BY
B. JALAJAKUMARI M. Sc.

REGIONAL RESEARCH LABORATORY (CSIR)
TRIVANDRUM-695 019
INDIA

JULY 1989

# STUDIES ON CLAY (KAOLINITE) POLYMER COMPOSITES

THESIS
SUBMITTED TO
THE UNIVERSITY OF KERALA
IN PARTIAL FULFILMENT
OF THE REQUIREMENTS
FOR THE DEGREE OF
DOCTOR OF PHILOSOPHY IN PHYSICS

BY
B. JALAJAKUMARI M. Sc.

REGIONAL RESEARCH LABORATORY (CSIR)
TRIVANDRUM-695 019
INDIA

JULY 1989

LIBRARY
Received on 27.07.95
Accession no G1/1595
Call no 666.32:678:620.16x:043
REGIONAL RESEARCH LABORATORY
TRIVANDRUM

(R)

M9

CR

549.623.9
620.16x; 666.32:678
618:666.32

G/1595
27.7.95

# C E R T I F I C A T E

This is to certify that the thesis entitled "STUDIES ON CLAY (KAOLINITE) POLYMER COMPOSITES" is an authentic record of the research work carried out by Miss B. Jalajakumari, M.Sc., under our supervision in partial fulfilment of the requirement for the Degree of Doctor of Philosophy of the University of Kerala and further that no part thereof has been presented before for any other degree.

(Dr. K.G. Satyanarayana)
Head, Materials Division
Regional Research Laboratory (CSIR)
Trivandrum 695 019

(Dr. K.G.K. Warrier)
Scientist
Regional Research Laboratory (CSIR)
Trivandrum 695 019

## ACKNOWLEDGEMENTS

It is with great pleasure I express my deep sense of gratitude and respect to Dr. K.G. Satyanarayana, Head, Materials Division, and Dr. K.G.K. Warrier, Scientist, Regional Research Laboratory, Trivandrum, for their valuable guidance, constant encouragement and continual support given to me throughout the course of this work. I am indebted to Dr. K.G.K. Warrier for his keen interest in this work. His amiable nature will always be a pleasant memory in my life.

I thank Dr. A.D. Damodaran, Director, R.R.L., Trivandrum, for his constant encouragement and for extending all the facilities to carry out my work. Also, thanks are due to Dr. A.G. Mathew, former Acting Director for his interest and encouragement during the initial stages of my doctoral work.

I gratefully acknowledge Prof. S. Bhattacherjee, Department of Physics, I.I.T., Kharagpur, for the whole-hearted discussions and for constructive suggestions after personally going through my work.

I am thankful to Dr. K.J.D. Mackenzie and Dr. R.H. Meinhold, DSIR, New Zealand for the NMR spectra, and Prof. M.R. Krishnadev, University of Laval, Canada, for SEM studies of the clay samples.

I thank Prof. K.V. Rao, Head, Department of Physics, I.I.T., Kharagpur, for extending the facility for dielectric measurements and Prof. G. Arul Das, Department of Physics, University of Kerala, for the Raman Spectra.

My thanks are due to Mr. P.V. Ravindran and Mr. K. Sreekumar, V.S.S.C., Trivandrum, Dr. Binodkumar, I.I.T., Kharagpur, Dr. P.S. Mukherjee, Mr. P. Guruswamy, Mr. K. Sukumaran, Mr. K.K. Ravikumar, Mr. S.G.K. Pillai, Mr. K. Athinarayanaswamy and Mr. Peter Koshy, R.R.L., Trivandrum for their help in different instrumental facilities.

I thank Dr. C. Pavithran, Scientist, R.R.L., Trivandrum for the useful discussions.

My heart-felt thanks go to Mr. H.K. Varma for his affectionate friendship and help during thesis preparation. The help of Mr. K.P. Kumar is duly acknowledged.

I take this opportunity to thank my colleagues of Ceramics and Glass Division of R.R.L., Trivandrum, Dr. (Mrs.) M. Lalithambika, Scientist-in-Charge of the Division, Messers K.R. Prasad, V. Sreekantan, P. Perumal, P. Krishna Pillai and P. Mukundan for providing a congenial atmosphere and the memories of which I shall cherish for ever.

Thanks are also due to Messers A.V. Philip, P. Vijayakumar, R. Babu and G. Sudhakaran for their help in the thesis preparation.

I acknowledge the Council of Scientific and Industrial Research, New Delhi, for the financial support during the course of this work.

I thank numerous friends and well wishers all of whom cannot be named here.

B. JALAJAKUMARI

## SUMMARY

Kaolinite, one of the most abundant material with good thermal stability, high surface area and fine particle size has been one of the most common fillers in polymer composites. Because of the hydrophilic nature of the surface of kaolinites, it becomes extremely difficult to disperse kaolinite in polymers, making it necessary to modify their surfaces by suitable methods. In this investigation detailed studies have been made to modify the surface of kaolinite by a thermal decomposition - hydration - redecomposition technique which results in product of increased surface area characterized by microporosity. The details of the investigation are presented below.

Chapter I gives an introduction to composites with particular reference to clay-polymer composites. The attempts made so far on the surface modification of clays for improving the compatibility factors between kaolinite and polymer matrices have been discussed with a view to improve the mechanical and electrical properties of such composites.

Chapter II deals with the techniques of characterization of kaolinite and also details on dehydroxylation of kaolinite. Further, mention has been made on the information gap in dehydroxylation of kaolinite.

Chapter III describes the surface modification of the kaolinite by a thermal decomposition-hydration redecomposition treatment. The surface modified kaolinite was characterized by Raman and solid state NMR techniques for understanding the extent of dehydroxylation in heat treated clays. Dielectric measurements on the heat treated (surface

modified) kaolinites show them to be more insulating than the pure kaolinite.

Chapter IV describes the effect of addition of the treated kaolinite in polymer matrices such as polyethylene, polyester and polyvinyl chloride so as to form polymer matrix composites. The microstructural features and mechanical and electrical properties of the composites prepared using treated and untreated kaolinite are discussed.

Chapter V presents a general discussion with a comparison of the properties of the three composites.

Chapter VI provides the effect of the treated kaolinite on the high temperature behaviour in ceramic composites.

Chapter VII gives the conclusions and suggestions for further work.

The work described in this thesis has partly been published/ is under publication, as indicated below:

1. Surface modification of kaolinite by controlled thermal treatment, J. Mat. Sci. Lett., 5 (1986) 865-868.

2. Suitability of kaolinite clay prepared by controlled heat treatment for use in particulate composites, Trans. Ind. Ceram. Soc., (1986) 45 (5) Sept.-Oct. 123-125.

3. Formation characteristics and microstructure of mullite from surface modified kaolinite, Proceedings of the National Seminar on Refractory Industry in India held at Trivandrum, 1987, p.53.

4. Mechanical and electrical properties of surface modified kaolinite-polyester particulate composites, J. Reinforced Plastics and Composites, 7 (5) 1988, 402-412.

5. Thermal dehydroxylation in surface modified kaolinite, J. Mat. Sci. (in press).

6. Preparation and properties of kaolinite polyethylene composites, Trans. Ind. Ceram. Soc. 48(1) Jan.-Feb. 1989, 5-10.

7. Raman spectra and electrical properties of surface modified kaolinite (communicated to Clay Minerals).

## LIST OF FIGURES


I.1 Classification of composites

I.2 Model for filled polymers

I.3 Theoretical curves for the elongation to break for the case of perfect adhesion and no adhesion between the filler and polymer phases

I.4 Theoretical curves for the tensile strength of filled polymers

II.1 Structure of unmodified kaolinite (WC)

II.2 Thermogravimetric analysis (TGA) of WC

II.3 Differential thermal analysis (DTA) of WC

II.4 Particle size distribution of WC

II.5 Scanning electron micrograph (SEM) of WC

II.6 Transmission electron micrograph (TEM) of WC

II.7 X-ray diffraction (XRD) pattern of WC

II.8 Infrared (IR) spectra of WC

II.9 Dielectric constant and dielectric loss of WC with frequency

II.10 DTA of metakaolinite (MK)

II.11 SEM of MK

II.12 TEM of MK

II.13 XRD of MK

II.14 IR spectra of MK

II.15 Dielectric constant and dielectric loss of MK with frequency

III.1 DTA of vacuum treated (surface modified) kaolinite (VT)

III.2 SEM of VT

III.3 TEM of VT

III.4 XRD of VT

III.5 IR spectra of VT

III.6 Raman spectra of WC, MK and VT

III.7 Solid state NMR spectra of WC, MK and VT

III.8 Dielectric constant and dielectric loss of VT with frequency

IV.1 SEM of polyethylene filled with WC and VT

IV.2 Tensile modulus of WC and VT filled polyethylene composites with filler content

IV.3 Tensile strength of WC and VT filled polyethylene composites with filler content

IV.4 Weight loss of WC and VT filled polyethylene composites with filler content during wear test

IV.5 SEM of the worn surface of WC and VT filled polyethylene composites

IV.6 Polyester resin filled with WC and VT

IV.7 Optical micrographs of polyester resin filled with WC and VT

IV.8 Load deformation curve of polyester composite

IV.9 Compressive strength of WC and VT filled polyester composites with filler content

IV.10 Weight loss of WC and VT filled polyester composites with filler content during wear test

VI.1 XRD of WC and VT heated at 1050$^{o}$C

VI.2 XRD of WC and VT heated at 1150$^{o}$C

VI.3 XRD of WC heated at 1350$^{o}$C and VT heated at 1250$^{o}$C

VI.4 Variation of dielectric constant with frequency of WC and VT heated at different temperatures

VI.5 Variation of dielectric loss of WC and VT heated at different temperatures

VI.6 SEM of WC and VT heated at different temperatures

## LIST OF TABLES


I.1 The effect of addition of an organo-titanium kaolinite filler in polymers and plastics

I.2 Properties of high and low density polyethylene filled with 20% of different fillers

I.3 Summary of informations on the surface modification of particulates in polymer based composites

II.1 Chemical analysis of the kaolinite (WC)

II.2 Particle size distribution of WC

II.3 X-ray powder data for WC

III.1 Band positions in the Raman spectra of WC, MK and VT

IV.1 Density and percentage porosities of WC and VT filled polyethylene composites

IV.2 Elongation of WC and VT filled polyethylene composites

IV.3 Dielectric constant of WC and VT filled polyethylene composites

IV.4 Dielectric loss of WC and VT filled polyethylene composites

IV.5 Density and % porosities of WC and VT filled polyester composites

IV.6 Wear rate of WC and VT filled polyester composites

IV.7 Dielectric constant of WC and VT filled polyester composites

IV.8 Dielectric loss of WC and VT filled polyester composites

IV.9 Density and % porosities of WC and VT filled polyvinyl chloride composites

IV.10 Compressive strength of WC and VT filled polyvinyl chloride composites

V.1 Comparison of the properties of the composites with polyethylene, polyester and polyvinyl chloride

V.2 Density and percent porosities of polyethylene, polyester and polyvinyl chloride containing WC and VT

V.3 Dielectric constant and loss values of polyethylene and polyester containing 10 volume percentage of WC and VT at a frequency of $10^3$ Hz

VI.1 Volume shrinkage of WC and VT fired at different temperatures

VI.2 Density data for WC and VT fired at different temperatures

# C O N T E N T S


| | | Page |
|---|---|---|
| | ACKNOWLEDGEMENTS | i |
| | SUMMARY | iii |
| | LIST OF PUBLICATIONS | v |
| | LIST OF FIGURES | vi |
| | LIST OF TABLES | viii |
| CHAPTER I | | |
| | GENERAL INTRODUCTION | 1 |
| | Definition and type of composites | 1 |
| | Effect of fillers on mechanical and electrical properties of particulate polymer composites | 6 |
| | Clay-polymer composites | 14 |
| | Summary of informations on the surface modification of particulates | 25 |
| | Applications | 27 |
| | Aim, objective and scope of the present investigation | 28 |
| CHAPTER II | | |
| | CLAY (KAOLINITE) - CHARACTERISATION AND THERMAL DEHYDROXYLATION | 31 |
| | Introduction | 31 |
| | Structure and chemistry of kaolinite | 32 |
| | Characterisation of the kaolinite under investigation | 34 |
| | Dehydroxylation of kaolinite | 52 |
| | Information gap in dehydroxylation of kaolinite | 60 |

| | | Page |
|---|---|---|
| CHAPTER III | | |
| | SURFACE MODIFICATION OF THE KAOLINITE | 61 |
| | Introduction | 61 |
| | Experimental | 61 |
| | Results and Discussion | 62 |
| | Conclusions | 74 |
| CHAPTER IV | | |
| | KAOLINITE-POLYMER COMPOSITES | 75 |
| | Introduction | 75 |
| | Kaolinite-polyethylene composites | 75 |
| | Kaolinite-polyester composites | 91 |
| | Kaolinite-polyvinyl chloride composites | 106 |
| CHAPTER V | | |
| | COMPARISONS OF THE THREE POLYMER SYSTEMS INVESTIGATED | 111 |
| CHAPTER VI | | |
| | LOW TEMPERATURE MULLITE FROM SURFACE MODIFIED KAOLINITE | 118 |
| | Introduction | 118 |
| | Experimental | 122 |
| | Results and Discussion | 123 |
| | Conclusions | 135 |
| CHAPTER VII | | |
| | CONCLUSIONS AND SUGGESTIONS FOR FURTHER WORK | 136 |
| | Conclusions | 136 |
| | Suggestions for further work | 138 |
| REFERENCES | | 140 |

# C H A P T E R  I

## GENERAL INTRODUCTION

# CHAPTER I

## GENERAL INTRODUCTION

Composite materials are finding ever new applications in different engineering fields, as they are capable of meeting diversified requirements in properties including high performance even in extreme conditions.

### I.1 DEFINITION AND TYPE OF COMPOSITES

A composite is a combined material consisting of two or more distinct constituent materials or phases. Thus, many of the natural materials like wood, bamboo etc. are also composites because in these materials cellulose fibres are embedded in a lignin matrix. But in a general sense the composite material should be man made and are combined materials created by the synthetic assembly of two or more components - a selected filler (particle) or reinforcing agent (fibre) and a compatible matrix binder (i.e., a resin, alloy or ceramics) to obtain specific characteristics and properties. The components of a composite do not dissolve or otherwise merge completely into each other, but neverthless act in concert. The component as well as the interface between them can usually be physically identified and it is the behaviour and properties of the interface that generally control the properties of the composite. The properties of the composite cannot be achieved by any of the components acting alone.

Three basic types of composite materials are: dispersion strengthened composite materials, particle reinforced composite

materials and fibre reinforced composite materials[1]. In each an elemental or alloy matrix has a second phase distributed within it. The second phase (usually harder than the matrix) is added to achieve some net property improvement. The different types are distinguished by their microstructures. Dispersion strengthened composite materials are characterised by a microstructure consisting of an elemental or alloy matrix within which fine particles of 0.01 to 0.1 $\mu$ in diameter are uniformly dispersed in a volume concentration of 1 to 15%. Particle reinforced composites differ from the dispersion strengthened composites since the dispersoid size exceeds 1.0 $\mu$ in size with the concentration extending upto 25 volume percent. The reinforcing phase in fibre composite materials spans the entire range of size, from a fraction of a micron to several mils in diameter and the entire range of volume concentrations from a few percent to greater than 70%[1]. The distinguishing microstructural feature of fibre-reinforced materials is that reinforcement has one long dimensions whereas the reinforcement particles of the other two composites do not.

Further, composite materials can be classified on the basis of matrix material or on the type of reinforcement. This is illustrated in Fig. I.1. The matrix material can be broadly classified into four groups such as polymeric, metal, cement and ceramic base. In each case, the form of reinforcements can be continuous fibrous, short fibrous or particulates. These reinforcements can be inorganic, organic, metallic or ceramic materials.

### I.1.1 Matrix materials

These include polyester, phenolic, epoxy, silicone, alkyd, melamine, polyimide, fluorocarbon, polycarbonate, acrylic, acetal,

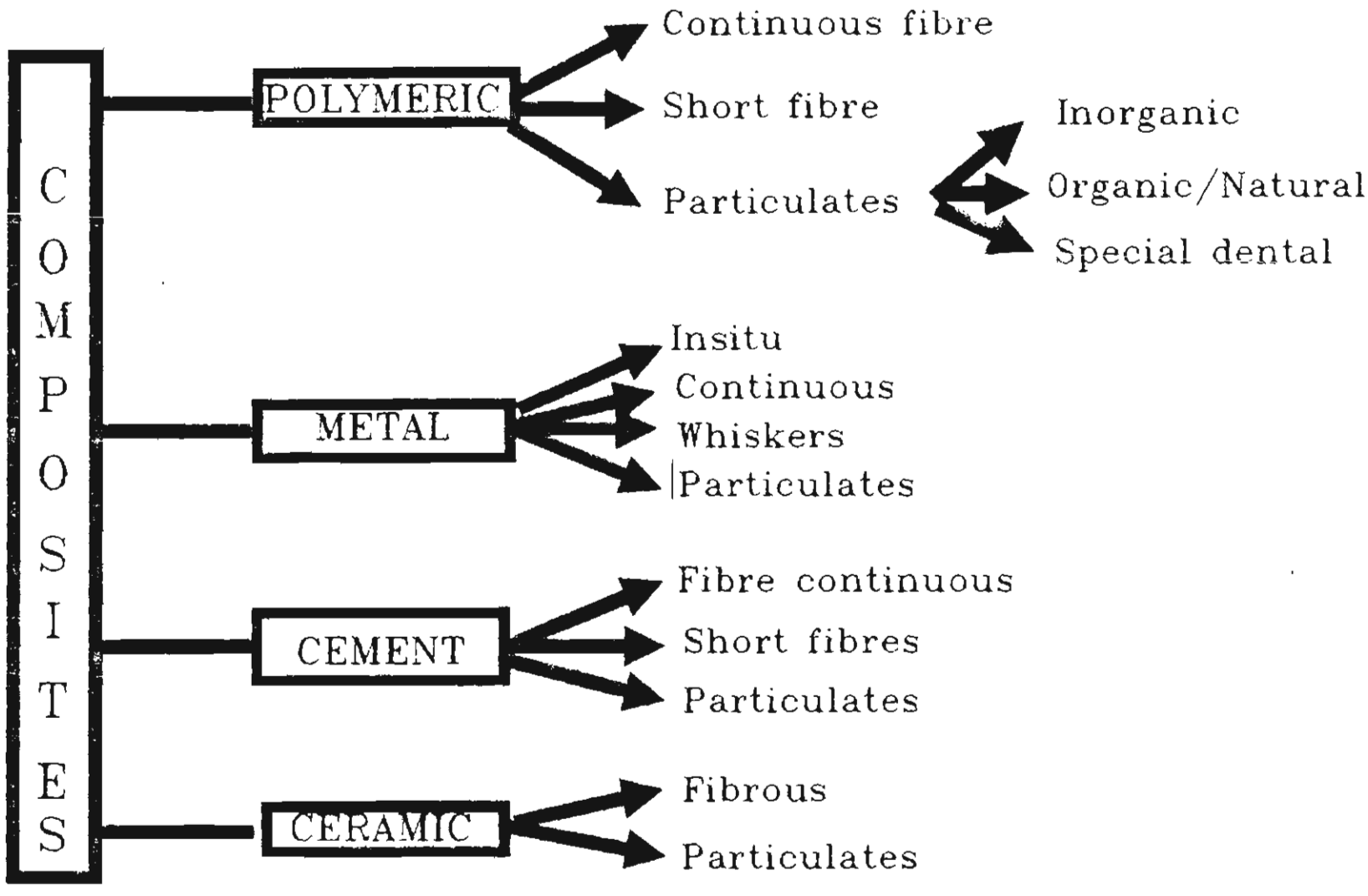


Fig. I.1 Classification of composites

polypropylene (acrylonitrile-butadiene-styrene) copolymer, polyethylene, polyvinyl chloride, polyisoprene and polystyrene. These resins can be further classified as thermoplastics (capable of being repeatedly hardened and softened by temperature) or thermoset (changing into substantially infusible and insoluble materials when cured by the application of heat or by chemical means). The metal matrix include Cu, Al, Ti etc. which find their use due to their light weight, high strength properties, high temperature capability as well as special properties such as wear resistance/abrasion resistance. Cement matrices are the portland cement and the conventional plaster of paris. They are in use due to their availability and low cost. The ceramics by virtue of its added advantage of low wear is the future hope of the matrices.

### 1.1.2 Reinforcements/and fillers

The commonly used reinforcing materials in polymer matrices are continuous or short fibres of glass, carbon and kevlar. In addition, a number of particulate fillers have been used to bring about not only cost effectiveness of expensive resins but also to positively contribute in improving certain properties such as stiffness, flame retardancy and smoke control.

#### 1.1.2.1 Particulate composites

Particulate composites have an additive constituent which is essentially one or two dimensional and macroscopic. In some composites however, the additive constituent is macroscopically non-dimensional, only on the microscopic scale does it become dimensional[2]. Particulate composites differ from the fibre and flake type in that distribution

of the additive constituent is usually random rather than controlled. Particulate composites are therefore usually isotropic. Fibre composites are anisotropic in properties having outstanding properties in one direction. Several authors have studied fibre composites[1,2]. Because of their isotropic nature, particulate composites show better properties in all directions[1].

The particulate composites have been classified into two categories.

1. Metal matrix - particulate composites
2. Polymer matrix - particulate composites

I.1.2.2 Metal matrix particulate composites

They are generally defined as a metal matrix containing a distribution of particles (eg. graphite, ceramic particles/whiskers such as SiC, $Al_2O_3$, intermetallics, second phase etc.) typically 5 $\mu$ to 200 $\mu$ in size and spaced over distances of the same order of magnitude. In this sense, the metal particulate composite differs from normal dispersion hardened materials where particle size varies between 0.1 $\mu$ and 2 $\mu$, the interparticle distance less than 5 $\mu$ and volume percent of dispersoid generally below 10%. Second phase particles are gnerally introduced to improve the thermal characteristics of the composites.

I.1.2.3 Polymer matrix particulate composites

Composite materials with polymeric matrices are emerging as strong candidates for load bearing structural applications in the commercial airplane and automotive industries. Metal or ceramic

particles embedded in polymer matrix is called polymer particulate composites. Examples are glass beads reinforced thermoplastics, silica reinforced epoxy resin, epoxy aluminium particles reinforced composites and epoxy iron particulate composites[3-10]. Also functions and uses of fillers such as asbestos, calcium carbonate, carbon black, kaolinite, mica and silica in the polymer industry have been studied by several authors[11].

## I.2 EFFECT OF FILLERS ON MECHANICAL AND ELECTRICAL PROPERTIES OF PARTICULATE - POLYMER COMPOSITES

Generally the properties of the composite materials are determined by the particle size and shape, properties of the components, morphology of the system and the nature of the interfaces between the phases.

### I.2.1 Modulus of filled polymers

A particulate second phase can strengthen or stiffen the matrix in a very complicated manner[12]. The particles appear to restrict the mobility and deformability of the matrix by introducing a mechanical restraint, the degree of restraint depending on the particulate spacing and properties of the particles and matrix. In the simplest case, the elastic modulus ($E_c$) of the composite is given by[12]

$$E_c = V_m E_m + V_f E_f \qquad \text{(case of equal strains)} \qquad (I.1)$$

$$E_c = \frac{E_m E_f}{E_m V_f + E_f V_m} \qquad \text{(case of equal stress)} \qquad (I.2)$$

where $V$ is the volume fraction and $E$ the modulus with $m$ and $f$ referring to the polymeric matrix and particulate filler phase respectively.

In many cases the experimental modulus values do not match with the theoretical values calculated by eqns. I.1 and I.2. Numerous studies have focussed on the micromechanics of particulate filled composites[10-28].

The theories predict that the elastic moduli of a composite material should be independent of the size of the filler particles. But an increase in moduli is observed as the particle size decreases. The possible reasons for this discrepancy between theory and experiment are (1) as particle size decreases surface area increases. If the polymer is changed in some manner at the interface as by adsorption, then the properties should change with particle size because of the change in surface area. (2) As particle size decreases, agglomeration of powders tends to increase with a corresponding decrease in maximum packing volume. (3) Most composite specimens have a surface "skin" which is rich in polymer as a result of being molded against surface. This skin thickness is proportional to particle size[27].

Generally the modulus of the composite is affected by the distribution of particle sizes. More dense packing is possible for mixtures of different particle sizes compared to mono dispersed particles. Thus a distribution of particle sizes gives a larger packing fraction $I_m$ of the filler, and hence lower modulus for a given concentration[27].

I.2.2 Strength and stress strain behaviour

Generally a dramatic reduction in elongation to break is observed for filled polymers[27]. The simplest model in which the filler particles are attached to the polymer is given in Fig.I.2. Perfect adhesion is assumed between the two phases. Shear effects around the filler particles,

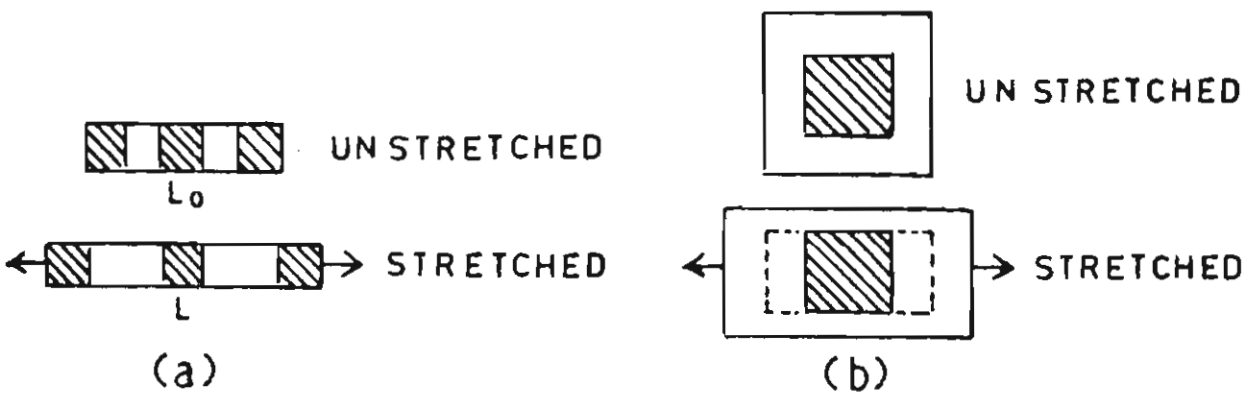


Fig.I.2 Models for filled polymers
(a) Perfect adhesion
(b) No adhesion

triaxial stresses in the polymer and effect due to poisson's ratio are all neglected here.

For a given elongation of the model, the actual elongation experienced by the polymer matrix must be greater than the measured elongation of the specimen. If one assumes that the polymer breaks at the same elongation in the filled system as the bulk unfilled polymer does and if the fracture path tends to go from one particle to another rather than giving a perfectly smooth fracture surface, then the elongation to break of the filled system relative to the unfilled polymer is[27]

$$\epsilon_{(\text{filled})} = (1 - V_f^{1/3}) \quad \epsilon_{(\text{unfilled})} \qquad \text{(I.3)}$$

where $\epsilon_{\text{unfilled}}$ is the actual elongation of the plastic, $\epsilon_{\text{filled}}$ is the overall elongation of the filled system (i.e., $\epsilon = \frac{L-L_o}{L_o}$ where L and $L_o$ are the final and initial specimen length , respectively) and $V_f$ is the volume fraction of filler. This equation is plotted in Fig. I.3. This curve shows the very dramatic decrease in elongation that can be brought about by only small amounts of filler. For poor adhesion and smooth fracture surface, the elongation to break may decrease more gradually than eqn. I.3 would indicate. Only in rare instances where fillers introduce additional crazing and at the same time act as arrestors to crack growth, polymers filled with rigid fillers have elongations to break which are equal to or greater than that of the unfilled polymer.

Fillers generally reduce the tensile strength of the composites[27]. By using eqn. I.3 with the theoretical equations for the modulus of

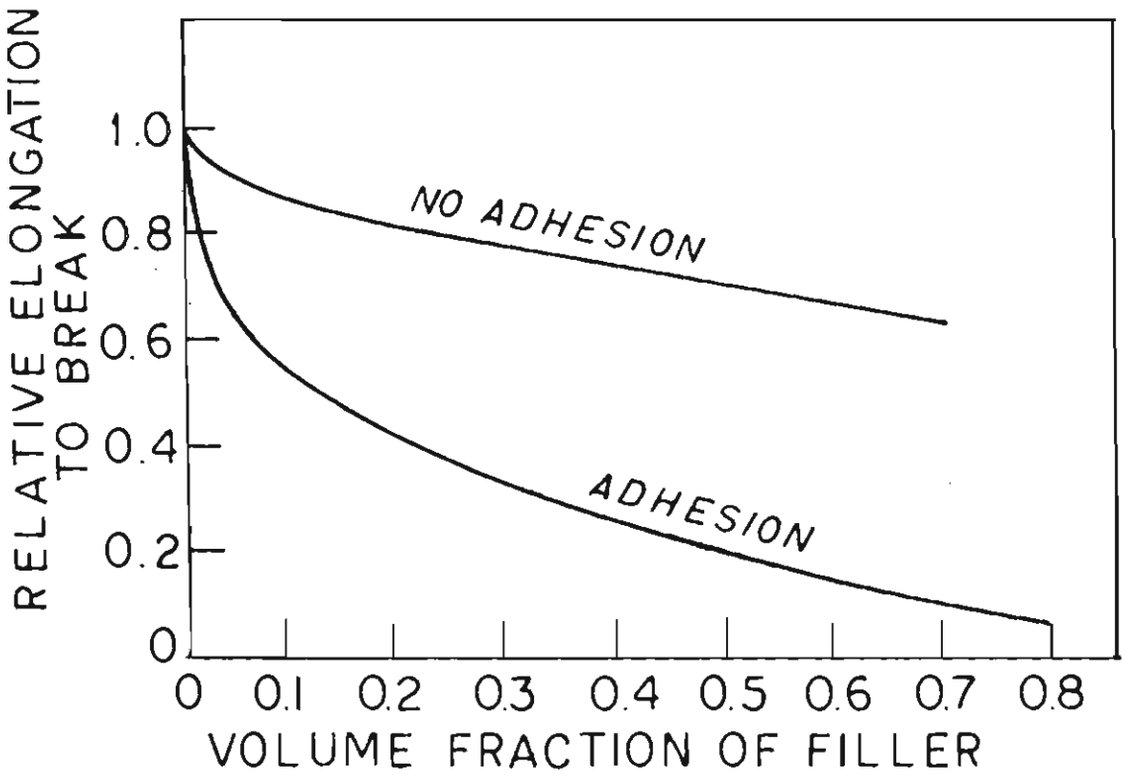


Fig. I.3 Theoretical curves for the elongation to break for the case of perfect adhesion and no adhesion between the filler and polymer phases[3].

filled systems containing spherical particles, tensile strength is given by[27]

$$\sigma_B = E \epsilon_B \qquad (I.4)$$

where E is the young's modulus of the filled polymer. The predicted values for tensile strength according to the theories of Kerner and Eilers - Van Dijck eqn. are given in Fig. I.4.

The tensile strength increases with added filler above a volume concentration of about 10%. The Eilers Van Dijck curve even predicts a value of tensile strength greater than that of the unfilled polymer at higher concentrations. Both theories predict a beneficial increase in tensile strength at high filler loadings, if there is good adhesion between filler and polymer and good dispersion of filler particles without aggregation.

If there is no adhesion, the filler particles cannot carry any of the load, so all the load must be carried by the matrix.

For a given cross section, the fraction occupied by the polymer is equal to the volume fraction occupied by the polymer and the tensile strength would be the product of the tensile strength of the unfilled polymer and the volume fraction of the polymer[27]. However, the filler particles distort the stress fields so that when the material breaks, the fracture travels from one filler particle or void space to another. Thus a model similar to that shown in Fig. I.2 b might be more realistic. This model accounts for the decrease in cross sectional area of the polymer phase with the addition of filler, but it does not enable us

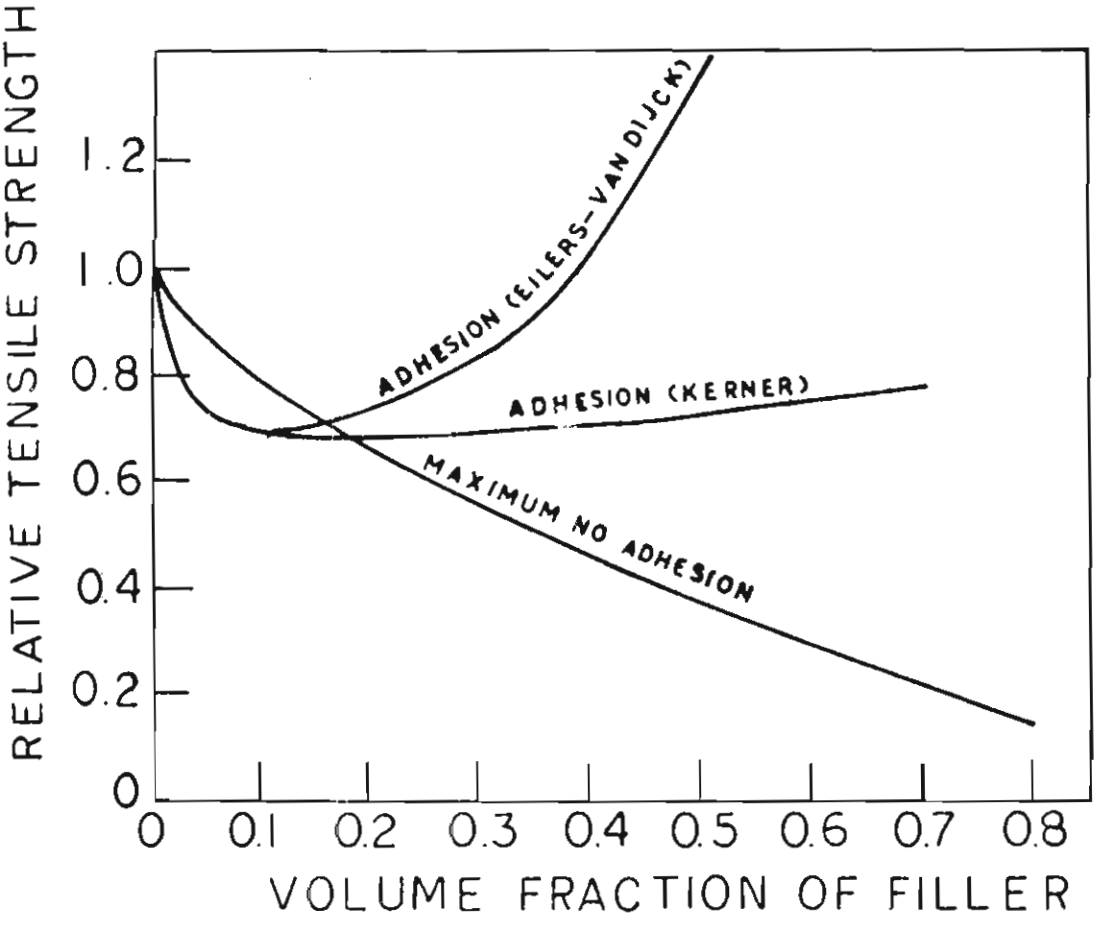


Fig. 1.4 Theoretical curves for the tensile strength of filled polymers.[3]

Curve for no adhesion was calculated using stress concentration factor $S' = 1$

to calculate the additional factor of stress concentration around the particles. Thus the calculated values of tensile strength based on this model may be considered as maximum values, stress concentrators will lower these values by an undetermined amount.

As the particle size decreases, tensile strength increases. With the decrease in particle size, the interfacial area per unit volume of filler increases. The stress fields near a particle are independent of the size of the particle. But when the particle size increases, the volume of polymer that experiences a given value of stress concentration increases. Hence the probability of finding a large flaw within this volume increases. If a large flaw exists within an area of stress concentration, the tensile strength will be reduced according to the Griffith's crack theory[27]. Also after dewetting, if the filler particles are large, large voids will be produced, larger voids are more harmful to strength than smaller voids[27].

Although fillers decrease the breaking strength in tension, they increase the strength in compression. Fillers such as wood and nut shell flours will reduce the compressive strength. But hard solid fillers increase the compressive strength provided that adhesion between the components is equal to or greater than the cohesive strength of the matrix.

I.2.3 Abrasion behaviour

The important factors which influence the property of abrasion are Mohs' hardness of the filler, shape of the filler particles, the strength of the interfacial bond, relative filler packing fraction and

the coefficient of friction. Irregular shaped particles of aluminium oxide in polytetra fluoroethylene increased the rate of wear by a factor of several time over that found with spherical particles in the same polymer[30]. Both particles increased the rate of wear over that of the unfilled polymer.

The abrasive wear of filled polymers is strongly dependent upon the relative size of the filler particles and the size of the abrasive. If the filler particles are large compared to the size of the abrasive particles and the adhesion between filler and matrix is good, wear is found to be least[27]. Fillers may either increase or decrease the rate of abrasion. The effects are difficult to predict because the final properties depend so strongly on the type of testing machines, on the type of fillers and upon the nature of the interface and the strength of the adhesion between the phases[30].

### I.2.4 Electrical properties

The subject of electrical conductivity in particulate composites had been under study for many years. Kerner assumed that the overall conductivity could be considered as a weighted linear superposition of the component conductivities, the weight is considered as the product of a geometrical factor (volume fraction of filler) and an intensity factor (ratio of the average value of the electrical field component in the direction of the applied field to the average value of the field in the bulk)[28].

## I.3 CLAY-POLYMER COMPOSITES

### I.3.1 Literature survey

Clays have been known and used as ceramic raw materials for

centuries. Detailed studies on the surface property relationships of the clay minerals have led to wealth of informations in this mineral from time to time. Presently clay is understood as hydrous alumino-silicate mineral which makes the colloidal fractions of soils and sediments.

In industry, clays are used as fillers and reinforcements in polymer systems such as elastomers, polyethylene, polyvinyl chloride and other thermoplastics. Clay, being the natural and most abundant material with properties of thermal stability, high surface area, fine particle size and low density, has been the most versatile filler for polymers[31]. Some of the objectives in adding a filler to a polymer matrix could be to stiffen the matrix and make it more rigid, to regulate thermal shrinkage, to reduce creep, to increase strength properties of the material, to improve electrical and rheological properties, above all to reduce the cost of the materials[31-33].

The efficiency of a filler to improve the physico-mechanical properties of a given system is affected by a number of factors such as shape and size of the particles, physico-chemical properties of the constituents, volume fraction of the filler, adhesive bond between the two phases, the type of dispersion and amount of particle agglomerations[34-39]. All these factors being equal, the degree of dispersion of the filler in the polymer matrix plays an important role in such systems[39]. Because of the hydrophilic nature of the clay surfaces it becomes extremely difficult to disperse clay in polymers. To make the clay more compatible with the polymer, it is necessary to modify the surface of the clay by suitable methods. This can be done either

by thermal or chemical treatments. The extensive literature on this subject has been reviewed by Theng[39].

A very simplest method of modifying the clay surface is by attaching a suitable organic compound to the mineral surface[40]. For porous and high surface area solids, the method is not very effective. The adsorbed organic coat may be displaced by solvents or during compounding[33,40]. Clay surfaces can be made compatible with organic phase in a better way by neutralising the acid washed material with an organic base which is then held by the exchange complex of the mineral as the corresponding cation. By replacing part or all of the exchangeable inorganic cations with small organic cations or poly cations, stable hydrophobic clays can be prepared[41-46].

To prepare organo-silicon modified kaolinites as fillers for rubber and diethyl polysiloxane (liquid) to kaolinite, the mixture is exposed to ultrasonic vibration and the unbonded polymer is removed by washing the system with toluene or tetrahydrofuran[39]. Significant improvements in modulus, abrasion resistance and compression set properties have been achieved by use of modified kaolin in rubber, modification being achieved by using an aminosilane, by which it is possible to attach the hydrolysed silanol group of the reagent to the kaolinite surface, leaving the pendent amino group free to react with the rubber during vulcanisation. Ep rubber filled with this type of clay had a tensile strength 55% higher than that containing the untreated kaolinite[47].

Kaolinites modified by reaction of tetraisopropyl titanate and oleic acid were effectively used as fillers for poly amides (nylon) and plastics[47]. The effect of the organo titanium clays so obtained

in polymers and plastics is given in Table I.1. In almost all the cases elongation is decreased by the filler. The toughness and heat distortion properties of plastics are improved by the addition of filler.

When a pendent amine group is introduced into the organic coating, the filler becomes more compatible with the polymer matrix[48]. Such mineral filled nylons which are commercially available show significant reductions in water uptake. This would give them improved dimensional stability in situations where there are large fluctuations in relative humidity. Clay filled polyamides may be obtained by introducing a catalytically active clay into the monomer. When montmorillonite treated with amino caproic acid is used for this purpose, the caprolactum monomer is apparently intercalated giving rise to a clay-polymer complex with an interlayer separation of 1.31 nm[48]. By heating methyl methacrylate in the presence of acid, clays and an organic radical initiator, sheets of high flexural strengths can be obtained[49].

Another fast developing technique to obtain better compatibility and hence strong bonding between filler and matrix, is to graft a suitable polymer onto the clay surface. Grafting normally implies that the polymer is attached to the mineral by primary (covalent) bonds. However, secondary interactions may also lead to extremely strong bonding between polymer and solid surface. For this reason, and because in many instances, some homopolymer is formed concurrently, the occurrence of true grafting is often difficult to demonstrate directly. A lot of investigations have been done on this aspect, because of the potential industrial applications of such graft[39,50-55].

Table I.1: The effect of addition of an organo-titanium kaolinite filler obtained by reacting the clay with tetraisopropyl titanate and oleic acid in polymers and plastics[47]

| Property | Polymer or plastic | | | | | | | | | | |
|---|---|---|---|---|---|---|---|---|---|---|---|
| | HDPE | Epoxy | Acetal | SAN | Nylon 6 | Polypro-pylene | Propy-lene co-polymer | Rigid PVC | ABS | Impact PS | Phenolic |
| Tensile strength | + | + | 0 | - | 0 | + | + | 0 | + | + | 0 |
| Tensile yield | 0 | + | 0 | 0 | 0 | 0 | + | 0 | 0 | 0 | 0 |
| % Elongation | - | - | - | 0 | - | - | - | - | 0 | - | 0 |
| Tensile modulus | + | 0 | + | + | + | + | 0 | + | + | + | 0 |
| Hardness | 0 | + | 0 | 0 | 0 | 0 | 0 | 0 | + | 0 | 0 |
| Heat distortion | + | + | + | 0 | + | + | + | + | + | 0 | 0 |

Plus and minus signs denote a + Ve and -Ve change in property while 0 represents no change.

HDPE high density polyethylene; SAN styrene acrylonitrile polymer; PVC polyvinyl chloride; ABS acrylonitrile-butadiene-styrene resin; PS polystyrene

When octadecyl ammonium (ODA) montmorillonite was mechanically dispersed in the presence of methyl methacrylate by means of vibration milling, polymethyl methacrylate was formed[50,51]. Because of the covering of the clay surfaces with a dense layer of long alkyl chains no grafting occurred in this case. However, the presence of dispersed clay particles in the matrix gave rise to a polymer which was harder and had a higher softening point than the corresponding unfilled material. When the same experiment was conducted on Na montmorillonite, considerable grafting was found to occur. The rate of polymerisation and the yield of polymethyl methacrylate were further increased when benzoyl peroxide was added to the system and graft polymers as well as homopolymers were formed. These observations were explained in terms of the adsorption onto the clay surface of the chemical initiator whose cleavage into radicals was promoted by the grinding process.

Polyfukha et al[39] have treated kaolinite with various organic initiating agents such as tert-butyl peracrylate, tert-butyl perpropionate, and β-hydroxy ethyl-tert-butyl peroxide etc. When such treated kaolinite was heated above the decomposition temperature of the initiator in presence of some organic monomers such as methyl methacrylate and styrene, polymerisation occurred. An appreciable proportion of the polymer formed was found to be non-extractable and hence assumed to be grafted onto the clay. The nature of the initiator and the strength with which it is adsorbed onto the mineral surface influences the amount of grafting.

When the complexes formed by treating 2,2'-azobisisobutyramidine with kaolinite and montomorillonite was decomposed, they gave free radicals and it was highly effective in initiating the polymerisation of monomers such as methyl methacrylate, acrylamide, vinyl acetate and 4-vinyl pyridine[53].

Fallick et al[56] described a method for treating the fillers in which filler particles are dispersed in the polymer melt, encapsulate them with a thin sheet of resin and bind this encapsulant to both the mineral and the polymer matrix. By this procedure they were able to develop a family of mineral reinforced linear polyethylene termed 'ceraplasts'. They showed considerable increase in tensile and impact strength over conventionally filled polyethylene. This was attributed to the presence of a modulus gradient in the encapsulant between the mineral and the polymer matrix. By using untreated or surface modified kaolinite to the polymer melt, the mechanical strength and stability of polymers such as polycaproamide and polyethylene can be increased[57,58]. On crystallization of the polymer, the clay particles tend to concentrate in the interspherulitic region. Hence the mobility of the polymer is reduced in these areas and also prevented particles from regrouping in the crystalline phase.

Howard[59] described a method for obtaining reinforced polyethylene by polymerising the monomer in the presence of a clay containing adsorbed catalytically active transition metals. Bixler and Fallick[60] obtained reinforced polyethylene by compounding the

polymer with clay particles which have been coated with an olefinic substance and a free radical generator. Baum[61] adopted a similar method in which he coated the clay samples with oxygen containing organic compounds having high boiling points ( $> 413^{\circ}K$) and an organic peroxide which could act as a crosslinking agent between the modified mineral surface and the polyethylene chain.

Homogeneous mineral ultra high molecular weight polyethylene composites were prepared by Howard et al[62] with metal oxides, clays, silica etc. that possess high modulus and low temperature impact resistance. High levels of clay can be incorporated homogeneously in ultra high molecular weight polyethylene by polymerization of $C_2H_4$ in catlytically activated mineral surfaces.

By the use of irradiation techniques thermoplastics such as polyethylene, polypropylene and polyvinyl chloride can be grafted to the clay surfaces[63,64]. If the clay surface is coated with organics having polyethylene like chains (eg. polyvinyl alcohol, polyethylene oxide, hexamethylene diamine) the extent of crosslinking can be increased. By exposing these modified clays to $\gamma$-rays in the presence of polyethylene, products of greater strength, excellent thermal stability and resistance to organic solvents are obtained[64-66]. By using minerals whose surface is grafted with polymethyl methacrylate, Uskov et al[50] were able to crosslink polystyrene to a layer of polymethyl methacrylate. Nagada and Tagami[64] claimed effective reinforcement of polyvinyl chloride, when a clay-polymethyl methacrylate composite obtained by irradiating methyl methacrylate in the presence of the mineral was

incorporated into the system.

The above methods were effectively used by Hawthorne et al[67] to prepare kaolinite fillers and were used to reinforce polyethylene. Here the mineral is heated at 383-393$^{o}$K in air, thereby making the clay surface initially acidic and so capable of initiating the cationic polymerization of various vinyl monomers (butadiene, isoprene, piperylene, propylene, styrene) and the remaining acidity is neutralised with ammonia or an organic phase. When such treated clay is compounded with polyethylene, grafting occurs between the encapsulating polymer layer and the matrix polymer. Polyethylene filled with such treated clays show significant improvements in processability, tensile and impact strengths as compared with the unfilled polymer or the material containing untreated fillers as presented in Table I.2.

Kaolinite can be coated with di-isopropoxy aluminium methacrylate polymer obtained by the insitu hydrolysis of adsorbed oxyaluminium derivatives in organic solvents[68]. When such treated clays are blended with polyethylene the product shows improved tensile and impact strengths.

Structure and properties of filled high density polyethylene was studied by Selivanova et al[69]. The effect of thermal aging at 60-90$^{o}$C for $<$ 2160 $h_r$ on the physico-mechanical properties and structure of low density polyethylene was reported by Abramova et al[70]. Percentage elongation ( $\epsilon$ ) of unfilled polyethylene was found to decrease from 560 to 3% and tensile strength ( $\sigma$ ) of unfilled polyethylene was found to decrease by a factor of 2 after 1500 hr aging at 90$^{o}$ compared to a decrease in $\epsilon$ from 400 to 200% and no decrease in $\sigma$ of kaolin filled polyethylene.

Table I.2: Properties of high and low density polyethylene filled with 20% of different fillers[68]

| Filler type | 95% confidence limits for yield kg/cm$^2$ | | Elongation at break, % | | Impact strength, kgm/m |
|---|---|---|---|---|---|
| | HDPE | LDPE | HDPE | LDPE | HDPE |
| None | 289 ± 4 | 90 ± 3 | 1300 | 700 | 2.63 |
| Untreated hydrite 10(H 10)[a] | 282 ± 5 | 96 ± 4 | 100 | 200 | 1.23 |
| Free port kaolin OX-3[b] | 285 ± 3 | 109 ± 1 | 40 | 140 | 1.30 |
| Commercial reactive encapsulated kaolin | 286 ± 3 | 96 ± 4 | 25 | 160 | 1.23 |
| SRF carbon black | 318 ± 2 | 110 ± 1 | 50 | 84 | 1.00 |
| H 10 + 4% isoprene[c] | 300 ± 2 | 110 ± 3 | 90 | 210 | - |
| H 10 + 4% piperylene[c] | 300 ± 4 | 111 ± 2 | 140 | 140 | 1.32 |
| H 10 + 4% styrene[c] | 299 ± 4 | 111 ± 6 | 45 | 190 | 1.56 |

a - From Georgia Kaolin Company

b - Coated with an organophilic compound

c - Polymerization terminated by ammonia encapsulating polymer oxidised before use

The effect of modifiers eg. di-buphthalate and SBR latex was studied by Jan Czak et al[71] in relation to the degree of filling in chalk and polystyrene composites. The mechano mechanical grafting of acronitryl, methyl methacrylate or vinyl chloride on mica, kaolin and volcanic tuff by vibration milling was studied by Opera et al[72]. The tensile properties of PVC was found to be the same with and without fillers ( $\leq$ 10%). The impact strength was increased when filled with grafted volcanic tuff.

When PMMA grafted kaolin was used as filler in polyvinyl chloride, modified physico-chemical properties were obtained. Improved electrical properties were observed by introducing calcined kaolinite in PVC, SB (styrene-butadiene) and butyl rubber[73].

Kulinskii and Lapko[74] observed that sorption of moisture by dehydrated fillers intended for ethylene propene rubbers used in high voltage cable insulation depends on the particle size distribution and calcining temperature.

De Nunzio and Held[75] have found a good correlation between the surface area of a number of clays and the degree of reinforcement in agreement with Black et al[36,37].

Table I.3 lists the different types of treatments generally adopted for surface modification of particulates for improved properties.

I.3.2 Inference drawn from the literature

The addition of fillers and reinforcing agents for obtaining modified physical properties of polymers has reached a lot of industrial

Table I.3: Summary of informations on the surface modification of particulates in polymer based composites

| | |
|---|---|
| Common particulates | Chalk, kaolinite, montmorillonite, carbon black, asbestos, silica, mica |
| Surface modification techniques | 1. Using coupling agents such as silane derivatives and organic titanates<br>2. Chemical grafting of macromolecules to the filler surface<br>3. Radiation grafting<br>4. Physico-chemical initiation<br>5. Fixation of active sites on filler surfaces |
| Common matrices | Polyethylene, polyvinyl chloride, polystyrene, polypropylene, polyamides |

importance. Inert particulate fillers such as carbon black, silica and clay are used primarily to reduce the cost of the composite material. Other factors such as improved physical and mechanical properties can be achieved by use of such fillers. Kaolinite being one of the most abundant materials with unique properties is one of the most important filler for polymer systems (will be discussed in detail in Chapter II). Because the surface of clays is hydrophilic, it exhibits a strong tendency to resist dispersion with the formation of stronqly bonded agglomerates. The reinforcing effect of clay can be improved by suitable surface treatment of the filler particles to promote wetting by and adhesion to the polymer matrix.

A number of novel techniques based on chemical methods have been developed and systematically studied for obtaining more reinforced filler polymer systems. This involves methods such as the attachment of a suitable organic compound to the filler surface by exchanging the inorganic cations with organic counterparts, treating the mineral with organosilanes, grafting a suitable polymer onto the filler surface and to encapsulate the mineral particles with a polymer layer.

Eventhough the process of dehydroxylation can make clay surface hydrophobic, not much attention has been given to study its effect in polymer composites. Aim of the present study is therefore to modify the clay surface by a thermal decomposition hydration - redecomposition technique (will be discussed in detail in Chapter III) and to study its effect in different polymer systems.

## I.4 APPLICATIONS

Cost reduction by using fillers is the most important application of the clay-polymer systems. Water soluble polymers have been used to stabilise soils in civil engineering applications such as construction of air fields, canals, highways and preparation of building sites for housing and industrial purposes.

Ceramics can perform well under the influence of various mechanical, thermal, electrical and magnetic environments. The major problem is the method of fabrication to arrive at the required shape, which is a requirement for the construction of automobiles and space vehicles. This problem can be solved by the injection molding technique. For this, a ceramic polymer composite may be prepared and moulded to the required shape by injection molding, then the polymer is evaporated by slow heating. Layer type clay-carbon composites may find wide applications as a refractory and a wear resistant material, in sliding applications and also as an electrical conducting material. For this, composite is prepared from a suitable clay and a long chain polymer; it is then carbonized which will result in a material with interlayer of clay and carbon which is expected to have entirely new mechanical, electrical and thermal properties.

Mineral filled nylons with improved tensile and flexural properties have proved very useful in the manufacturing of objects such as carburettor bodies, fan blades and skate boards.

Clays can be effectively used as fillers for rigid and flexible urethane foams to provide exceptional cost reduction and to improve properties such as uniformity and finer cell volume.

Heat sealed and welded joints are improved by the inclusion of fillers in thermoplastics due to the improvement in conductivity, but the flow of the melt gets reduced. Magnetic, high frequency and inductive bonding require a magnetically susceptible filler in the thermoplastic or at the interface to generate heat[31].

Mechanical fastening frequently involves the use of metal fastners. Since fillers reduce the coefficient of expansion of plastics to more nearly that of metals, composites are more compatible where temperature changes may produce joint separation due to differential expansions. Low density crushable fillers also provide reduction in crack propagation as impact especially in thick sections and help to grip nails or punched inserts[31].

Thermosetting resins such as epoxy resin or a resin prepared from aromatic cyanic acid esters containing conducting filler such as kaolin is bonded to the walls of slots in electrical machines to give heat conducting electrical insulation[31]. Clay fillers are extensively used in polyvinyl chloride which is used as electrical insulators, phonographic records and floor coverings.

## I.5 AIM, OBJECTIVE AND SCOPE OF THE PRESENT INVESTIGATION

From the foregoing it becomes evident that for commercial applications, most of the polymeric materials are compounded with reinforcing agent, colcurants or fillers for various purposes. The composite material is then molded or shaped for a variety of end use. Clay being the most abundant material and having unique properties such as thermal stability, high surface area, fine particle size and low density is a common filler for polymers. Because of the hydrophilic nature of

clays, they exhibit a strong tendency to resist dispersion in polymers by forming strongly bonded agglomerates. To increase the compatibility factor between the clay and the polymer matrix, it is necessary to make the clay surface organophilic prior to blending or compounding the filler with the polymer. It has been reported that increased surface area of clay particle is an important factor for polymer adsorption. Simple calcination of clay minerals does not give any increase in surface area. Thermal decomposition - hydration - redecomposition technique has been proved to be an effective method for obtaining high surface area clay powders. Thus in the present work an attempt has been made to modify the surface of kaolinite by the above technique which results in a product of increased surface area characterized by microporosity. The surface modified kaolinite has been characterized by Raman and solid state NMR techniques for understanding the extent of dehydroxylation in heat treated clays. Dielectric measurements of the surface modified kaolinite were made to evaluate their insulating properties in comparison to the pure kaolinite.

The effect of addition of the surface modified kaolinite in three different polymer matrices such as polyester, polyethylene and polyvinyl chloride would lead to development of new materials with improved properties. The mechanical and electrical properties and microstructural features of the composites prepared using the treated and untreated kaolinite are compared.

As part of the characterization of the surface modified kaolinite, a high temperature transformation reaction usually studied on kaolinite has also been performed. The transformation above 950-1000$^{o}$C is known as premullite or spinel, which is followed by the actual formation of

mullite, one of the most important phase in the alumina-silica system. Low temperature conversion of kaolinite to mullite has been a subject of study by various methods, one of them being addition of impurities or dopants in the reaction step. However, it would be quite possible for kaolinite with higher surface area could enhance the formation of mullite. XRD, microstructural observations,and measurements of electrical properties of sintered clay samples at temperatures above 1000$^{o}$C,are the tools used to identify the mullite.

# C H A P T E R II

## CLAY (KAOLINITE) - CHARACTERISATION AND THERMAL DEHYDROXYLATION

# CHAPTER II

## CLAY (KAOLINITE) - CHARACTERISATION AND THERMAL DEHYDROXYLATION

### II.1 INTRODUCTION

Clay minerals occur in a wide variety of geological environments in the form of soils, weathering products, sedimentary rocks and as hydrothermal clays. Geologically clays are composed of various minerals of primary and secondary origin, all of which constitute fine powders of average size around 2 microns.

Clays which are hydrous layer silicates belong to the larger family of phyllosilicates. Their structure essentially consists of tetrahedral and octahedral sheets condensed together in varying proportions and stacked on top of each other in a definite way. Each tetrahedron is linked with its neighbouring tetrahedra to form hexagonal rings which in turn are connected to form two dimensional sheets. The bases of the tetrahedra are in the same plane and the tips point in the same direction, towards the octahedral sheet. The tetrahedral sheets have the composition $(Si_2O_5)^{2-}$. By union with the positively charged octahedral sheet electrical neutrality is achieved. The octahedra also form sheets. Both trivalent and divalent cations may be present. When the cation is a trivalent ion, such as $Al^{3+}$, only two thirds of the possible cationic sites are normally filled and the structure is termed dioctahedral. If the octahedrally coordinated cation is divalent, such as $Mg^{2+}$ or $Fe^{2+}$, all the possible sites are normally filled and structure is termed trioctahedral.

Depending on the ratio of tetrahedral to octahedral sheets in

one respective layer the following three major groups of clay minerals have been identified:

| Tetrahedral sheet to octahedral sheet ratio | Group |
|---|---|
| 1 : 1 | dimorphic |
| 2 : 1 | trimorphic |
| 2 : 2 or 2 : 1 : 1 | tetramorphic |

Each group has a variety of names depending on the compositional and structural variations.

Kaolinite belongs to the 1:1 type and is described in the following section.

## II.2 STRUCTURE AND CHEMISTRY OF KAOLINITE

The word 'kaolin' which is believed to have been derived from the Chinese word kaolin, has a structural formula $Al_4 Si_4 O_{10} (OH)_8$, and chemical composition, $Al_2O_3.2\ SiO_2.\ 2\ H_2O$. Kaolinite is the simplest member of the kaolin family consisting of one layer per unit cell with a triclinic symmetry.

The structure of kaolinite consists of a hexagonal network of Si-O tetrahedra with a superimposed layer of Al-O(OH) octahedra sharing the oxygen atoms at the apices of the tetrahedra as shown in Fig.II.1. Each silicon atom is tetrahedrally surrounded by three oxygens in the basal plane and fourth in the layer above. The latter is shared with two Al atoms, each of which is octahedrally coordinated to oxygens and four hydroxyl groups, three in the uppermost layer and one coplanar with the apex oxygen. The Si tetrahedron shares corner with three other tetrahedra while each Al - octahedron has three edges in common with

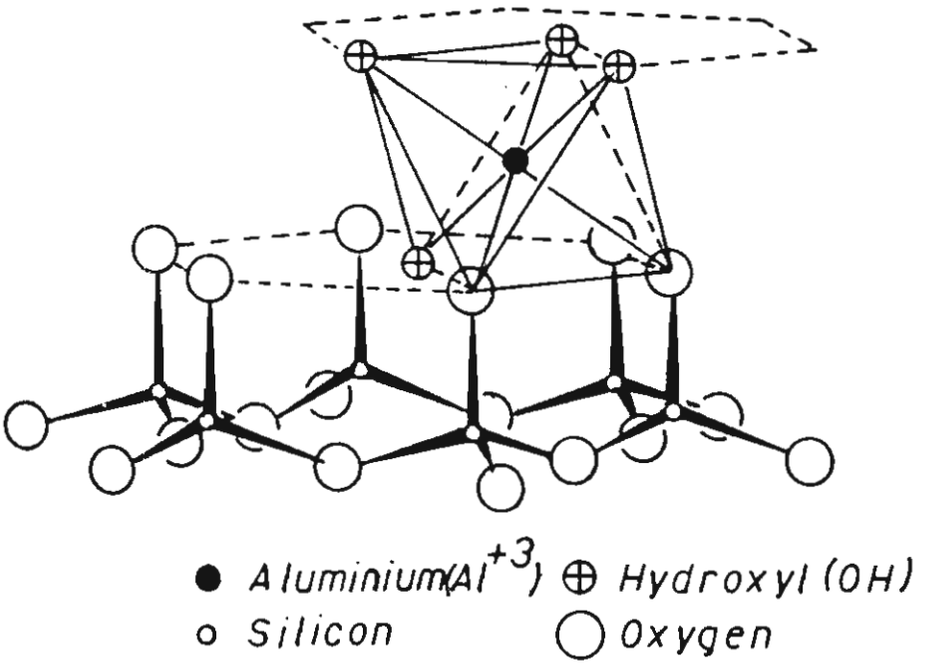


Fig. II·1 The structure of kaolinite,[7,8]
$Al_4Si_4O_{10}(OH)_8$

other octahedra. In the layer common to the octahedral and tetrahedral groups two-thirds of the atoms are shared by silicon and aluminium. In a normal layer only two third of all possible octahedral sites are filled by aluminium forming a dioctahedral layer and the (OH) groups in the wholly hydroxyl layer lie in lines parallel to the bases. Hence in ideal case, successive layers are so arranged that oxygen atoms and (OH) groups of adjacent layers approach each other in pairs as shown in Fig.II.1.

Several workers have carried out detailed verification and refinements of the basic structure[78-84]. Excellent reviews on the studies of kaolinite structure are provided by Grim[83] and Brindley and Brown[84].

### II.2.1 Dehydration of kaolinite

Dehydration of a clay mineral involves the loss of adsorbed water and the interlayer or lattice OH water which may result in considerable changes in the structure of the clay. The DTA of kaolin minerals show an endothermic reaction in the 500-700$^{o}$C range which leads to the meta-kaolinite formation. The meta phase has been studied by several researchers[85-101]. Most of the earlier workers obtained very diffuse band at the metakaolin range and considered it to be an amorphous phase. The dehydration characteristics of the kaolinite will be discussed in detail in the following sections.

## II.3 CHARACTERISATION OF THE KAOLINITE UNDER INVESTIGATION

### II.3.1 Experimental

#### II.3.1.1 The kaolinite

The clay used in the present investigation was supplied by M/s. English Indian Clays Ltd., Trivandrum, India. The kaolinite

as received was further sieved through a 45 micron sieve and dried.

II.3.1.2 Methods

II.3.1.2.1 Chemical analysis: Chemical analysis of the kaolinite was carried out according to the rapid methods of silicate analysis reported by Kumar et al[102]. Alumina content was determined by complexometric method using EDTA and $Fe_2O_3$ and $TiO_2$ by colorimetric method. The amount of alkalies was estimated using a flame photometer and the loss on ignition value was determined at 1050°C.

II.3.1.2.2 Density: Density measurements of the kaolinite particle were made by the specific gravity bottle method.

II.3.1.2.3 Thermogravimetric analysis: TGA was done on 0.5 g clay samples at a heating rate of10°C/min using Perkin Elmer Model with an automatic recorder.

II.3.1.2.4 Differential thermal analysis: DTA was taken on 0.1 g of the sample using calcined alumina as standard material and at a heating rate of 10°C/min using a Perkin Elmer Model.

II.3.1.2.5 Particle size distribution: The particle size measurement of the material was studied by using a Micromeritics Model Sedigraph 5000 D Particle Size Analyser and the particle size distribution of the material was obtained in a graph with cumulative mass percent versus particle diameter in microns. This instrument works on the sedimentation principle using a modified Stokes law given by[103]

$$r = \sqrt{9\,h\eta/2\,(D_1 - D_2)\,gt} \quad \text{(in microns)}$$

where

$\eta$ = viscosity of the defloculant employed

h = height from the top to where measurement was done

$D_1$ & $D_2$ = Densities of sample and solvent respectively

g = acceleration due to gravity

t = time allowed for settling of the dispersion

The deflocculant used for preparing the dispersion was $Na_4P_2O_5$ (Tetron).

II.3.1.2.6 Surface area: The surface area $S_{BET}$ ($m^2\ g^{-1}$) of the sample was calculated by the Brunauer-Emmett Teller (BET) method.

II.3.1.2.7 Scanning Electron Microscopy: Fine dispersion of the clay particles in acetone was prepared and deposited on a brass stud. SEM studies were done at University of Laval, Canada.

II.3.1.2.8 Transmission Electron Microscopy: TEM studies were done on a JEOL JEM 100 B. For this purpose clay particles were dispersed in acetone and deposited on the carbon film.

II.3.1.2.9 X-ray diffraction (XRD) studies: XRD patterns of the clay was obtained by the powder diffraction technique on Philips Model PW 1710 X-ray diffractometer with $CuK\alpha$ radiation using nickel as filter at a setting of 40 kv and 20 mA. The identification of the mineral was done using ASTM Card index of powder diffraction patterns and also from other available literature.

II.3.1.2.10 Infrared (IR) spectra: IR absorption spectra of the clay in the range 4000-400 $cm^{-1}$ was automatically recorded in the form of a chart using Perkin Elmer Model IR Spectrophotometer with KBr.

II.3.1.2.11 Dielectric measurements: Thin circular pellets of 2 mm thickness and 10 mm diameter were prepared by hot pressing to avoid moisture and air gaps. Room temperature silver paste was applied for electrodes on either side of the sample. The dielectric measurements were done on a meter of model GR 716 in the frequency range $10^2$-$10^5$ Hz and on a Marconi circuit magnification meter (type 7 F 329 G) in the range $10^5$-$10^7$ Hz by following the resonance curve method as described by Bhattacherjee[104].

II.3.2 Results and Discussion

II.3.2.1 Chemical analysis

Result of the chemical analysis of the kaolinite under investigation is given in Table II.1.

The total colouring oxides ($Fe_2O_3$ + $TiO_2$) is 1.57% which is low. The total alkali content ($K_2O$ + $Na_2O$) is only 0.63% and is well within the limits of specification for ceramic industries. Thus because of the low alkali and alkaline earth oxides and of the higher alumina content, the clay used was ideal as a constituent for the ceramic body.

II.3.2.2 Density

The density of kaolinite under investigation was 2630 kg $m^{-3}$ which is comparable to the theoretical density of ( 2609 kg $m^{-3}$) of kaolinite computed from the structure.

II.3.2.3 Thermogravimetric analysis

The TG curve for the clay is presented in Fig.II.2. The initial

Table II.1: Chemical analysis of the kaolinite under investigation

| Constituent | Percentage content |
|---|---|
| $SiO_2$ | 46.02 |
| $Al_2O_3$ | 37.30 |
| $Fe_2O_3$ | 0.90 |
| $TiO_2$ | 0.67 |
| MgO | 0.28 |
| CaO | Trace |
| $K_2O$ | 0.45 |
| $Na_2O$ | 0.18 |
| LOI | 14.20 |

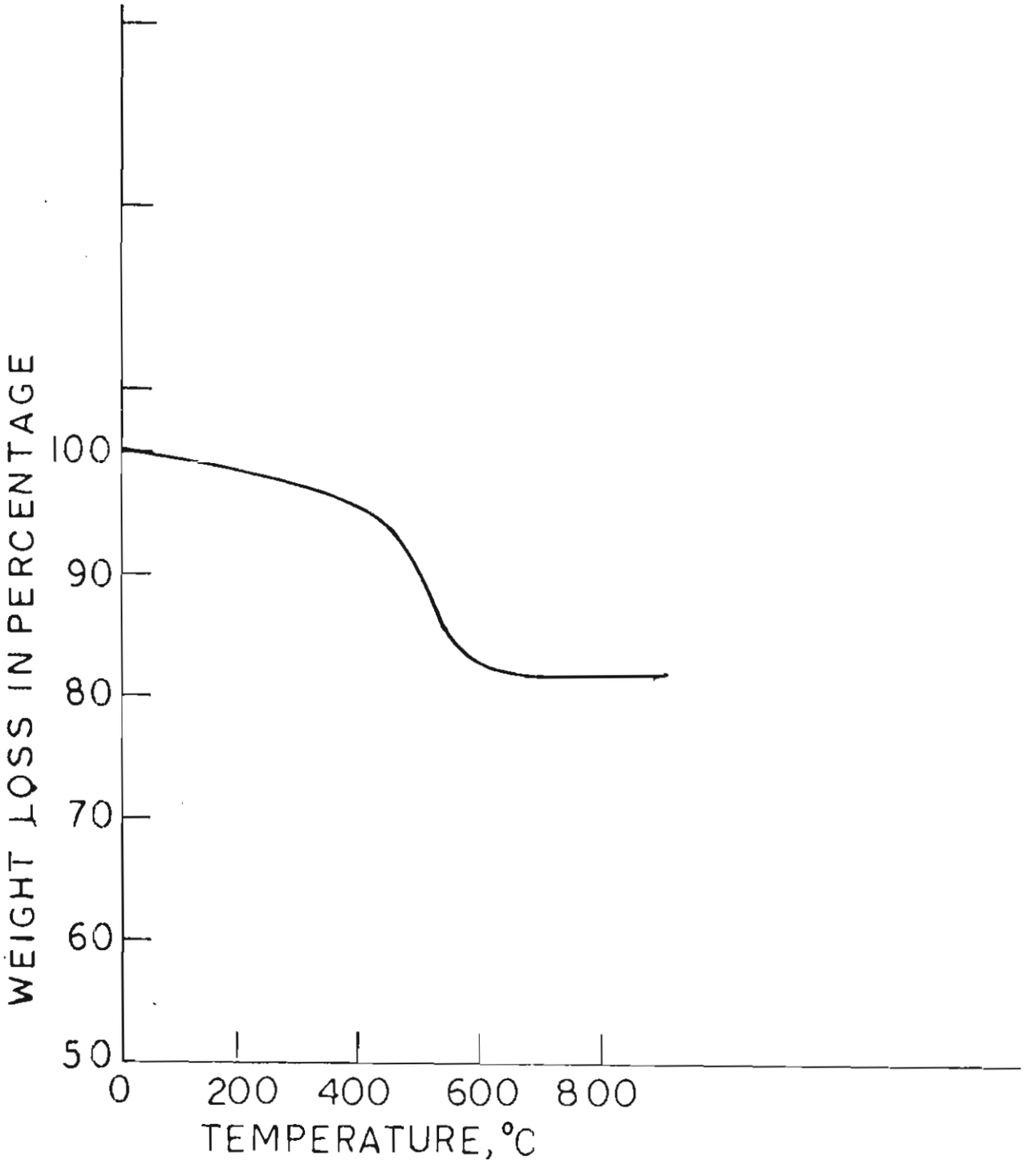


Fig. II.2 T G curve for the kaolinite (W C)

weight loss is due to the loss of physically adsorbed water. The percentage weight loss of 13.6% in the range of 500-630°C comparable to the theoretical loss of 13.9% is essentially due to the dehydroxylation of the clay and the formation of the metakaolinite[83,105,106]. The closer values between the theoretical and observed loss shows that the clay under investigation is high in kaolin content.

II.3.2.4 Differential thermal analysis

DTA of the kaolinite is shown in Fig.II.3. The three characteristic peaks are

(a) Endothermic peak at 110°C due to the removal of adsorbed water

(b) Endothermic peak at 590°C due to the dehydroxylation of the structural water[105,106]. The removal of hydroxyls take place from 450 to 700°C, the temperature varying from one type of kaolinite to another and this variation can be explained by a variation of the size of the particles[83]. But this variation may also be caused by the degree of crystallisation because more feebly crystallised kaolinite losses hydroxyls more readily than the well crystallised ones[83]. Thus the higher magnitude and peak temperature in the higher range clearly indicate the probability of a more orderly arrangement of the structural layer of the kaolinite.

(c) Exothermic peak at 975°C due to a structural reorganization indicating the crystallization of spinel/premullite. The exothermic effect is also different in shape and temperature for well crystallised varieties as compared to the more feebler ones. When kaolinite is feebly crystallized, the exothermic effect is less

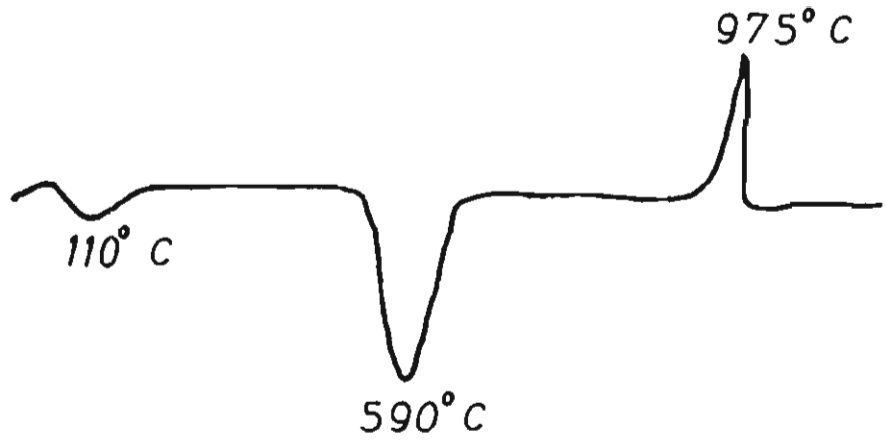


Fig. II.3 DTA curve of WC

intense, taking place in a broad temperature range[83]. The nature of the endothermic and exothermic peaks suggest the higher degree of crystallinity of the clay under investigation.

In fact, kaolin with a formula $Al_2O_3 \cdot 2\ SiO_2 \cdot 2\ H_2O$ undergoes thermal decomposition as follows

$$6\ (Al_2O_3 \cdot 2\ SiO_2 \cdot 2\ H_2O) \xrightarrow[-12\ H_2O]{450\text{-}700^{\circ}C} \underset{\text{Metakaolin}}{6\ (Al_2O_3 \cdot 2\ SiO_2)}$$

$$\xrightarrow[-3\ SiO_2]{900\text{-}1000^{\circ}C} \underset{\text{Spinel}}{3\ (2\ Al_2O_3 \cdot 3\ SiO_2)} \xrightarrow[-5\ SiO_2]{1350^{\circ}C} \underset{\text{Mullite}}{2(3\ Al_2O_3 \cdot 2\ SiO_2)} \qquad \text{(II.1)}$$

At higher temperature ( $>$ 1300°C) spinel transforms to mullite.

II.3.2.5 Particle size distribution

The result of the particle size analysis is given in Fig.II.4 and Table II.2. The clay used is very fine with average particle size of 0.25 microns.

II.3.2.6 Surface area analysis

The surface area of the clay under investigation is found to be 15 $m^2\ g^{-1}$. Specific surface area is not a characteristic of any particular clay mineral, since it varies with particle size distribution and particle shape.

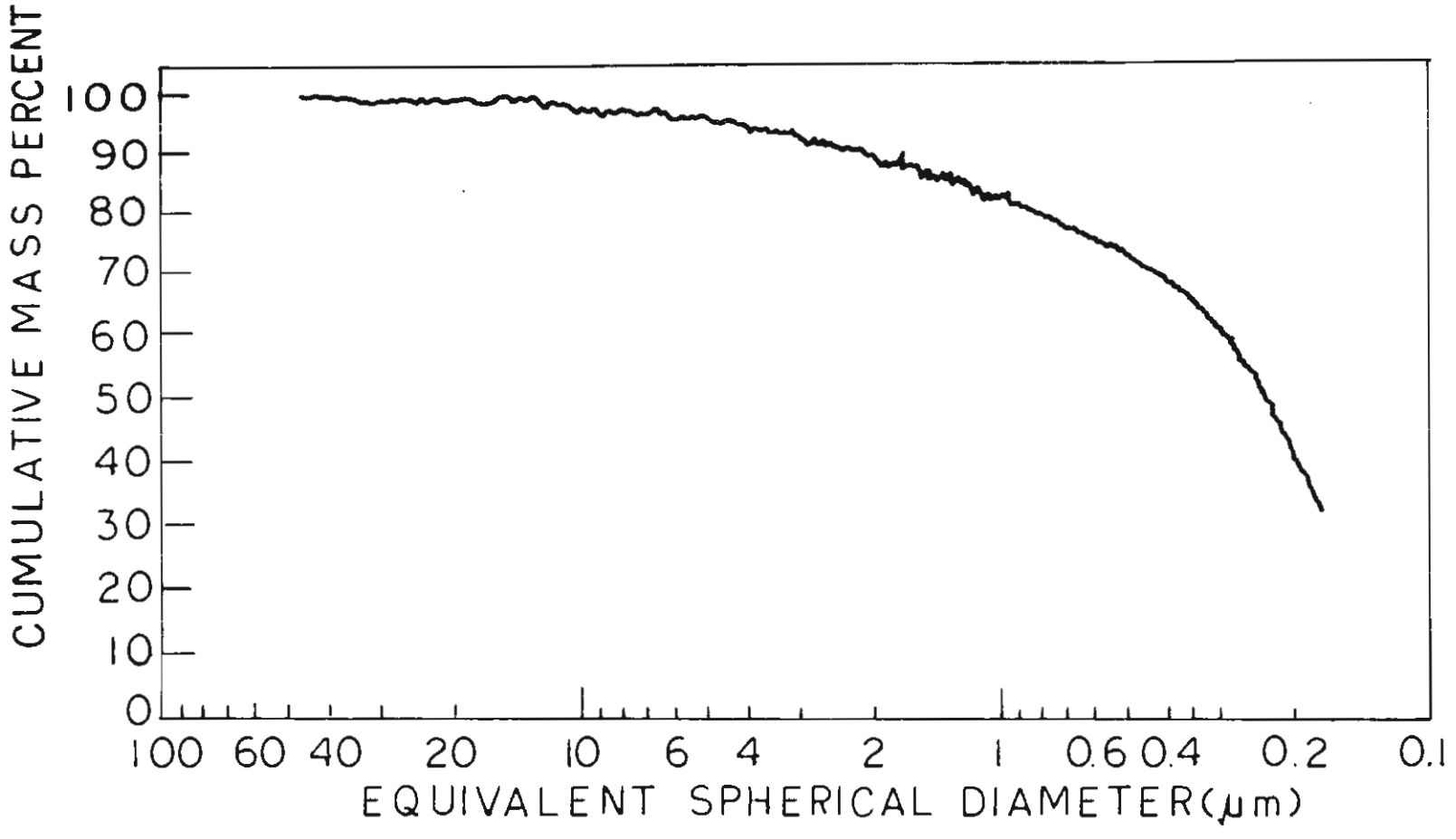


Fig.II.4.Particle size analysis of Washed Clay (WC)

Table II.2: Particle size distribution of the kaolinite clay used

| Particle size (microns) | Percentage |
|---|---|
| < 20 | 100 |
| < 10 | 100 |
| < 5 | 98 |
| < 2 | 92 |
| < 1 | 85 |
| <0.5 | 76 |
| Average particle size (APS) | 0.25 microns |

II.3.2.7 Electron microscopy

Fig.II.5 shows the SEM photograph of the kaolinite. From the micrographs the hexagonal six sided platy structure which is characteristic of kaolinite clay is clearly evident. The kaolinite used in the experiments is relatively of ordered structure and also highly laminated. The degree of crystallinity of the clay used is very high.

Fig.II.6 shows the transmission on electron micrograph showing the flaky nature of kaolinite.

II.3.2.8 X-ray diffraction (XRD) studies

The x-ray diffraction pattern of the kaolinite clay is given in Fig.II.7. Table II.4 lists interplanar spacings (calculated and observed). The x-ray pattern of well ordered kaolinite is featured by a number of well marked lines at 7.164 $A^{\circ}$ , 4.31 $A^{\circ}$, 3.57 $A^{\circ}$, 2.34 $A^{\circ}$, 1.99 $A^{\circ}$, 1.66 $A^{\circ}$, and 1.49 $A^{\circ}$ (79,83, 107-117). All these peaks are observed in the clay sample under investigation.

According to Brindley[79], a highly crystalline kaolinite will show well resolved doublet at 4.18 $A^{\circ}$ and 4.13 $A^{\circ}$. It can be seen that this doublet is present in the clay under investigation. Also XRD pattern indicates that the free quartz has been removed during washing.

II.3.2.9 Infrared (IR) spectrum

Fig.II.8 shows the IR spectrum of the kaolinite. The peaks at 3705 and 3630 $cm^{-1}$ are due to the hydroxyl groups[109-118], the ratio of the intensities of these two peaks determines the crystallinity of the clay. If the ratio is of the order of one, the clay is well ordered, if it is 0.25 then it will be a disordered one[118]. In the

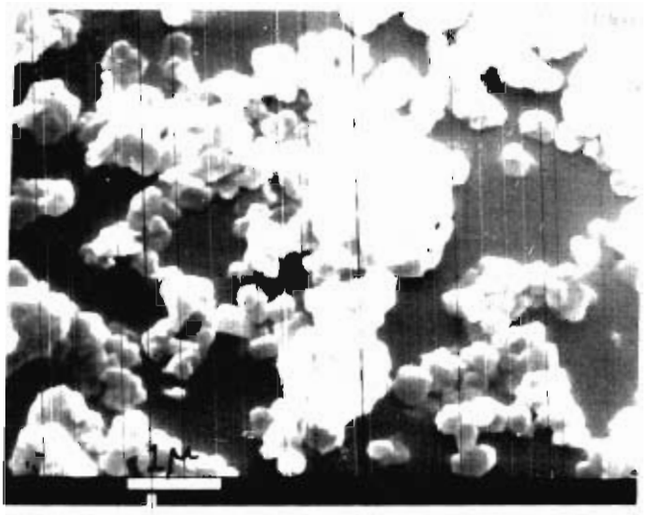

Fig. II.5: Scanning electron micrograph of kaolinite (WC)

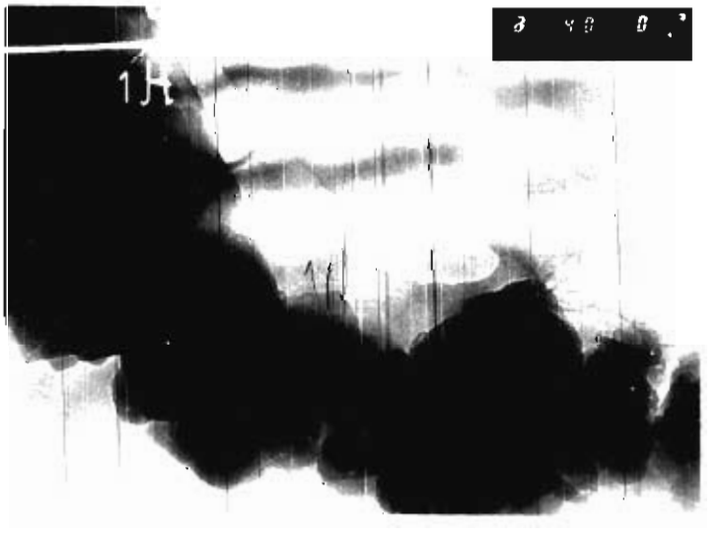

Fig. II.6: Transmission electron micrograph of kaolinite (WC)

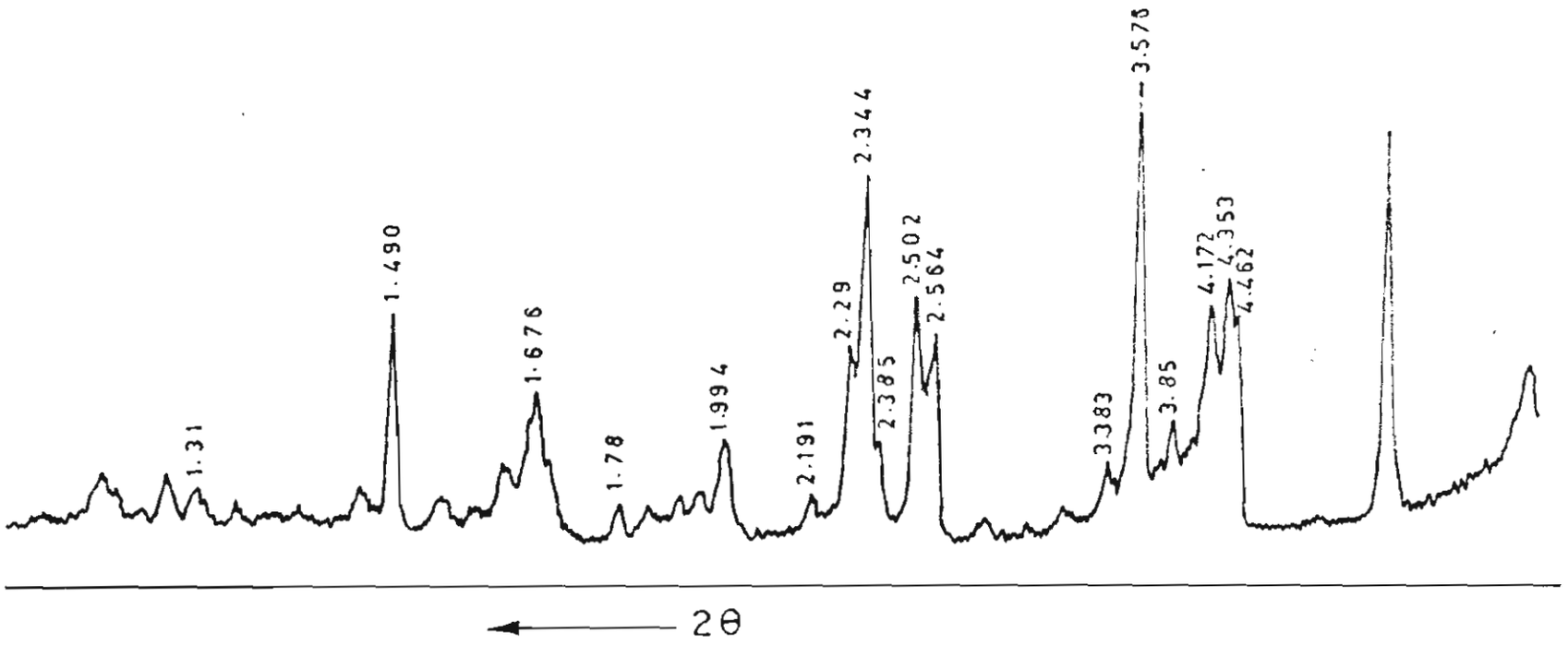


Fig. II.7. XRD pattern of Kaolinite (WC)

Table II.3: X-ray powder data for kaolinite

| Interplanar spacing d $A^{o}$ | Relative intensity $\frac{I}{I_o}$ | $d_{calcu.}$ $A^{o}$ | Miller indices hkl |
|---|---|---|---|
| 7.168 | 9 | 7.150 | 001 |
| 4.462 | 5 | 4.469 | 020 |
| 4.360 | 6 | 4.370 | $1\bar{1}0$ |
| | | 4.332 | 110 |
| 4.172 | 5 | 4.180 | $1\bar{1}1$ |
| 4.130 | | 4.125 | $1\bar{1}\bar{1}$ |
| 3.850 | 3 | 3.849 | $02\bar{1}$ |
| 3.576 | 10 | 3.573 | 002 |
| 2.564 | 5 | 2.566 | $1\bar{3}0$ |
| | | 2.563 | $20\bar{1}$ |
| 2.502 | 5 | 2.500 | $1\bar{3}\bar{1}$ |
| | | 2.490 | 200 |
| | | 2.483 | 112 |
| 2.385 | 2 | 2.383 | 003 |
| 2.344 | 8 | 2.342 | $20\bar{2}$ |
| | | 2.341 | $1\bar{3}1$ |
| 1.994 | 2 | 1.994 | $20\bar{3}$ |
| | | 1.989 | $1\bar{3}2$ |
| 1.787 | 1 | 1.786 | 004 |
| 1.676 | 3 | 1.687 | $24\bar{1}$ |
| | | 1.666 | $20\bar{4}$ |
| 1.490 | 5 | 1.490 | 060 |
| | | 1.487 | $33\bar{1}$ |
| | | 1.486 | $33\bar{1}$ |

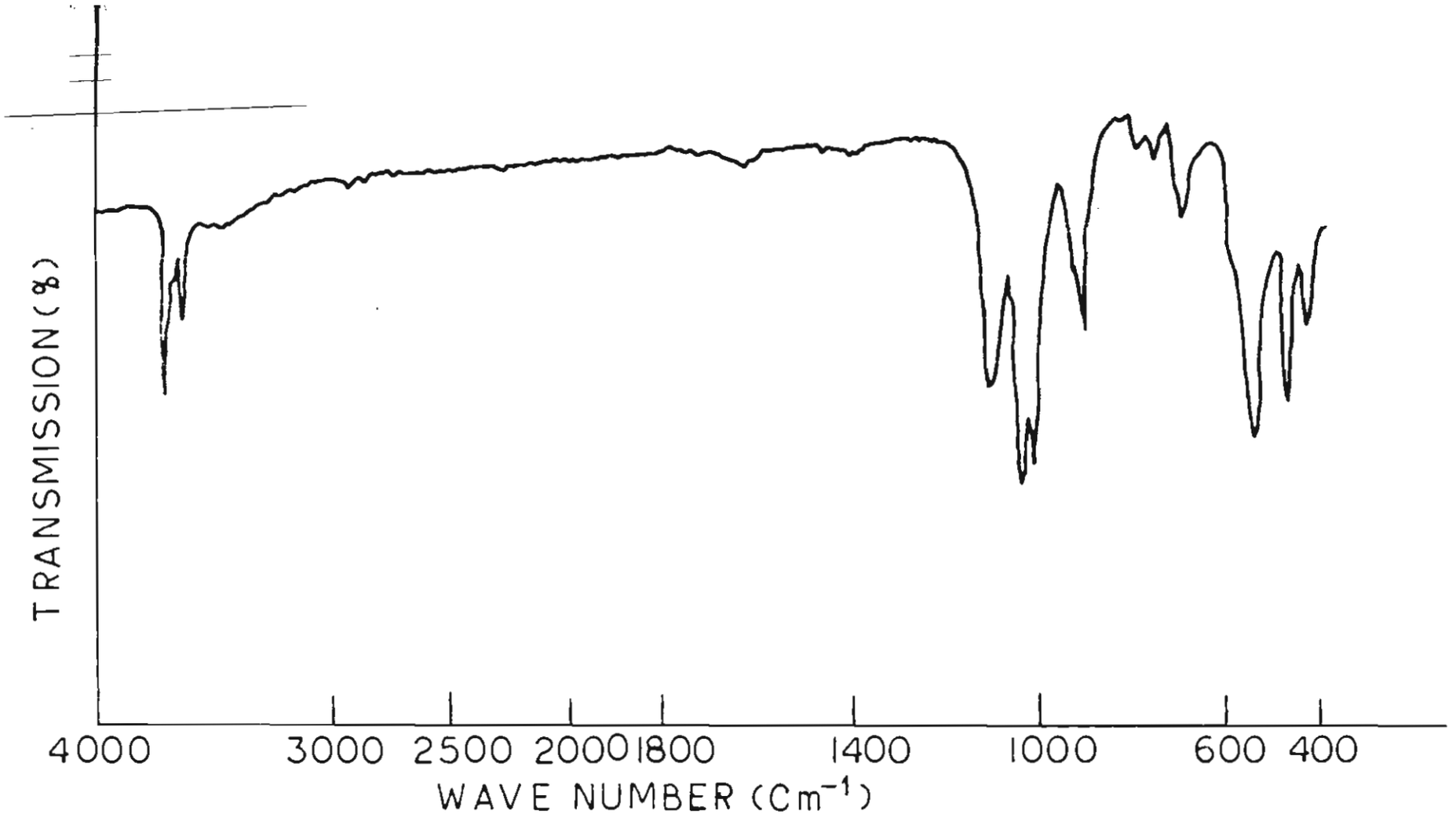


Fig. II.8 I R spectra of kaolinite (W C)

present case the ratio is of the order of 0.8 which is near to one.

The absorption bands between 1150 to 400 $cm^{-1}$ are due to lattice vibration[119-123]. The bands at 1105, 1027 and 1005 are due to (Si-O) stretching vibrations. The band at 1105 $cm^{-1}$ due to (Si-O) stretching vibrations (opical oxygen), the large band at 1027 $cm^{-1}$ is due to (Si-O) combined stretching and bending vibrations (basal oxygen). The presence of band at 1120 and 925 $cm^{-1}$ are also an indication of the ordered clay and are due to Al-(OH) vibrations[119]. The small peak at 830 $cm^{-1}$ is due to Si-O-Al vibrations. The peaks below 550 $cm^{-1}$ are due to metal-oxygen stretching or Si-O bending vibrations.

II.3.2.10 Dielectric properties

Fig.II.9 shows the frequency variations of dielectric constant (k) and dielectric loss ($\tan\delta$) of WC at room temperature. It can be seen that both k and $\tan\delta$ values are considerably frequency dependent having larger values at lower frequencies, they attain frequency independent values beyond $10^5$ Hz. This observation is similar to other layer and double chain silicate minerals[104, 124-128]. The k value of 2.8 at a frequency of $10^6$ Hz agrees with the one reported by Bhattacherjee for kaolinite[104].

The properties of the dielectric materials can be explained by the extent of electric polarisation. Different types of polarisations are electronic, ionic and orientation polarisation of dipoles present. It is well known that when a solid is placed in an electric field, the movement of charge carriers and their accumulation at the interfaces of the sample and electrodes in addition to the various types of polarisations, which display different types of frequency dependence plays a

G/1595

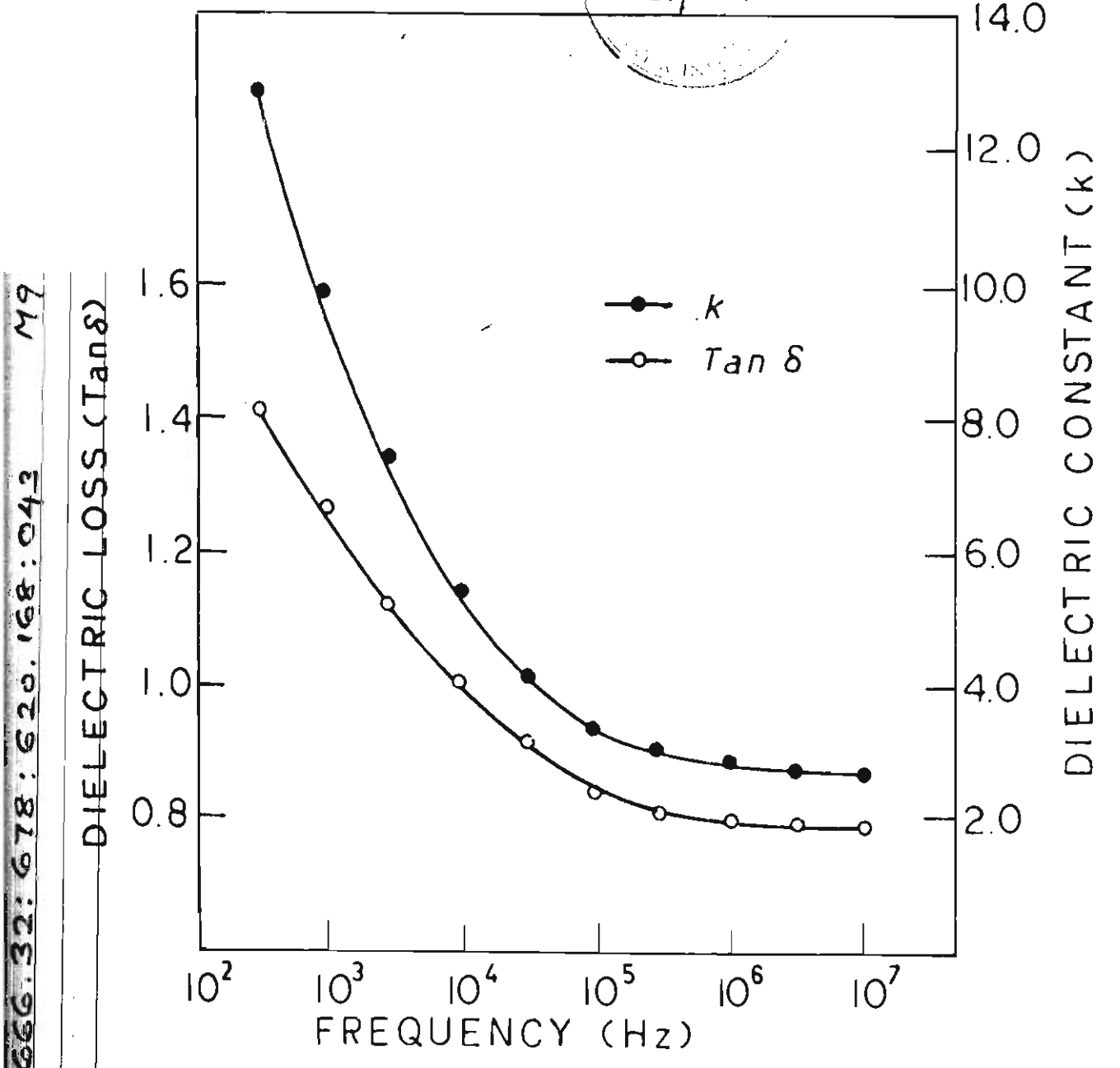


666.32:678:620.168:043 M9

Fig. II.9 Variation of dielectric loss (tanδ) and dielectric constant (k) with frequency of WC at room temperature

dominant role in deciding the nature of dielectric constant and loss. In fact, the variations of k and tan $\delta$ with frequency will be indicative of the type of polarisation operative in the sample. Also different types of water present in the clay samples play significant role in controlling their electrical properties. The appreciably high values of k and tan $\delta$ at lower frequencies and at room temperature can very well be attributed to the dipolar and space charge polarisation due to the presence of free charge carriers, inherently present in the sample (such as water molecules and impurity ions) which follow the electric field that is applied and pile up at the surface of the crystal or at major defect regions inside the sample. Such accumulation of the charge carriers leads to a barrier whose height is a measure of the trapped charge carrier concentration. The capacity of the sample consequently increases with increase in height of the barrier which in turn increases the dielectric constant of the sample. However, at higher frequencies both space charge and dipolar polarisation becomes practically inappreciable[104]. This is so because as the contribution of space charge polarisation to k and tan $\delta$ is inversely proportional to the frequency, the rate of variation of k and tan $\delta$ are less at higher frequencies compared to that of lower frequencies.

## II.4 DEHYDROXYLATION OF KAOLINITE

The dehydroxylation of kaolinite as observed from the thermal analysis of kaolinite (Fig.II.3) takes place around 550°C where essentially the water in the lattice is removed. Hence kaolinite is heated to 650°C which is slightly above the dehydroxylation temperature.

II.4.1 Experimental

About 10 g of washed clay (WC) (Section II.4) was calcined at 650°C for 5 hr . This is abbreviated as MK.

II.4.1.1 Methods

The instrumental methods are as in Section II.3.1.2.

II.4.2 Results and discussion

II.4.2.1 Differential Thermal Analysis (DTA)

DTA curve of MK presented in Fig.II.10 shows a small endothermic peak at 110°C which is due to the adsorbed water. The endothermic peak at 590°C present in the kaolinite is absent in MK because of the decomposition occurred during thermal treatment. The exothermic peak at 975°C in kaolinite is present in MK at the same temperature.

II.4.2.2 Surface area

BET surface area of MK is found to be 14 $m^2 g^{-1}$. A small decrease in surface area is observed after decomposition at 650°C in line with the observation made by Petro et al[129] and it is probably due to the simultaneous dehydroxylation of kaolinite and formation of metakaolinite.

In general when kaolinite decomposes, the water loss occurs more or less uniformly from all unit cells with a decrease in the number of oxygen atoms per unit cell. This may lead to a partial collapse of the silicate layer, thereby explaining the small decrease in textural parameters.


Fig. II.10 DTA curve of MK

II.4.2.3 Electron microscopy

SEM photograph of MK presented in Fig.II.11 shows that it retains the hexagonal pattern of kaolinite to some extent (with an average particle size of 0.75 $\mu$ ) although the original hexagonal plate like structure is distorted.

Fig.II.12 presents the transmission electron micrograph of MK. It can be seen that on heating to 650$^{o}$C, kaolinite acquired an agglomerated structure with an average particle size of about 0.75 $\mu$.

II.4.2.4 X-ray Diffraction (XRD) studies

XRD of MK is shown in Fig.II.13. It does not show any powder pattern, because of the lack of crystallinity.

II.4.2.5 IR Spectra

IR spectrum of MK is given in Fig.II.14. The spectrum is not sharp in the region of OH possibly due to the collapse of the gibbsite and silica layers by the dehydroxylation process. Further, the bands in the range 1100-400 $cm^{-1}$ are broad and diffuse because of the collapse of the Si-O and Al-OH linkages. The strong absorption bands at 1100, 1027 and 915 $cm^{-1}$ in kaolinite (Fig.II.7) are replaced by a single broad band at 1030 $cm^{-1}$.

II.4.2.6 Dielectric properties

Fig.II.15 gives the frequency variations of k and tan $\delta$ of MK. It can be seen that with frequency, both k and tan $\delta$ are found to decrease, but the amounts of decrease here are not that steep

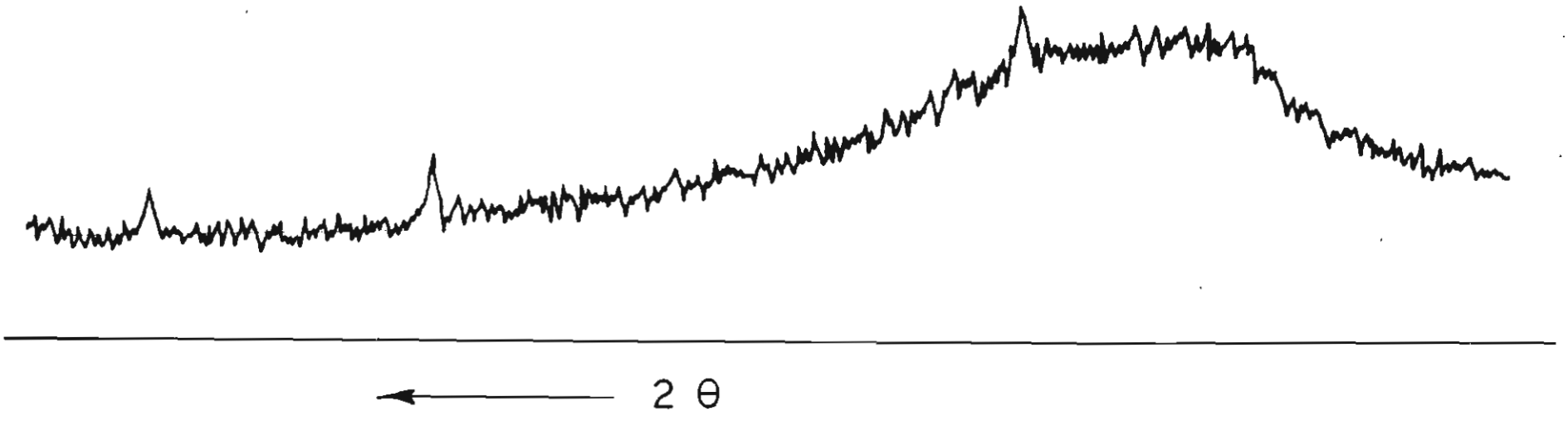


Fig. II.13 XRD pattern of MK

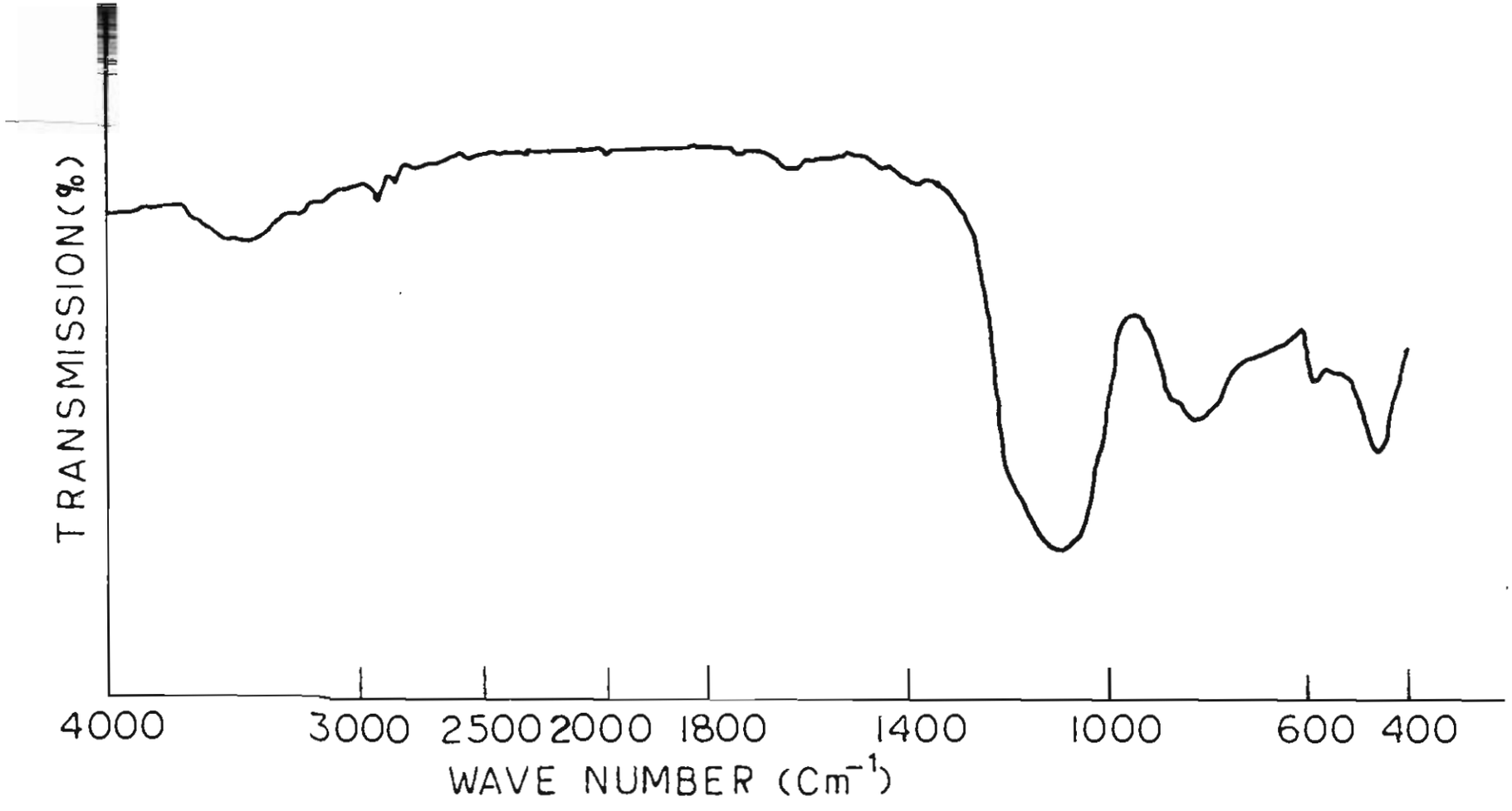


Fig. II.14 IR spectrum of MK

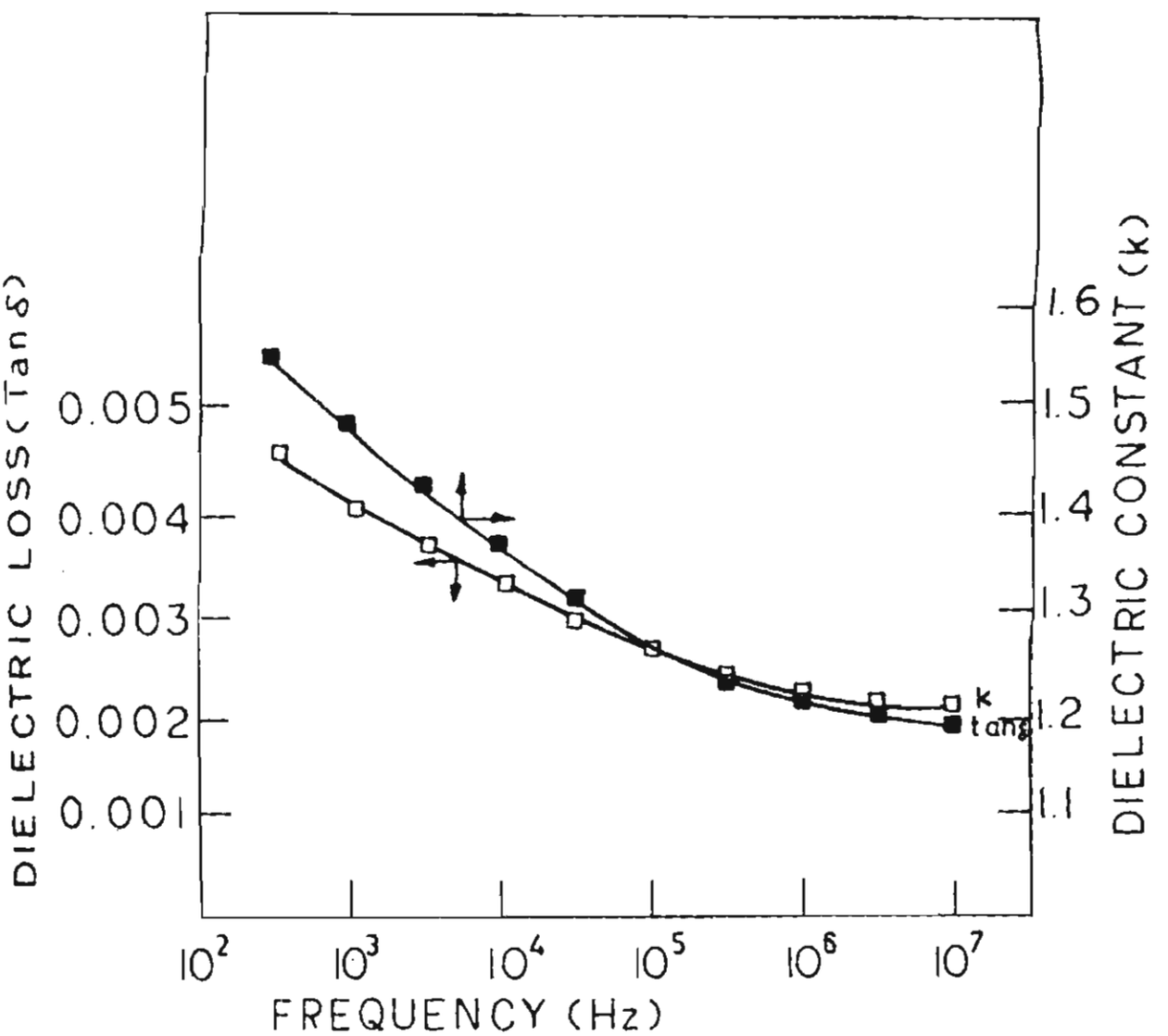


Fig. II.15. Variation of dielectric loss (tan δ) and dielectric constant (k) with frequency of MK at room temperature

as in the kaolinite clay (Fig.II.9) because of the prior removal of the hydroxyl groups.

## II.5 INFORMATION GAP IN DEHYDROXYLATION OF KAOLINITE

The kaolinite under investigation is pure and has a high order of crystallinity as seen from infrared spectrum as well as from XRD. Information can be generally obtained on the dehydroxylation of kaolinite from data on infrared spectrum and thermal analysis. The XRD pattern however, exhibits a non-crystalline feature. Heat treatment of kaolin in the range 550°C-650°C definitely undergoes dehydroxylation. However, recent studies have shown[101] doubtlessly that simple heat treatment in the above range of temperature results only in partial dehydroxylation, although speculative studies were reported much earlier. Possibly the absence of suitable method for identifying exactly the extent of dehydroxylation was one of the reasons for this.

The thermal decomposition-hydration-redecomposition sequence investigated in the present work has shown evidence of a metakaolinite with increased surface area and dielectric property, thus indicating the possibility of formation of a modified metakaolinite. This has been further investigated using the solid state NMR and Raman spectral data within the limits of available information in view of the recent application of these tools in the study of dehydroxylation of kaolinites. Since increased surface area and surface dehydroxylation of kaolinite are essential requirements for better compatibility with polymer matrices in general, attempt has been made to incorporate the surface modified kaolinite in selected polymers and to evaluate the improvement in mechanical as well as electrical properties of the composites over those of kaolinite incorporated composites.

# C H A P T E R III

## SURFACE MODIFICATION OF THE KAOLINITE

# CHAPTER III

## SURFACE MODIFICATION OF THE KAOLINITE

### III.1 INTRODUCTION

This Chapter describes the surface modification of kaolinite by a thermal decomposition hydration - redecomposition treatment, as reported for talc-magnesite and serpentine-magnesite[130,131]. This treatment involves heating of kaolinite at a moderately high temperature followed by rehydroxylation and decomposition at a lower temperature under vacuum. An attempt has been made to characterise the product by using solid state NMR and Raman Spectra since the conventional techniques such as XRD and IR cannot probably explain its characteristics.

### III.2 EXPERIMENTAL

#### III.2.1 Preparation of the surface modified kaolinite

About 10 g of the washed clay (WC) (Section II.3.1.1) was calcined at 650°C at a heating rate of 200°C/hr for 5 hr to metakaolinite (MK). It was then immersed in cold water at room temperature under vigorous stirring. It is dried at 110°C in an air oven for 16 hours. Redecomposition of the hydroxylated product was performed in a tube furnace at 450°C (VT) at a heating rate of 200°C/hr for 4 hr under vacuum.

#### III.2.2 Methods

The DTA, IR surface area, XRD and electron microscopy studies were carried out on the sample as discussed in Chapter II.

III.2.2.1 Raman spectra

Raman spectra was recorded with a Spex Ramalog instrument using the 4880 A line of a spectra physics 165 $Ar^+$ laser for excitation.

III.2.2.2 Solid state NMR

Solid state magic angle spinning NMR spectra of samples were obtained on a XL 200 Varian Spectrophotometer at magic angle spinning speeds upto 2600 rps.

III.3 RESULTS AND DISCUSSION

III.3.1 Differential thermal analysis (DTA)

DTA curve of VT shown in Fig. III.1 gives a small endothermic peak at 110°C which is due to the adsorbed water. The endothermic peak at 590°C in kaolinite is absent in VT as in MK. The exothermic peak at 975°C in the kaolinite present in MK at the same temperature (Figs. II.3 and II.10), has been shifted down to 940°C in the case of VT. The shift in this peak showed the possible increase in thermal reactivity of VT.

III.3.2 Surface area

BET surface area of VT is found to be 29 $m^2\ g^{-1}$. It is almost double that of kaolinite (Section II.3.2.6).

The kaolinite type of clays decomposed with a limited degree of shrinkage such that during dehydration, partial rehydroxylation takes place[129] i.e., water is forced between the dehydroxylated layers. This dehydrated product will be stable and will resist collapse upon heating at 450°C. This mechanism could explain the marked


Fig. III. 1 D T A curve of V T

increase in surface area of the specifically treated powder.

III.3.3 Electron microscopy

Fig. III.2 is scanning electron microphotograph of VT showing the distorted structure of VT with surface porosities. To some extent VT also retains the hexagonal plate like structure of kaolinite. But it should be noted that the tendency of retention of the kaolinite structure is less in VT compared to that of MK (Fig. II.11).

Fig.III.3 shows the transmission electron micrograph of VT particles. Here deagglomeration of MK to fines of average particle size 0.45 $\mu$ is found to take place.

III.3.4 X-ray diffraction (XRD)

XRD of VT shown in Fig. III.4 is similar to that of MK (Fig.II.13). It also does not show any powder diffraction pattern due to the lack of crystallinity.

III.3.5 IR Spectra

IR spectrum of VT (Fig.III.5) is broad and diffused as that of the MK (Fig. II.14).

III.3.6 Raman spectra

Fig. III.6 shows the Raman spectra of WC, MK and VT while Table III.1 shows the band positions of OH stretching region in the Raman spectra of kaolinite, MK and VT.

The Raman spectra of the kaolinite is similar to that of kaolinite reported earlier[132,133]. MK and VT retained the peaks appeared at

Fig. III.2: Scanning electron micrograph of VT

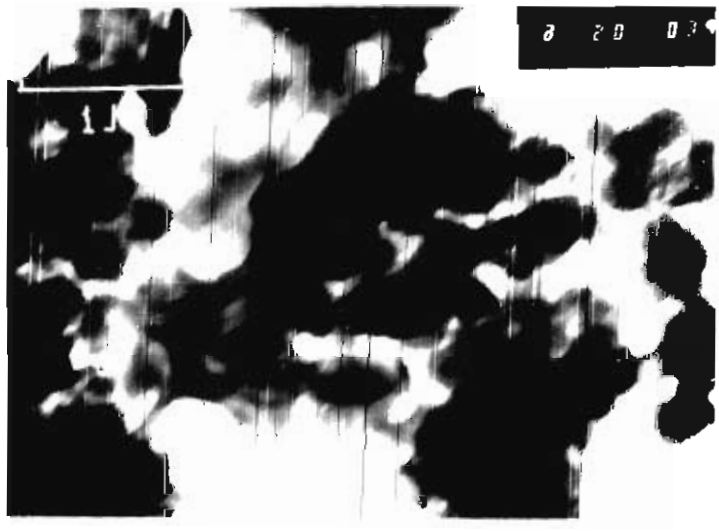

Fig. III.3: Transmission electron micrograph of VT

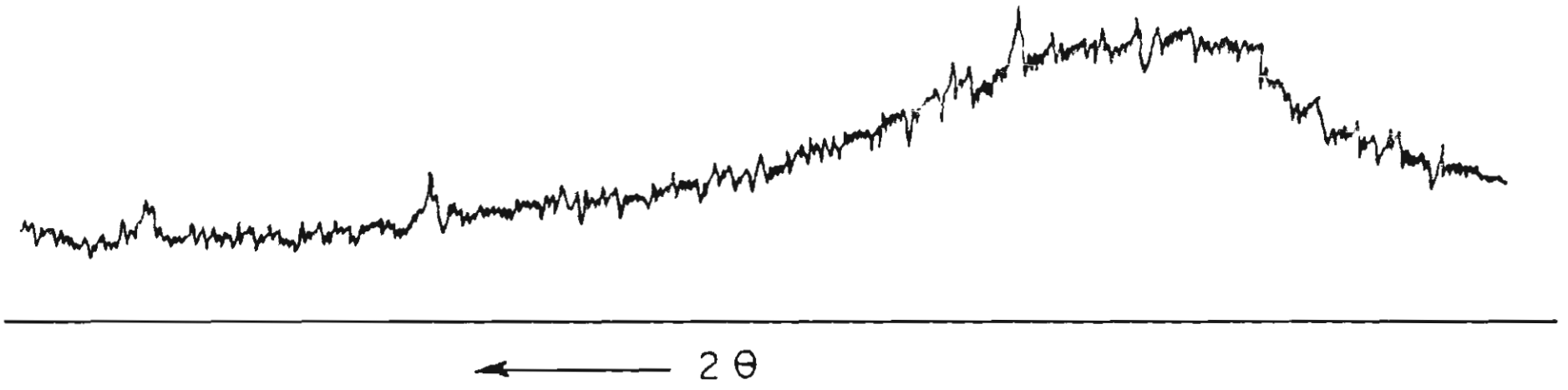


Fig. III. 4 XRD pattern of VT

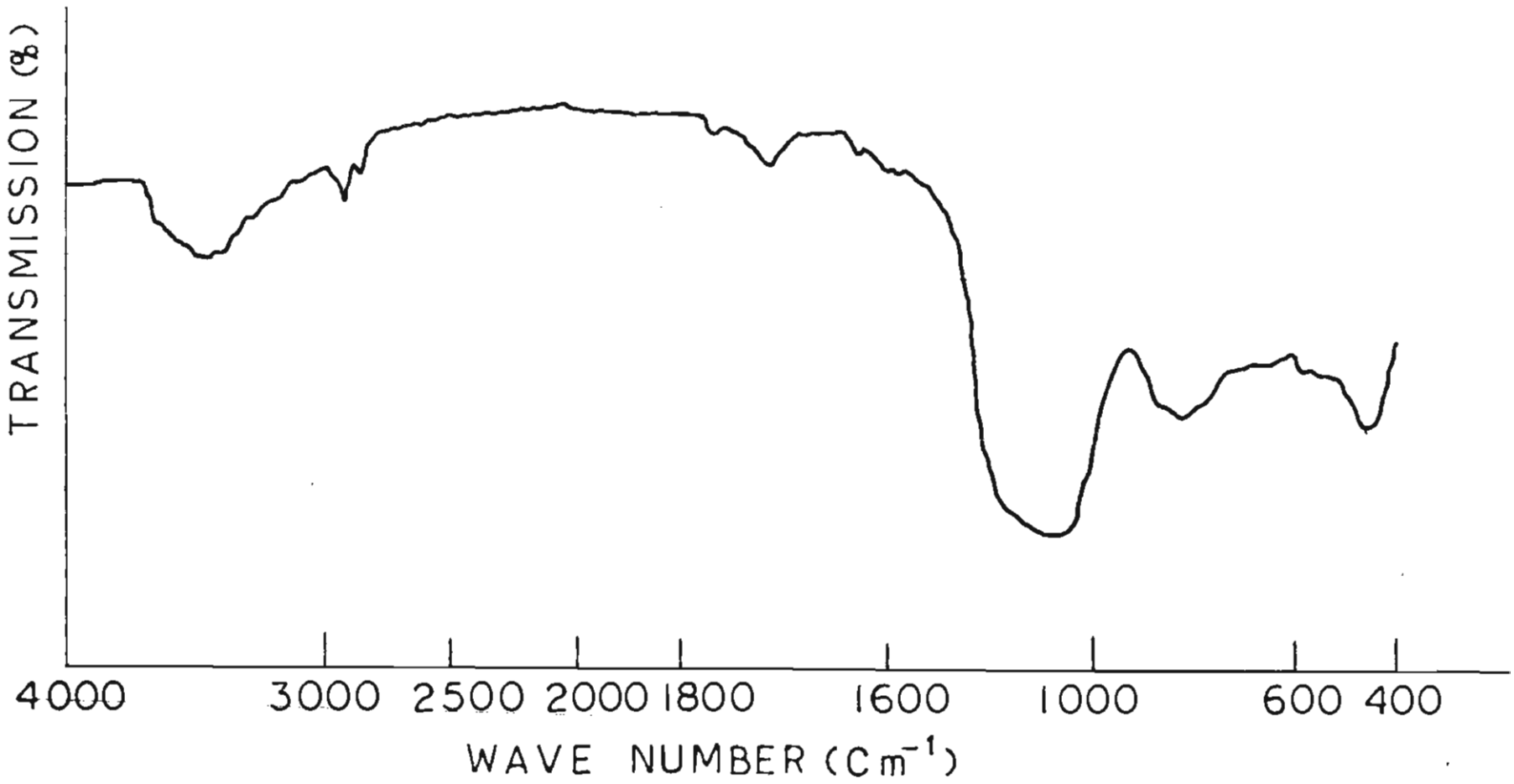


Fig. III. 5 IR spectrum of VT

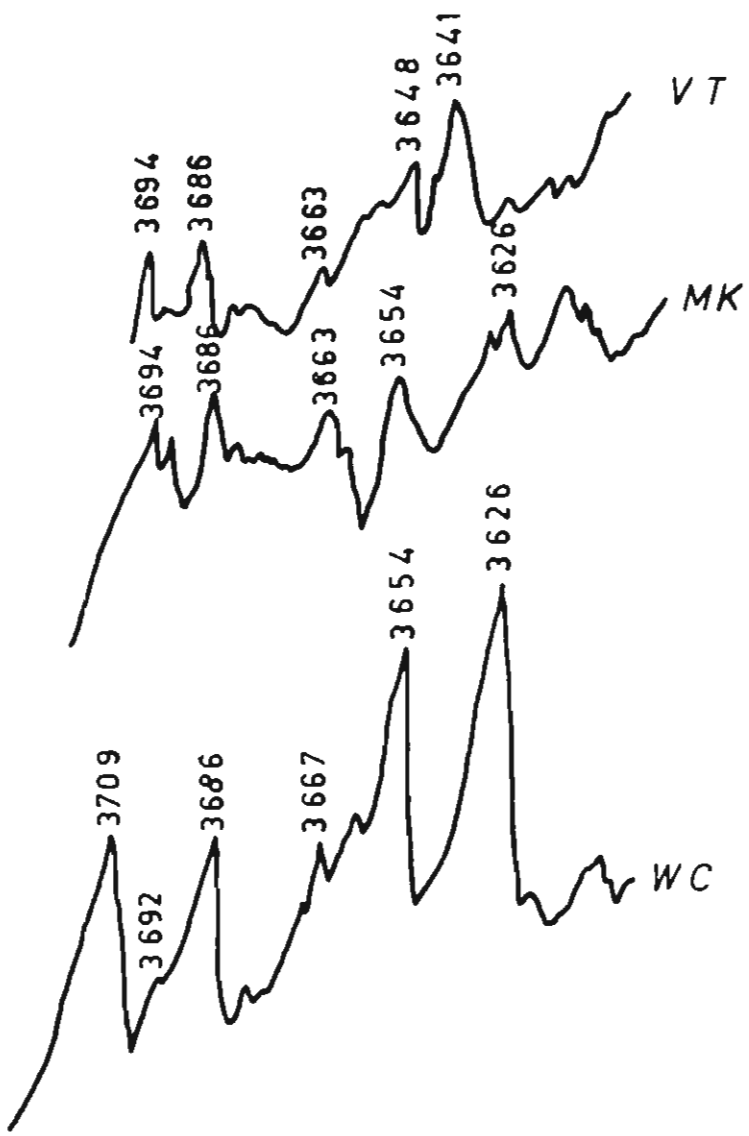


Fig. III.6 Raman spectra of WC, MK and VT in the 3620 – 3775 $cm^{-1}$ region

Table III.1: Band positions ($cm^{-1}$) in the Raman spectra of WC, MK and VT

| WC | MK | VT |
|---|---|---|
| 3692 | 3694 | 3694 |
| 3686 | 3686 | 3686 |
| 3667 | 3663 | 3663 |
| 3654 | 3654 | - |
| 3626 | 3626 | - |

3686 and 3692 $cm^{-1}$ in kaolinite at almost the same positions. There was a slight shift for the 3692 $cm^{-1}$ peak to 3694 $cm^{-1}$ in MK and VT. The peaks at 3626 $cm^{-1}$ and 3654 $cm^{-1}$ in kaolinite although retained in MK are surprisingly absent in VT. This could be a clear evidence for the further removal of hydroxyls which is retained in MK. The reduction in the intensity of the peak at 3667 $cm^{-1}$ and subsequent shift to 3663 $cm^{-1}$ also are indications of the partial removal of the hydroxyls further from metakaolinite as a result of vacuum treatment. However, the peak at 3686 $cm^{-1}$ observed in kaolinite has been retained in MK with reduced intensity and still retained in VT. Reduction of the intensity of this peak indirectly indicates the removal of inner hydroxyls. More detailed Raman studies may bring out a clear cut means of predicting these structures.

III.3.7 Solid state NMR

The $^{29}Si$ NMR spectrum shown in Fig.III.7(A) gives a single sharp resonance at -91.5 PPM relative to tetramethyl silane (TMS) which is in well agreement with the previous results[134], although the peak splitting reported by Barron et al[135] is not observed. The hydrogen bonding present in kaolin results in a separation of $\sim$ 0.7 nm between the aluminium or silicon layers of adjacent sheets, this interlayer hydrogen bonding causes a deshielding in kaolinite. The mean Si-O-Si(Al) bond angle $\theta$ can be calculated from the chemical shift $\delta$ of the silicon resonance using the relation[134]

$$\delta = -176.65 - 55.821 \sec\theta \qquad \text{(III.1)}$$

For kaolinite, the calculated value of chemical shift from the structural

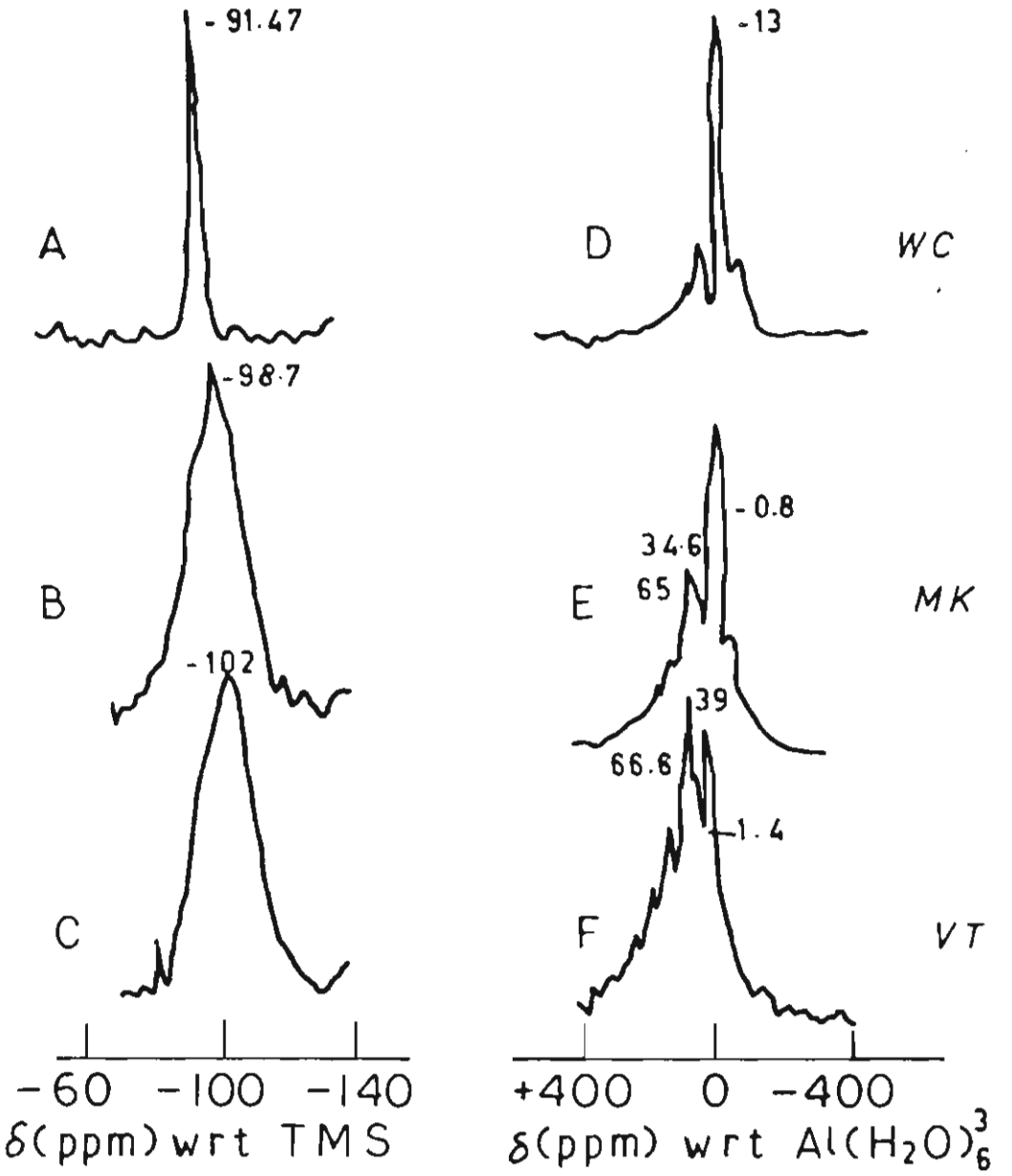


Fig.III.7 High resolution solid state NMR spectra of WC, MK and VT

Spinning speed ≈ 2600 rps

A–C $^{29}Si$ spectra

D–F $^{27}Al$ spectra

data using eqn.III.1 is -90.3. This is in well agreement with the observed shift of -91.5 PPM.

MK shows a single broad resonance centered at about -98.6 PPM with respect to TMS (Fig.III.7(B)). Mackenzie et al[101] reported a similar spectrum for metakaolinite. Metakaolinite retains about 12% of its original hydroxyls, which even after heating to 800°C could not be completely eliminated. The $^{29}Si$ NMR spectrum of VT (Fig.III.7(C)). shows the shift of the broad peak to -102 PPM. This broadening of the peak probably indicates further removal ofhydroxyls from MK.

The $^{27}Al$ NMR spectrum for the kaolinite is given in Fig.III.7(D). The principal resonance at -0.6 PPM is in the expected position for octahedral aluminium coordinated hydroxyl groups. The splitting is due to the presence of more than one silicon site or to the effect of an electric field gradient (efg) at the quadrupolar aluminium nucleus[101].

Figs. III.7(E)&(F) show the $^{27}Al$ NMR spectra of MK and VT. MK shows octahedral aluminium resonance at about -0.8 PPM and tetrahedral signals at about 65 PPM. Additional peak at 34.6 PPM could be detected as reported for metakaolinite[101] and dehydroxylated pyrophyllite by Mackenzie et al[136]. The peak at 65 to 66 PPM is characteristically tetrahedral, the other at 34 to 39 PPM has been reported for dehydroxylated pyrophyllite by Mackenzie et al[136] for which both the Si and Al NMR spectra are remarkably similar to those of metakaolinite.

III.3.8 Dielectric properties

Fig. III.8 gives the frequency variations of dielectric constant (k) and dielectric loss (tan $\delta$) of VT. Both k and tan $\delta$

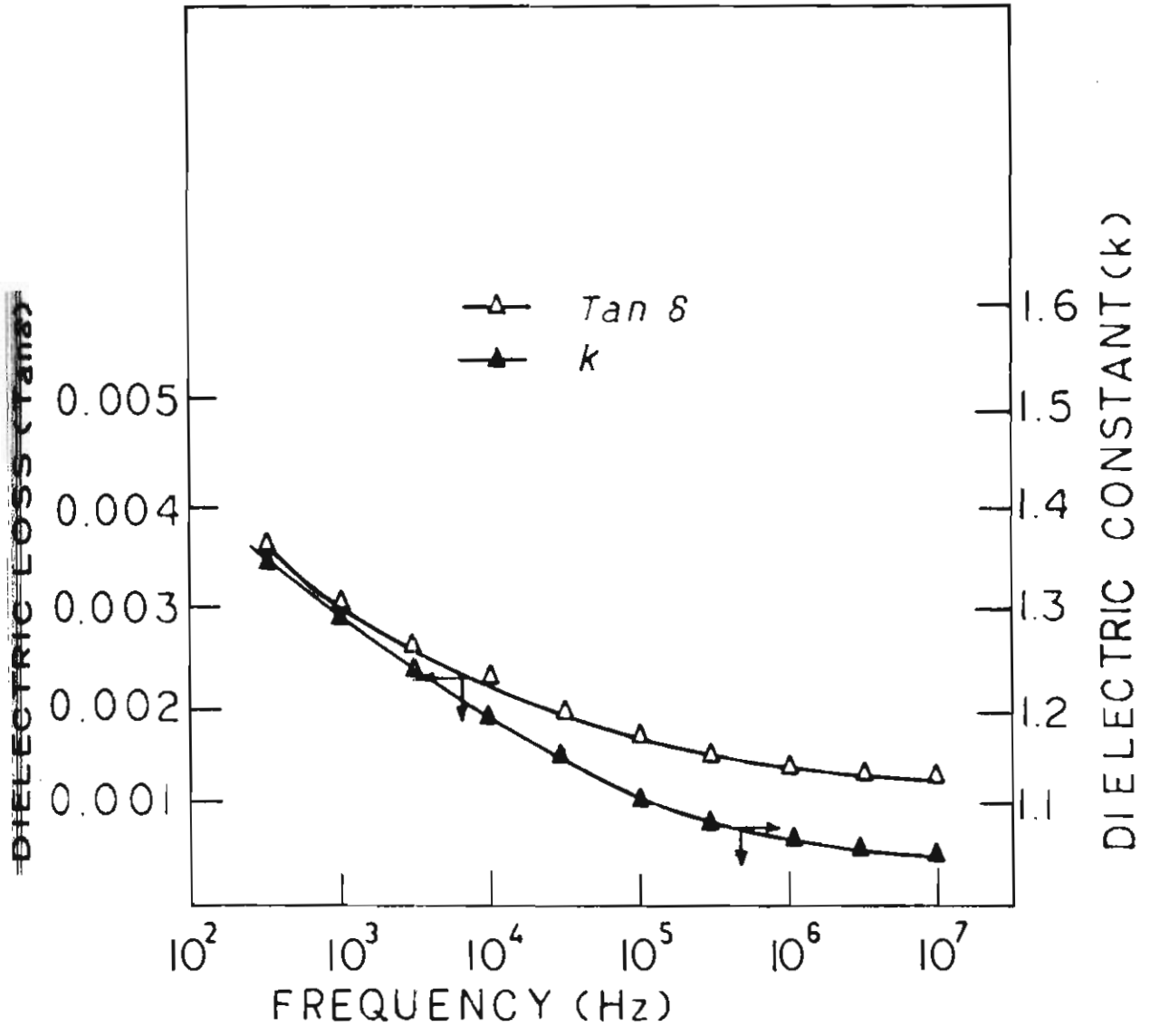


Fig.III.8 Variation of dielectric loss (Tan $\delta$) and dielectric constant (k) with frequency of V T at room temperature.

are found to decrease with frequency. The absolute values of k and tan $\delta$ at frequencies in VT are less than those in MK (Fig. II.15) essentially due to the further removal of hydroxyls from MK by the vacuum treatment, decreasing the dipolar contributions in the range of the experiment.

## III.4 CONCLUSIONS

The observations made from the thermal analysis curve and surface area measurements show that the dehydroxylation followed by vacuum treatment adopted to prepare VT has resulted in a type of metakaolinite with increased activation and surface area characterized by microporosity compared to the metakaolinite prepared by simple calcination. However, IR spectra and XRD of MK and VT could not explain probably the characteristics of these particles. Raman and solid state NMR techniques have been used for detecting the extent of dehydroxylation in vacuum treated clays and have been found to be useful tools in such studies. SEM and TEM studies show the change in size and shape of the particles brought about by the thermal treatments. The decrease in dielectric constant and dielectric loss can be explained based on the stepwise gradual dehydroxylation which could be supported by solid state NMR, Raman and microscopic studies as discussed.

# C H A P T E R IV

## KAOLINITE-POLYMER COMPOSITES

# CHAPTER IV

# KAOLINITE-POLYMER COMPOSITES

## IV.1 INTRODUCTION

Because of the importance of composite materials it becomes increasingly important to study the performance, cost and potential of the available composite materials. In this Chapter, an attempt has been made to study the effect of kaolinite (WC) and the surface modified kaolinite (VT) on the electrical, mechanical and other physical properties of polymeric composites. Polyester, polyethylene and polyvinyl chloride were selected as the matrices since the methods of processing are different such as cold setting, hot extrusion and hot compression molding. Experiments were optimised so as to get appreciably uniform dispersion of the particulates in the various matrices used in the study.

## IV.2 KAOLINITE-POLYETHYLENE COMPOSITES

### IV.2.1 Introduction

Although polyethylene has many desirable properties for commercial uses, they do not possess sufficient rigidity for some application. By incorporating fillers into polyethylene, greater rigidity can be achieved. This section deals with the incorporation of kaolinite and surface modified kaolinite into polyethylene and their effects on physical, mechanical and electrical properties of polyethylene.

IV.2.2 Experimental

IV.2.2.1 Materials

The details of the kaolinite under investigation and the preparation of the surface modified clay have been presented in detail in Chapter II and III respectively. Polyethylene used was low density polyethylene of density 920 kg $m^{-3}$ manufactured by Mehta & Co., Bombay, India.

IV.2.2.2 Preparation

Composites were prepared by an injection molding technique. Weighed quantities of clay and polyethylene (both in the powder form) were mixed thoroughly using a Y-cone blender. The premixed material was heated to plastic flow (at 180$^{o}$C) and injected into the die through a 4 mm diameter extruder. Composites were prepared out of kaolinite (WC) and surface modified kaolinite (VT). Slightly higher temperatures and molding pressures are required for high filler fractions.

IV.2.2.3 Methods (Testing and Evaluation)

IV.2.2.3.1 Density measurement: The densities of the samples were determined by kerosene displacement method.

IV.2.2.3.2 Microscopic studies: Microstructural evaluations were carried out on the polished surface using a JEOL 35C scanning electron microscope.

IV.2.2.3.3 Tensile properties: The tensile properties were determined in accordance with ASTM D 882 - 75 b using an Instron Testing Machine and on ASTM type IV specimens.

IV.2.2.3.4 Abrasive wear measurements: The abrasion test was performed on 16 mm diameter samples in a roller type abrasion tester with a load of 500 g fixed with 220 grit silicon carbide paper. After each test the abrasive paper was replaced with a fresh one so that the sample surface was always in contact with the fresh wear track. Initial weight of the sample and weight of the sample after wear test were taken accurately.

The wear surfaces were examined under scanning electron microscope after the samples were cleaned ultrasonically to free of any abrasive particles sticking to the worn out surfaces.

IV.2.2.3.5 Dielectric measurements: Dielectric measurements were done as in Section II.3.1.2.11.

IV.2.3 Results

IV.2.3.1 Density

Table IV.1 gives the measured and calculated values of the densities of the WC and VT filled polyethylene composites. It can be seen that measured density values are lower in all the cases than the calculated ones. Density of the composites increases with increasing clay content in both cases, with VT incorporated composites having higher values than those incorporated with WC. Also the percentage porosities in WC composites increases with increasing filler fraction (10.9% to 13.2%) whereas it remains almost constant (about 6%) in the case of VT composities in all the cases investigated.

Table IV.1: Density and % porosities of WC and VT filled polyethylene composites

| | WC polyethylene composites | | | | VT polyethylene composites | | | |
|---|---|---|---|---|---|---|---|---|
| | Volume percentage of filler content | | | | Volume percentage of filler content | | | |
| | 5 | 10 | 15 | 20 | 5 | 10 | 15 | 20 |
| Calculated density, kg $m^{-3}$ | 1010 | 1091 | 1176 | 1262 | 1010 | 1091 | 1176 | 1262 |
| Measured density, kg $m^{-3}$ | 900 | 963 | 1025 | 1095 | 948 | 1025 | 1103 | 1183 |
| % Porosity | 10.90 | 11.730 | 12.840 | 13.230 | 6.140 | 6.050 | 6.210 | 6.260 |

IV.2.3.2 Dispersibility

Figs. IV.1a and b show the distribution of WC and VT containing 20 volume percentage in the polyethylene matrix. VT filled composites showed a more uniform dispersion with less agglomeration of dispersoids compared to WC composites. The average particle size in VT composite is 0.54 $\mu$ whereas that in WC composite is 0.3 $\mu$.

IV.2.3.3 Tensile properties

Fig. IV.2 gives the change in tensile modulus with the addition of filler in polyethylene matrix. Modulus in general is found to increase with the filler content. Also, the modulus is high in VT composites compared to WC composites in all ranges of compositions investigated.

Table IV.2 shows the percentage elongation to break of WC and VT filled systems. Elongation is found to decrease with the filler fractions.

Fig. IV.3 shows the change in tensile strength with filler content in WC and VT filled polyethylene. The strength in general is found to decrease with the addition of both WC and VT. However, WC incorporated polyethylene composite showed almost linear decrease from 11.99 MPa at 5% to 6.96 MPa at 20 volume percentage. Further, an addition of 5% reduces the strength of the composite by about 25% while the reduction is only about 15% in the case of VT filled composites under identical conditions of testing. The strength of VT incorporated composites decreases upto 12.93 MPa for 15 volume percentage while the

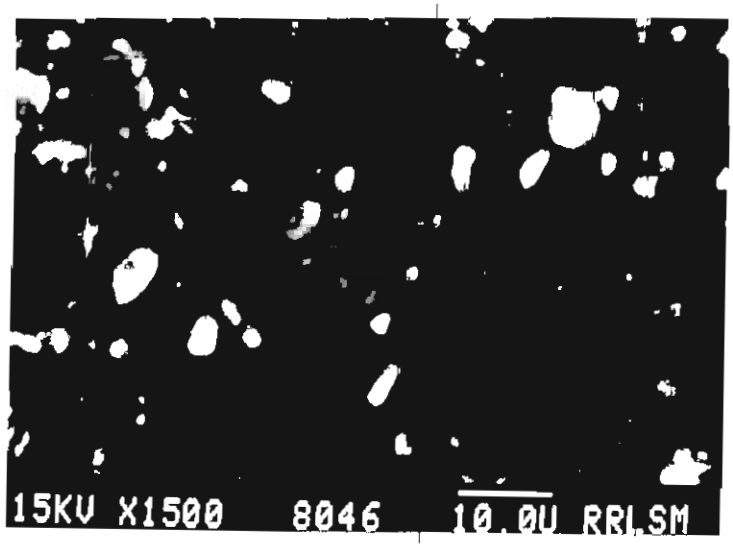


(a)

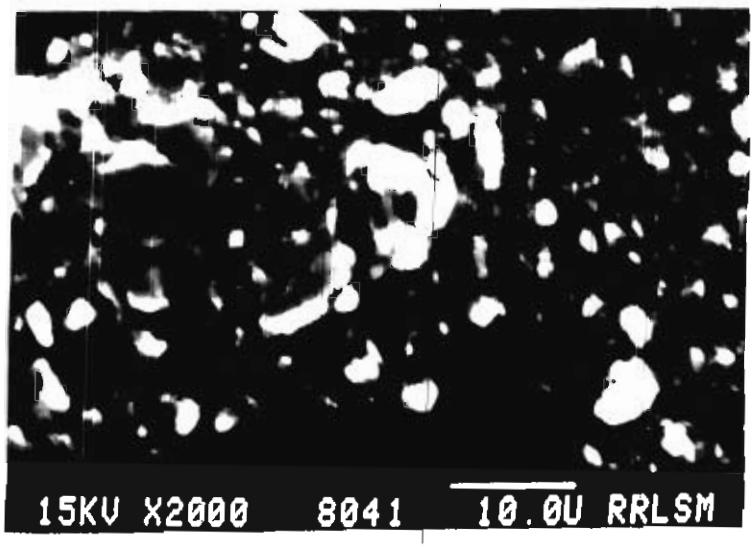


(b)

Fig. IV.1: Scanning electron micrographs of the polyethylene filled with (a) WC (20%), (b) VT (20%)

Table IV.2: Elongation of WC and VT filled polyethylene composites

| Volume percentage of filler content | % Elongation of WC | % Elongation of VT |
|---|---|---|
| 0 | 160 | 160 |
| 5 | 150 | 130 |
| 10 | 138 | 99 |
| 15 | 114 | 76 |
| 20 | 98 | 48 |

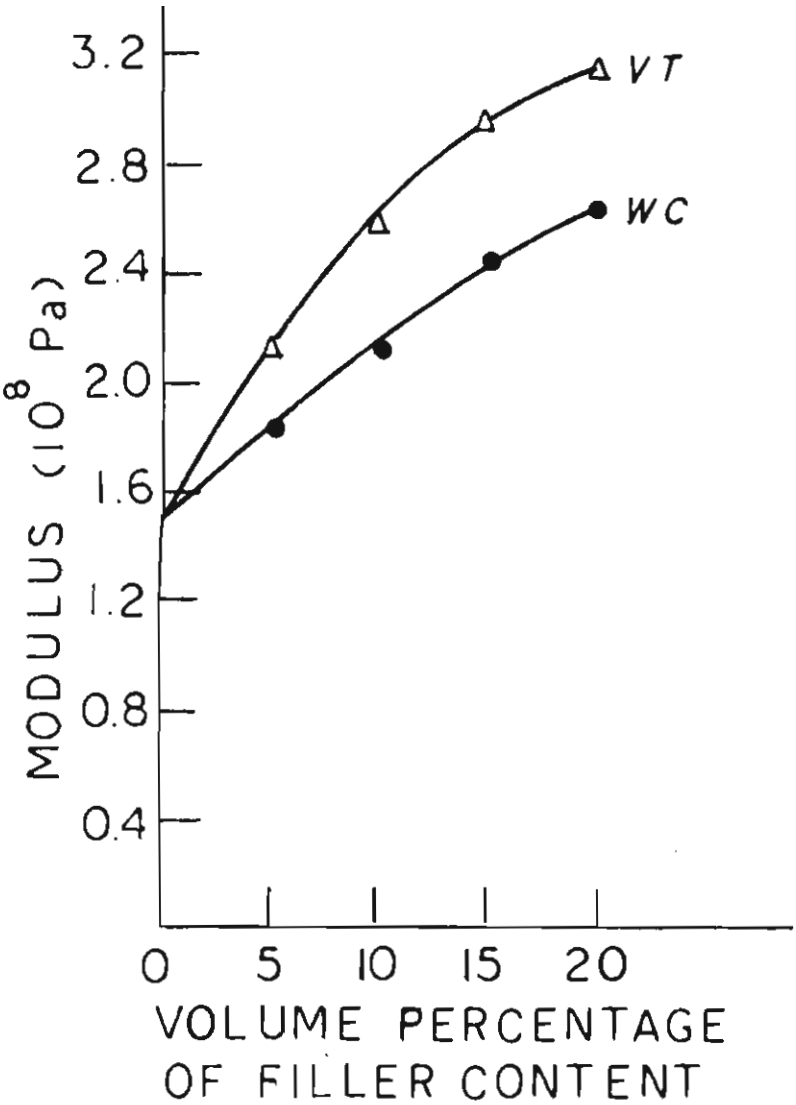


Fig. IV.2 Tensile modulus of WC and VT filled poly ethylene composites with filler content.

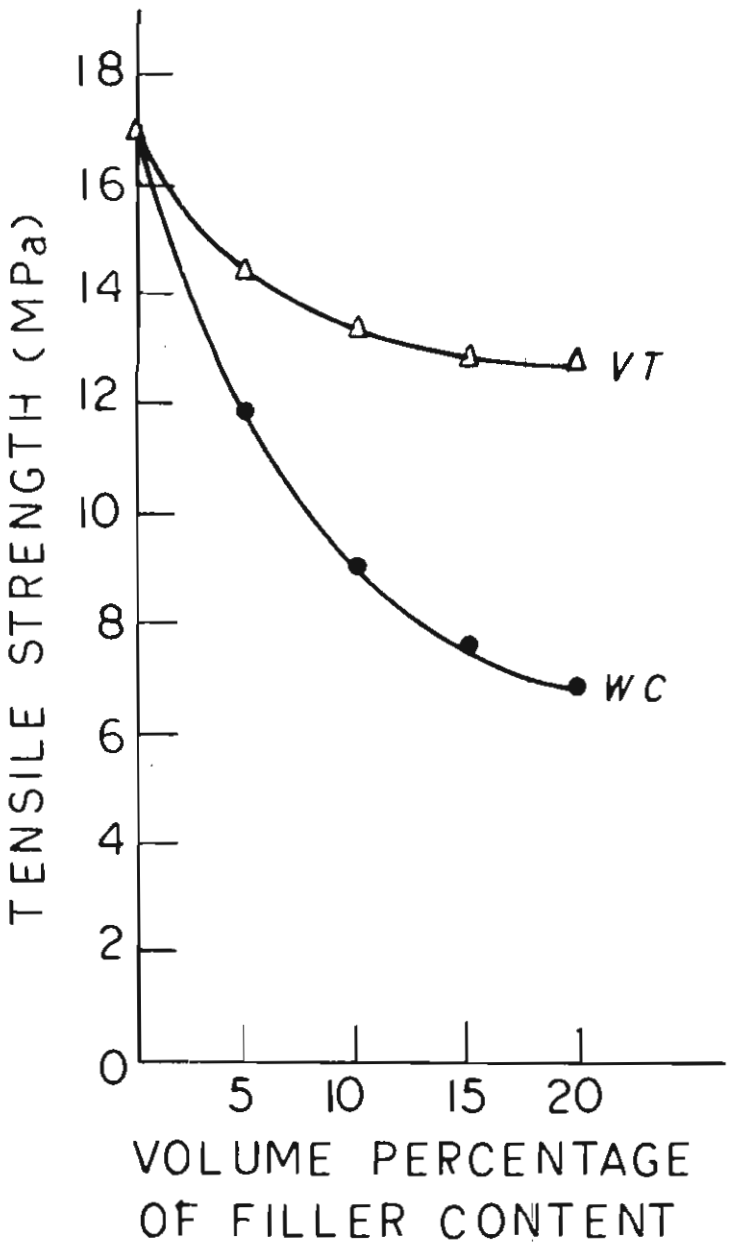


Fig.IV-3.Variation of tensile strength of WC & VT filled polyethylene composites with filler content.

strength for the same filler content in WC composite is reduced to 7.8 MPa.

IV.2.3.4 Abrasive wear

The weight loss vs filler content is given in Fig. IV.4. In both the cases, the percentage wear loss increases with filler content, the VT filled composites had relatively low wear loss. For a composite containing 20 volume percentage of VT the wear loss is 4.91% as compared to 5.8% for the same volume fraction of WC.

Fig. IV.5a shows the wear surface of WC-polyethylene composite where the wear track is clearly seen, the clay particles have been either pulled out or cut off, and the wear track with an average track width of 5 $\mu$ has gone deep into the matrix. On the other hand, the VT filled composites showed much shallower tracks with the VT particles remaining at random on the side of the track as seen from Fig. IV.5b.

IV.2.3.5 Dielectric properties

Tables IV. 3 & IV. 4 show the variations of dielectric constant (k) and loss (tan $\delta$ )values of WC and VT composites with frequency for different filler fractions. K and tan $\delta$ values decrease with frequency for both WC and VT composites. However, VT filled composites show low values compared to WC composites. K and tan $\delta$ values increase with filler content for WC composites whereas it decreases for VT composites.

IV.2.4 Discussion of results

As already mentioned in the introduction (Section I.2), properties

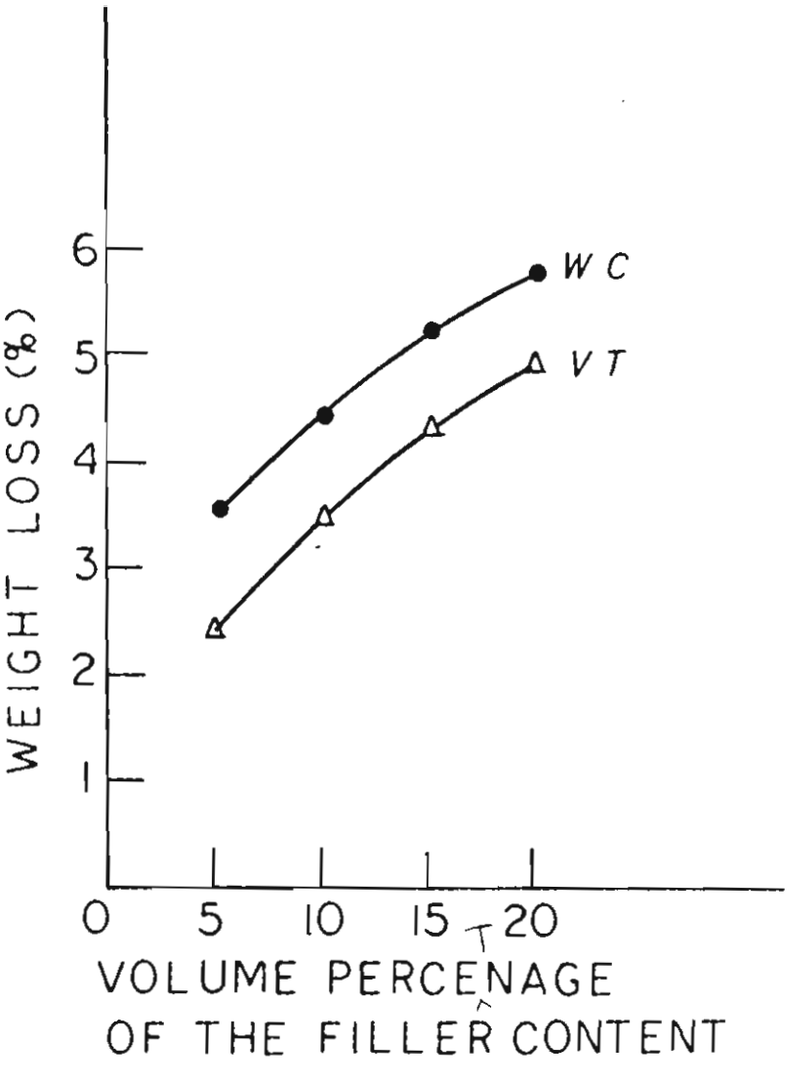


Fig.IV.4 Weight loss of WC and VT filled polyethylene composites with filler content.

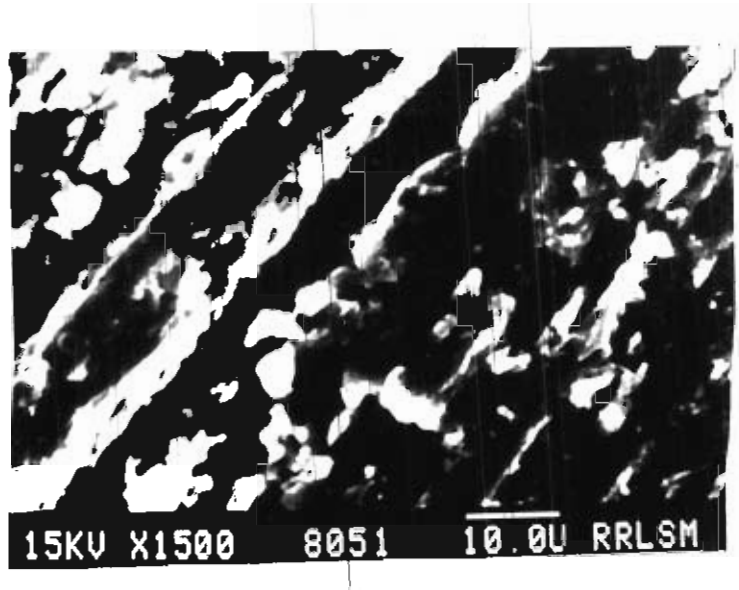


(a)

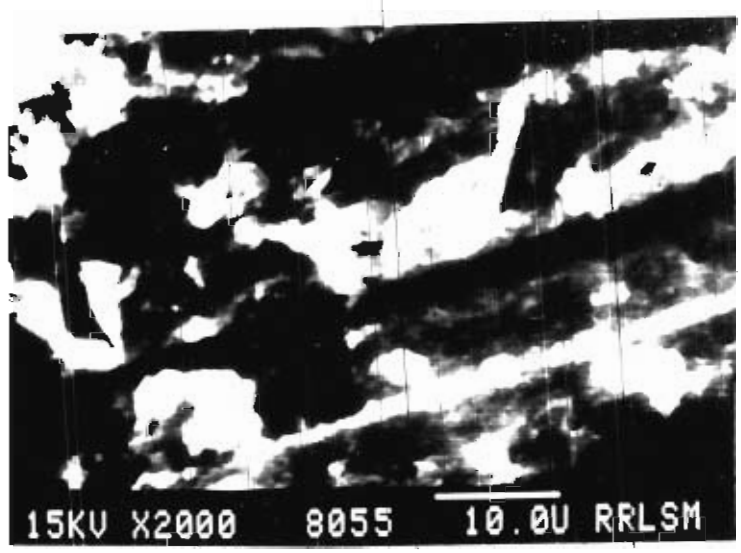


(b)

Fig. IV.5: Scanning electron micrographs showing the worn surfaces (a) WC (20%) polyethylene composite, and (b) VT (20%) polyethylene composite

Table IV.3: Dielectric constant of WC and VT filled polyethylene composites for different $V_f$ of fillers

| Frequency Hz | Dielectric constant | | | | | | |
|---|---|---|---|---|---|---|---|
| | Polyethylene | Volume percentage of filler content | | | | | |
| | | 5 | | 10 | | 15 | |
| | | WC | VT | WC | VT | WC | VT |
| $10^3$ | 2.370 | 3.750 | 3.320 | 4.120 | 3.260 | 4.490 | 3.210 |
| $10^4$ | 2.368 | 3.520 | 3.310 | 3.670 | 3.250 | 3.820 | 3.190 |
| $10^5$ | 2.365 | 3.410 | 3.300 | 3.460 | 3.238 | 3.510 | 3.170 |
| $10^6$ | 2.350 | 3.370 | 3.290 | 3.390 | 3.220 | 3.420 | 3.160 |

Table IV.4: Dielectric loss (tan $\delta$ ) of WC and VT filled polyethylene composites for different $V_f$ of fillers

| Frequency Hz | Dielectric loss | | | | | | |
|---|---|---|---|---|---|---|---|
| | Polyethylene x $10^{-6}$ | Volume percentage of filler content | | | | | |
| | | 5 | | 10 | | 15 | |
| | | WC x $10^{-6}$ | VT x $10^{-6}$ | WC x $10^{-6}$ | VT x $10^{-6}$ | WC x $10^{-6}$ | VT x $10^{-6}$ |
| $10^3$ | 215 | 420 | 390 | 650 | 290 | 730 | 230 |
| $10^4$ | 202 | 390 | 360 | 620 | 260 | 700 | 210 |
| $10^5$ | 198 | 370 | 320 | 590 | 240 | 680 | 200 |
| $10^6$ | 193 | 360 | 300 | 570 | 210 | 650 | 197 |

of the composite materials are determined by the properties of the individual components. The increase in densities of the composites with increasing clay content is the generally expected effect because of the higher density of the clay (2630 kg $m^{-3}$) against that of the polyethylene (920 kg $m^{-3}$). According to the rule of mixture, the density of the pore free composite is given by

$$\begin{aligned} \rho &= V_f \rho_f + V_m \rho_m \\ &= V_f \rho_f + (1 - V_f) \rho_m \\ &= V_f (\rho_f - \rho_m) + \rho_m \\ &= V_f C + \rho_m \end{aligned} \qquad \text{(IV.1)}$$

where $C = (\rho_f - \rho_m)$; $\rho_f$ and $\rho_m$ being the densities of the filler and matrix and $V_f$ is the volume fraction of the filler.

So long as $C$ is a positive quantity, density will increase with increase in volume fraction of the filler, however small it may be. For the pore free composites of WC and VT, densities will be almost same for the same volume fraction of the filler, irrespective of the filler surface treatment since there is no appreciable difference of densities in WC and VT. Introduction of pores will reduce the density of the composites from that given by eqn. IV.1. The surface modification of filler possibly leads to better wettability and dispersion in the case of VT composites, thereby reducing its porosity from that of WC composites. The difference in dispersion of WC and VT particles are clear from Figs. IV.1a & b.

The increase in modulus with the addition of clay in polyethylene matrix is the normally expected filler effect as have been observed in systems such as wollastonite, mica and talc[137-139].

As was already mentioned in the Introduction that a considerable decrease in elongation to break is observed if there is good adhesion of the filler to the matrix and if there is poor adhesion more gradual decrease is observed. In the present case WC shows a gradual decrease in elongation to break with filler content indicating that only weak adhesion of the filler and the matrix is possible in the case of WC. The behaviour for VT shows that the decrease is more rapid which concludes that there is comparatively good adhesion between the matrix and the VT particles.

WC polyethylene composites contain more agglomerates. Agglomerates are generally weak points in the material and break easily when a stress is applied to them. A broken agglomerate then behaves as a strong stress concentrator. Also agglomerates are larger than the primary filler particles, hence they produce weaker materials than composites containing the dispersed particles. Also they produce larger voids after rewetting. The tensile strength variation for WC composites matched with other systems with inert fillers when there was no adhesion between the particles and matrix. The trend in VT composite is much more similar with the case of adhesion as shown in Fig. I. . Eventhough the particle size is larger in VT (Section III.3), because of the dispersibility and less tendency for agglomeration, strength is higher for VT composites than WC composites in all the ranges investigated. The observation is in agreement with Hawthorne[68].

Since the clay is softer with low Mohs' hardness (2)[105] than the abrasive it is readily ground or abraded. The wear of filled polymers depends upon the particle size of the filler. When the particles are large and there is good adhesion between particles and the matrix, wear is found to be less. This explains the low wear of VT polyethylene composites compared to WC polyethylene composites.

With frequencies both WC and VT composites show a decrease in dielectric constant and loss values in line with the observations made for WC and VT (Figs. II.9 and III.8). The lower values of dielectric constant and dielectric loss for VT polyethylene composite clearly demonstrates that compared to WC composites, VT composites are better insulators, probably due to the absence of water content which escpaes under vacuum. It is also interesting to note that the tan $\delta$ and k values are drastically changed especially at lower frequencies for WC composites compared to pure polyethylene and VT composites which obviously indicates the predominance of water molecules forming the dipolar contributions at this frequency range.

Since absolute values of k and tan $\delta$ are less for VT compared to the polyethylene matrix, both the values show decrease with increase in filler content. The values are higher for WC and hence the increased values for WC composites.

## IV.3 KAOLINITE-POLYESTER COMPOSITES

### IV.3.1 Experimental

#### IV.3.1.1 Materials

The polyester resin (HSR (8131)), hardner (MEK peroxide (8021)) and catalyst (cobalt naphthanate (8013)) used were received from M/s. Hylam Ltd., Madras, India.

IV.3.1.2 Preparation

Polyester based composites were prepared in the following manner. A weighed quantity of the resin containing initiator and accelerator (1% each) is taken in a 150 ml beaker to which known quantity of clay powder was added and a smooth paste was prepared by mixing with a glass rod. The mixture was then kept in a desiccator under vacuum for 2 hr in order to remove the air bubbles during mixing. The mixture was then cast in glass tubes of required dimensions and allowed to set for about 2 hr . The cast sample was taken from the glass tube and allowed to cure at 100$^{o}$C in an oven for 2 hr . In view of the limitations in processing, it has not been possible to make composites with filler content above 10 volume percentage.

IV.3.1.3 Methods

IV.3.1.3.1 Density measurements: The densities of the samples were determined by water displacement method.

IV.3.1.3.2 Microstructural studies: Microstructural evaluations were carried out on the polished surface using a Leitz Metalloplan Optical Microscope.

IV.3.1.3.3 Strength measurement: The compressive strengths of the composites were evaluated on 10 x 20 mm cylindrical samples according to ASTM D 695 with a cross head speed of 2 mm/min using an Instron Testing Machine.

IV.3.1.3.4 Abrasive wear: The procedure is as discussed in Section IV.2.2.3.4.

IV.3.1.3.5 Dielectric studies: The details of dielectric measurements are as reported in Section IV.2.2.3.5.

IV.3.2 Results

IV.3.2.1 Dispersibility

WC particles showed a tendency to settle down to the bottom during resin cure which resulted in poor non-uniform dispersion (Fig. IV.6a). But VT showed a good uniform dispersion of the clay particles (Fig. IV.6b). Fig. IV.7 gives the microstructure of WC and VT filled polyester. $V_f$ being 20% by vol.(Fig. IV.7b), the microstructure of VT polyester system showed more uniform dispersion of particles with limited tendency for agglomeration, while WC system (Fig. IV.7a) showed a non-uniform dispersion with lot of agglomerations. The larger particles in Fig. IV.7b are not agglomerates, but single particles, VT being more coarser than WC particles (Section III.3).

IV.3.2.2 Density

Table IV.5 lists values of both experimentally measured density and calculated density using the densities of resin (1100 kg $m^{-3}$) and clay particles and the percentage porosities in the clay polyester composites. The following deductions can be made from the table.

a. The absolute density of the composites increased with increasing clay content.

b. The densities of composites prepared using VT are higher than those of composites made from WC for the same volume fraction of the clay content.

(a)

(b)

Fig. IV.6: Polyester resin filled with (a) WC, (b) VT

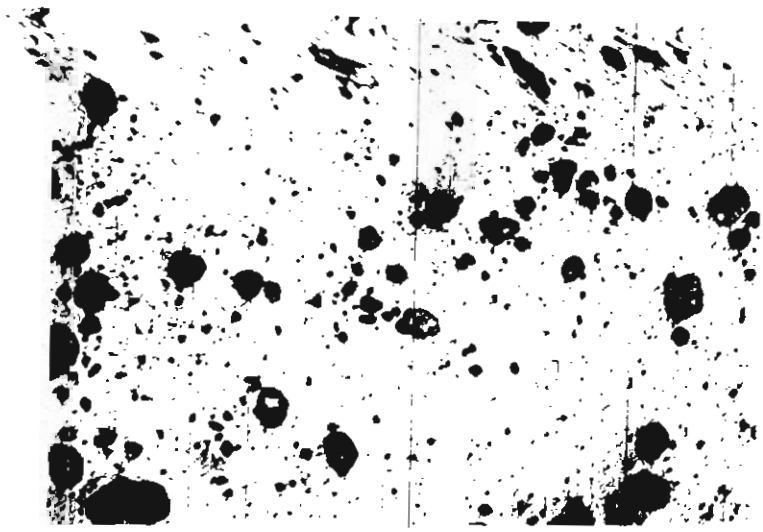

(a)

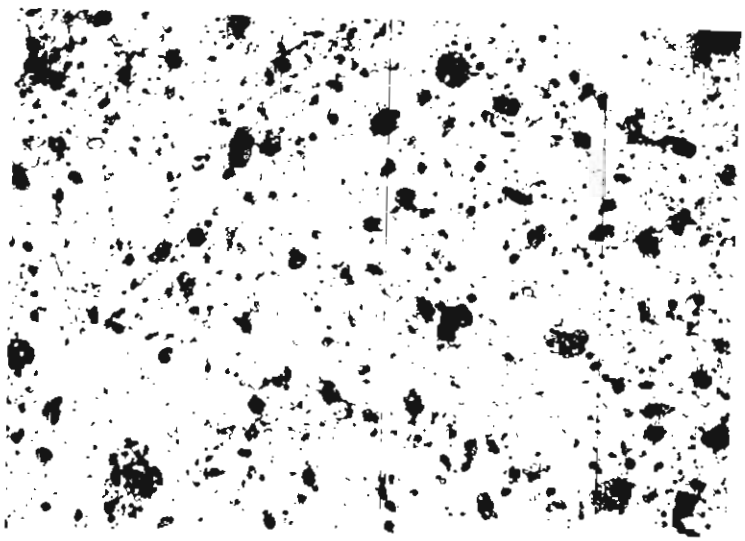

(b)

Fig. IV.7: Optical micrograph of polyester resin filled with (a) WC X50, (b) VT X50.

Table IV.5: Density and % porosities of WC and VT filled polyester composites

| | WC polyester composites | | | | VT composites | | | |
|---|---|---|---|---|---|---|---|---|
| | Volume % of filler content | | | | Volume % of filler content | | | |
| | 2.33 | 4.7 | 7.4 | 10 | 2.33 | 4.7 | 7.4 | 10 |
| Calculated density, $kg\ m^{-3}$ | 1224 | 1260 | 1300 | 1334 | - | - | - | - |
| Measured density, $kg\ m^{-3}$ | 1120 | 1150 | 1190 | 1220 | 1200 | 1240 | 1260 | 1290 |
| % porosity | 8.50 | 8.73 | 8.46 | 8.55 | 2.00 | 1.58 | 3.00 | 3.30 |

c. The percentage porosities are less in VT composites than those in WC composites.

It is interesting to note that the extent of porosity is more than double in WC filled composites when compared with VT composites for samples prepared under identical conditions.

IV.3.2.3 Compressive strength

The load displacement curves of the matrix (resin) and composite are shown in Fig. IV.8 which reveal the following points:

a. Elastic deformation of the composites takes place upto the matrix failure strain.

b. Thereafter cracking of the matrix and transference of load to the filler takes place.

c. Furtheron, the composite starts to deform in a non-linear manner upto its ultimate failure strain.

Fig. IV.9 shows the compressive strength of WC and VT filled polyester with filler concentration, ranging from 0 to 10 volume percent. It is observed from the curve that

a. Compressive strength for clay filled polyester composites increases directly with the filler loading upto 7.4% in the case of WC composite (345 $N/mm^2$) and upto 10% in the case of VT composites (406 $N/mm^2$). Further increase in filler content results in a decrease in the strength values.

b. Compressive strength of VT filled composite is higher than that of WC filled composites.

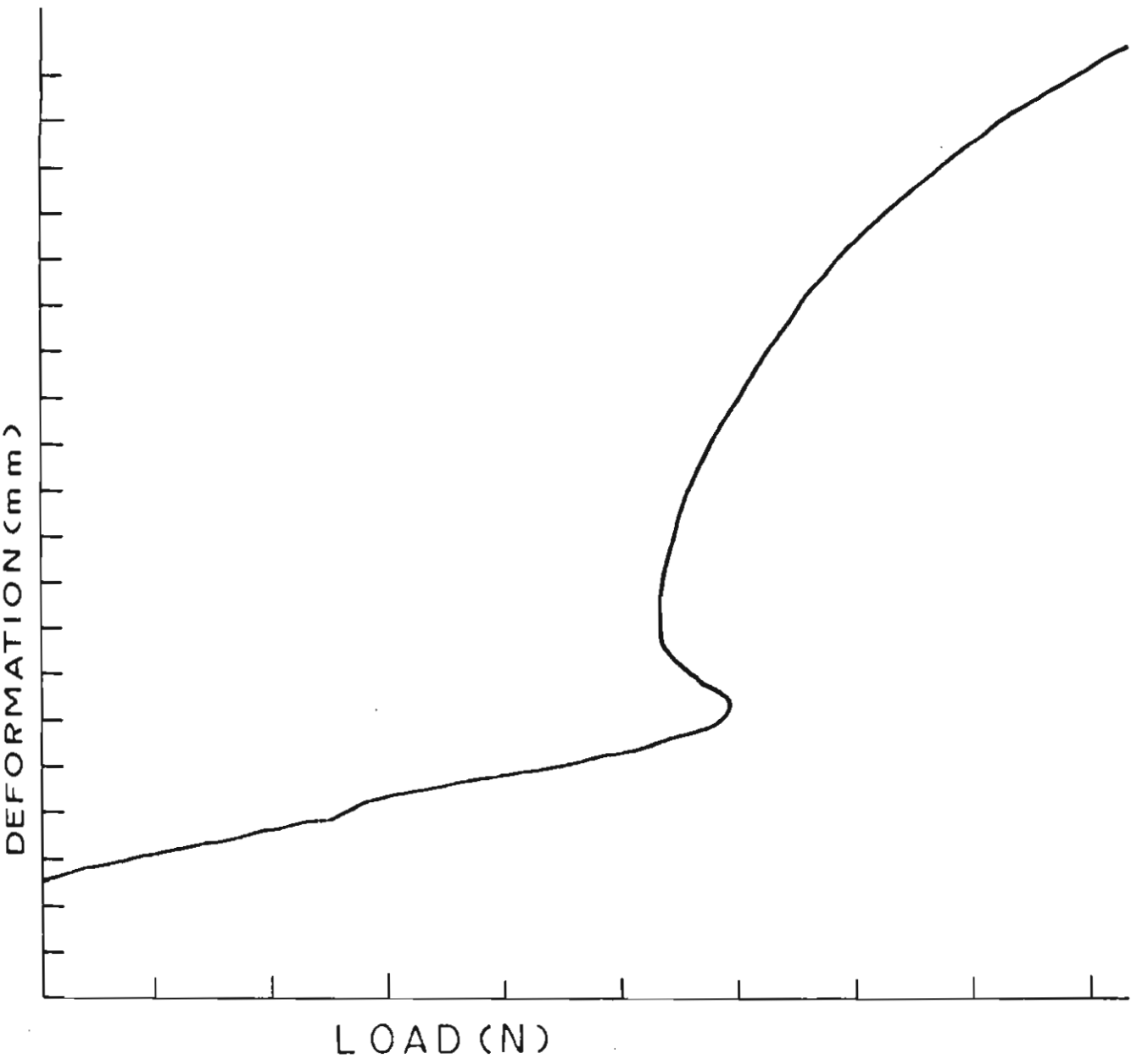


Fig. IV. 8 Load deformation curve for the Matrix cracking in a Clay–Polymer composite

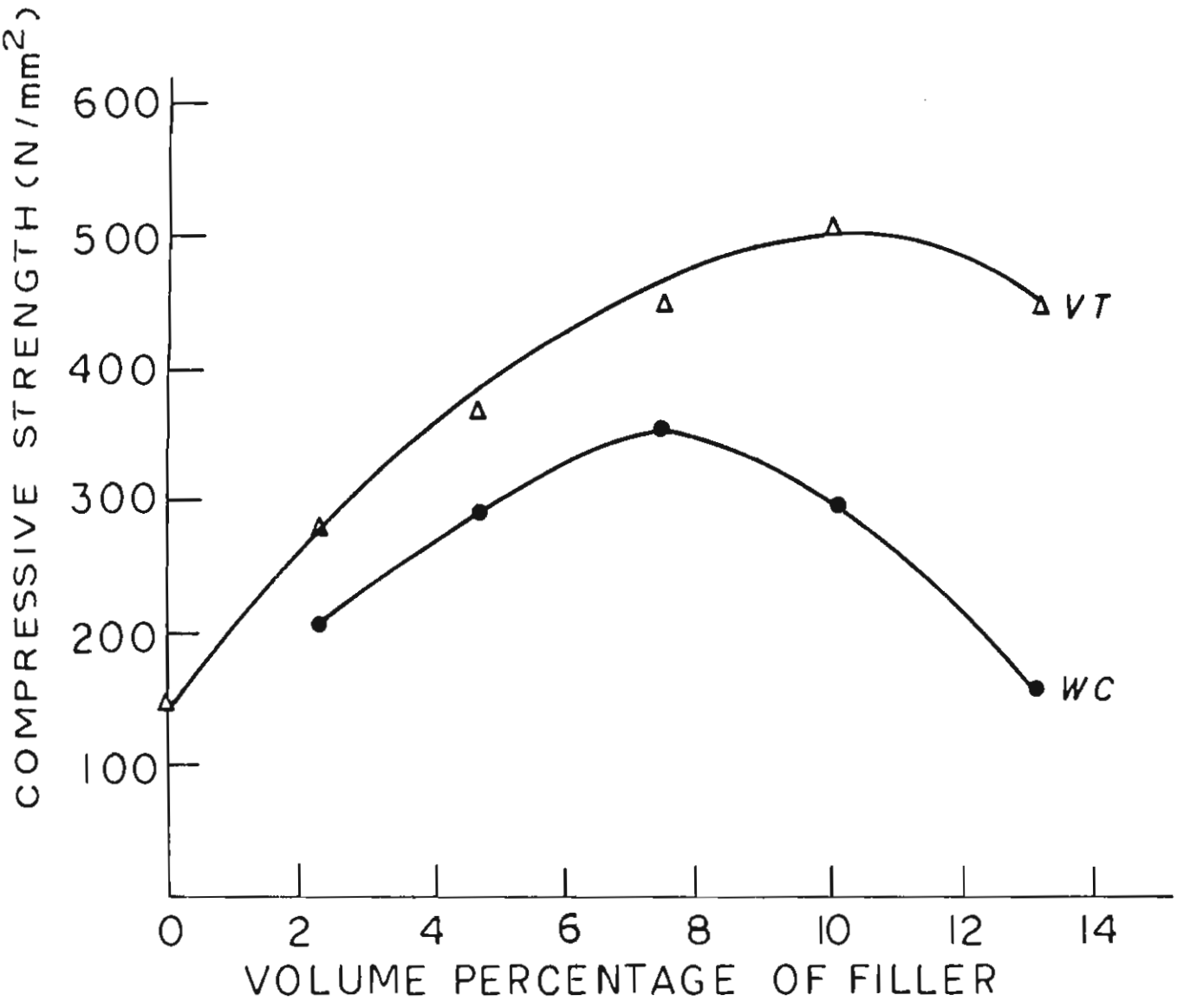


Fig. IV.9 Variation of compressive strength of WC and VT filled polyester composites

c. It is possible to incorporate more VT in the polyester matrix than WC.

IV.3.2.4 Abrasive wear

Fig. IV.10 shows plot of weight loss versus percentage of filler content in clay polyester composites. It can be seen that weight loss increases with percentage of filler content for both WC and VT filled composites.

The dimensionless wear rate $\dot{W}$ was calculated using the expression[140]

$$\dot{W} = \frac{M}{ASP} = \frac{V}{AS} \qquad \text{(Iv.2)}$$

where M is the weight loss; A is the apparent area in contact, $P$ is the density of the composite, V is the wear volume and S is the sliding distance. The wear rate is given in Table IV.6. The wear rate of VT composites is found to be the same as that of the matrix.

IV.3.2.5 Dielectric properties

Table IV.7 and IV.8 show the variation of dielectric constant(k) and dielectric loss (tan $\delta$ ) of WC and VT filled with polyester resins for different volume percentage of fillers. In all the cases both k and tan $\delta$ decrease with frequency. In the case of WC composites increase in values are observed with increasing filler content. But for VT both the values decrease with increase in filler content. Similar observation was made for polyethylene composites also (Section IV.2.3.5).

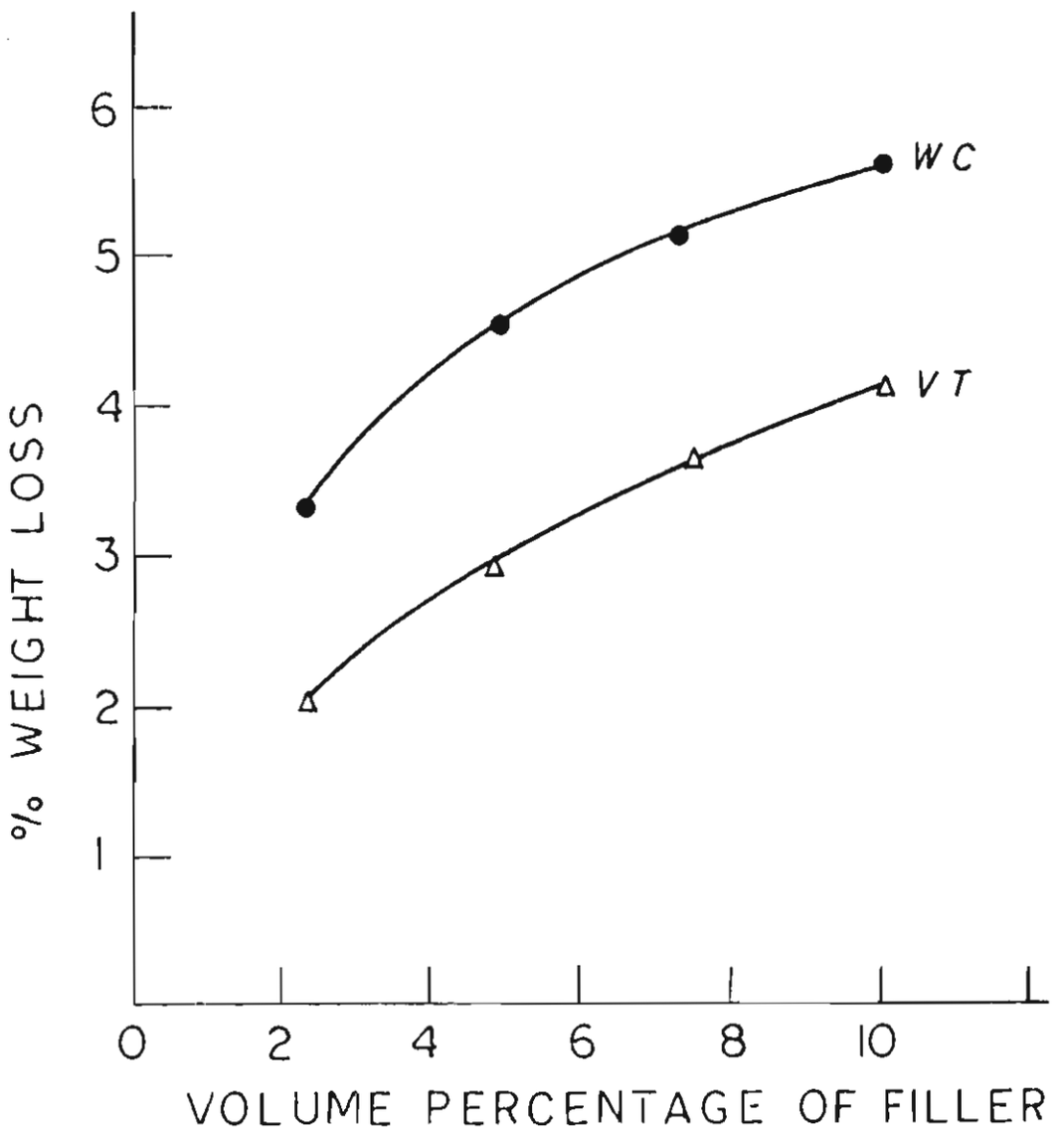


Fig. IV.10 Weight loss of WC and VT filled polyester composites with filler content

Table IV.6: Wear rate of the polyester composites filled with WC and VT of different compositions

| Material | Volume percentage of filler content | | | |
|---|---|---|---|---|
| | 2.33 | 4.7 | 7.4 | 10 |
| Matrix ($\times 10^{-5}$) | 15 | | | |
| WC composite ($\times 10^{-5}$) | 17 | 18 | 18 | 18 |
| VT composite ($\times 10^{-5}$) | 15 | 14 | 15 | 15 |

Table IV.7: Dielectric constants (k) of WC and VT filled polyester composites for different $V_f$ of fillers

| Frequency Hz | Polyester | Dielectric constants | | | | | |
|---|---|---|---|---|---|---|---|
| | | Volume percentage of filler | | | | | |
| | | 2 | | 6 | | 10 | |
| | | WC | VT | WC | VT | WC | VT |
| $10^3$ | 4.2 | 4.40 | 4.38 | 4.50 | 4.29 | 4.62 | 4.26 |
| $10^4$ | 3.9 | 4.10 | 3.96 | 4.20 | 3.94 | 4.40 | 3.92 |
| $10^5$ | 3.7 | 3.88 | 3.79 | 3.92 | 3.76 | 4.10 | 3.73 |
| $10^6$ | 3.5 | 3.71 | 3.69 | 3.82 | 3.62 | 3.90 | 3.48 |

Table IV.8: Dielectric loss (tan $\delta$ ) of WC and VT filled polyester with volume percentage of filler and with frequency

| Frequency Hz | Dielectric loss | | | | | | |
|---|---|---|---|---|---|---|---|
| | Polyester | Volume percentage of filler | | | | | |
| | | 2 | | 6 | | 10 | |
| | $\times 10^{-4}$ | WC $\times 10^{-4}$ | VT $\times 10^{-4}$ | WC $\times 10^{-4}$ | VT $\times 10^{-4}$ | WC $\times 10^{-4}$ | VT $\times 10^{-4}$ |
| $10^3$ | 220 | 500 | 230 | 990 | 216 | 1490 | 209 |
| $10^4$ | 190 | 400 | 198 | 800 | 182 | 1200 | 179 |
| $10^5$ | 160 | 340 | 162 | 679 | 159 | 970 | 143 |
| $10^6$ | 130 | 292 | 131 | 608 | 123 | 910 | 118 |

## IV.4 KAOLINITE-POLYVINYL CHLORIDE COMPOSITES

### IV.4.1 Introduction

Polyvinyl chloride (PVC) is one of the most important commercial synthetic materials which is widely used in wire and cable industries. PVC was apparently the first thermoplastic to be systematically filled with mineral materials. The present Chapter describes the effect of incorporation of the surface modified and unmodified clays on the properties of polyvinyl chloride. Density, compressive strength and microstructures are reported.

### IV.4.2 Experimental

#### IV.4.2.1 Preparation

The uniformly mixed powder of weighed quantities of clay and polyvinyl chloride was compression moulded at a temperature of 160$^{o}$C and at a pressure of about 4 $Nm^{-2}$. The material was preheated in the die before applying the pressure.

#### IV.4.2.2 Methods

Methods of testings are similar to that reported in Sections IV.3.1.3 and IV.4.1.3.

### IV.4.3 Results

#### IV.4.3.1 Density

Table IV.9 shows the densities of the kaolinite-PVC composites. It also shows increase in density with filler fraction.

Table IV.9: Density and % porosities of WC and VT filled polyvinyl chloride composites

| | WC-polyvinyl chloride composites | | | | | VT-polyvinyl chloride composites | | | | |
|---|---|---|---|---|---|---|---|---|---|---|
| | Volume percentage of filler content | | | | | Volume percentage of filler content | | | | |
| | 5 | 10 | 15 | 20 | 25 | 5 | 10 | 15 | 20 | 25 |
| Calculated density, kg $m^{-3}$ | 1433 | 1496 | 1559 | 1622 | 1754 | - | - | - | - | - |
| Measured density, kg $m^{-3}$ | 1290 | 1346 | 1410 | 1460 | 1564 | 1326 | 1378 | 1440 | 1510 | 1630 |
| % porosity | 9.98 | 10.03 | 9.60 | 9.99 | 10.80 | 7.50 | 7.90 | 7.10 | 6.90 | 7.10 |

It is observed from the Table IV.9 that percentage porosity is least at 15 vol.% of WC whereas it is least at 20 vol% of VT. After that it shows an increase.

IV.4.3.2 Compressive strength

Table IV.10 gives the compressive strength values of WC and VT composites with volume fraction of filler content. The strength values are seen to increase with the filler content upto a maximum ($9.1 \times 10^7$ Pa for WC at 15 $V_f$ and $10.23 \times 10^7$ Pa for VT at 20 $V_f$) and then decreases with the filler content.

Initially there is an increase in compressive strength for both WC and VT composites. After giving a maximum value of a particular volume fraction (15 volume percentage for WC and 20 volume percentage for VT) the values decrease.

*IV.4.3.3 Microstructure*

Figs. IV.11(a) and (b) show the microstructure of WC and VT (10%) filled polyvinyl chloride. VT composite shows uniform dispersion of the particulate in the PVC matrix with less agglomeration compared to WC composites.

*IV.4.4 Discussion*

The thermal decomposition hydration - redecomposition treatment has resulted in product of increased surface area. This resulted in increased dispersion of VT in polyvinyl chloride and hence lower porosity in the case of VT-PVC composites compared to the WC-PVC composites. This accounts for the improved strength values for VT composites compared to the WC composites.

Table IV.10: Compressive strength of polyvinyl chloride filled with WC and VT for different volume percentage of the filler content

| Volume percentage of filler | Compressive strength | |
|---|---|---|
| | WC (x $10^7$) Pa | VT (x $10^7$) Pa |
| 0 | 6.8 | |
| 5 | 7.1 | 7.5 |
| 10 | 7.9 | 8.2 |
| 15 | 8.9 | 9.1 |
| 20 | 8.6 | 9.8 |
| 25 | 8.3 | 9.1 |

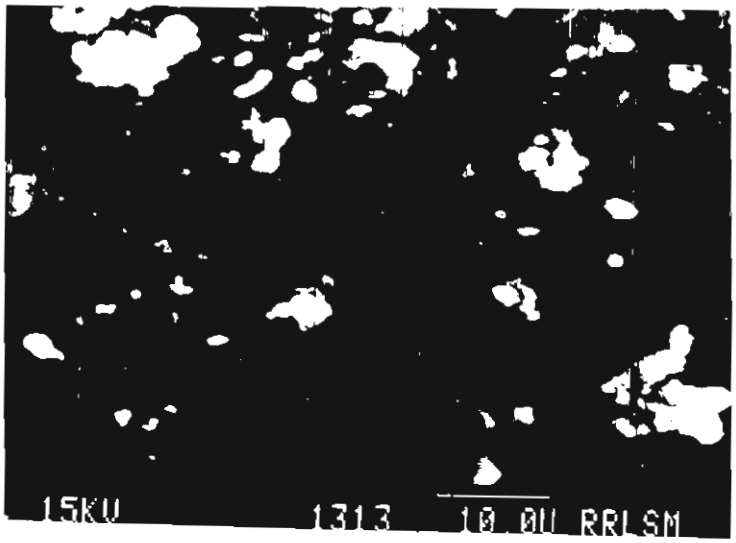


(a)

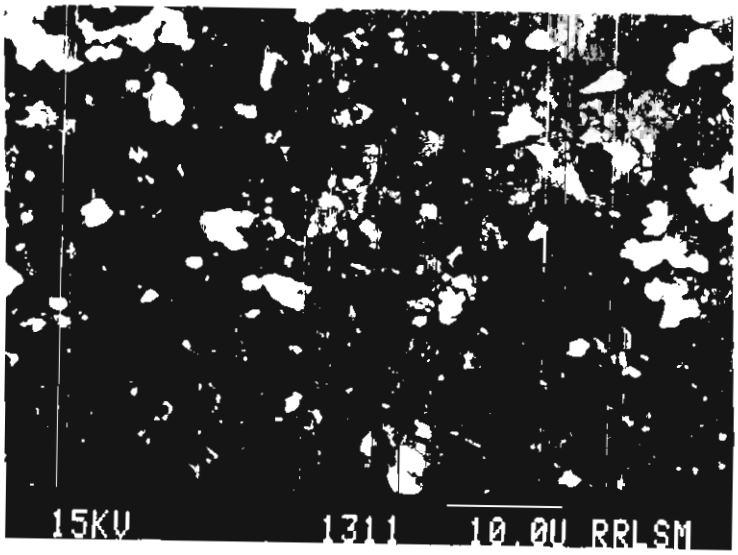


(b)

Fig. IV.11: Scanning electron micrographs of the polyvinyl chloride filled with (a) WC (10%), (b) VT (10%)

# CHAPTER V

## COMPARISON ON THE THREE POLYMER SYSTEMS INVESTIGATED

# CHAPTER V

## COMPARISON ON THE THREE POLYMER SYSTEMS INVESTIGATED

In the present investigation, the three polymer systems were selected with a view to understand different methods of formation of the composites and the relative behaviour of such composites. With respect to the possible interaction between the particulates and the matrices, there seems to be no appreciable differences in three polymer systems. The polyester could be easily molded at the room temperature conditions with a curing at 100°C. The polyethylene based composites were hot extruded at 180°C, while the polyvinyl chloride ones were prepared by hot compression molding at 170°C. Although the method of preparation may have a certain level of influence on the particulate matrix interaction, major contribution could be expected from properties of the particulates. In this respect, although the absolute values of the various properties could be different, possibility exists to compare the general trends as a function of the particulate with and without surface modification.

General observations in the properties of the various composites investigated are provided in Table V.1. The thermal modification resulting in the dehydroxylated kaolinite has been clearly seen invariably in all the composites by the considerable improvement in all the properties of the composites prepared using VT as compared to WC.

Table V.2 lists the comparison of density and percentage

Table V.1: Comparison of the properties of the composites with polyethylene, polyester and polyvinyl chloride

| Polyethylene | Polyester | Polyvinyl chloride |
|---|---|---|
| 1. Density: WC composite has lower value than VT | WC composite has lower value than VT | WC composite has lower value than VT |
| 2. Porosity: VT composites are less porous than WC composites | VT composites are less porous than WC composites | VT composites are less porous than WC composites |
| 3. Tensile properties:<br>Improved tensile strength and tensile modulus values are observed for VT composites as compared to WC composites. Percentage elongation is less in the case of VT composites. | Compressive strength:<br>Absolute values are higher for VT composites. After registering a maximum value it decreases with filler content. Maximum value was obtained for WC at a filler loading of 7.4% whereas for VT maximum is obtained for 10%. | Compressive strength:<br>Absolute values are higher for VT composites. Maximum value for WC composite (89 MPa) is obtained at a filler loading of 15% compared to VT (98 MPa for 20%) is obtained at 20%. |

Table V.1 Contd.

| Polyethylene | Polyester | Polyvinyl chloride |
|---|---|---|
| 4. Abrasive wear: | | |
| Lower wear values are obtained for VT composites compared to WC composites. | Lower values are observed for VT composites comapred to WC composites | - |
| 5. Electrical properties: | | |
| Lower dielectric constant for VT composites and hence good insulators than WC composites. Similar behaviour for dielectric loss also. | Lower dielectric constant for VT composites and hence good insulators than WC composites. Similar behaviour for dielectric loss also. | - |

porosities of composites prepared out of polyethylene, polyester and polyvinyl chloride and 10 volume percentage of WC and VT.

From the table it is clear that VT polyethylene composites are about 48% less porous while the VT polyester composite is 61% and polyvinyl chloride is 21%. The behaviour of particulate composites generally depend on the method of processing and nature of polymers.

The microstructural features with respect to the particulate distribution and agglomeration in all the three polymer systems indicate in general that the WC composites contain loose agglomerates of WC, although the basic particle size is very fine. Despite general care taken to reduce the extent of agglomeration of particles, there is a preferential tendency for agglomeration in WC as compared to VT, due to the surface hydroxyls and possibility of hydrogen bonding. The VT also has been showed to have agglomerates of loose type to a much less order. On the other hand, polyvinyl chloride has an absolutely different microstructure with a very homogeneously distributed kaolinite particles. Although agglomerates are seen, the polymer seems to have wetted the surfaces making the microstructure coherent.

The mechanical properties of the various composites could be discussed with respect to the tensile as well as compressive behaviour. Because of the limitations in processing, it has not been possible to compare all properties in the composites. The percentage elongation in polyethylene composite was reduced (Table IV.2) indicating the increased brittleness of the composites. This is expected for composites containing inorganic filler particles. The high extent of compatibility and adhesion of VT with the matrix has resulted in about 28% decrease

in the percentage elongation. Because of the higher dispersibility and lesser tendency for agglomeration both strength and modulus values are higher for VT polyethylene composites compared to WC composites. Similar trend for compressive strength are observed in both polyester and polyvinyl chloride.

Micrographs of the worn out surfaces of polyethylene composites bring out the even wear track in VT as compared to WC composite and indicating the nature of adhesion of the particle to the matrix. Similar behaviour could be expected in the composites based on polyester and polyvinyl chloride.

The electrical properties of kaolinite have been investigated with respect to temperature[104]. The general observation has been a reduction in dielectric constant and dielectric loss due to the removal of hydroxyls. Further, there is a general trend in the reduction of the above properties with respect to increase in frequencies. In this respect, the WC composites also keep the same trend. However, the specific values of dielectric constant and loss are still lower for VT than WC (Table V.3). This is observed in composites of both polyethylene and polyester.

The percentage reduction in dielectric constant for VT polyethylene composites is 21% and VT polyester composite is 8% whereas the reduction in dielectric constant for VT polyethylene composite is 55% and VT polyester composite is 86%. However PVC composites were not tested for dielectric properties.

Table V.2: Density and percent porosities of polyethylene, polyester and polyvinyl chloride containing 10 volume percentage of WC and VT

| Matrix | Property | Filler particle | |
|---|---|---|---|
| | | WC | VT |
| Polyethylene | Density kg $m^{-3}$ | 963 | 1025 |
| | Porosity (%) | 11.73 | 6.05 |
| Polyester | Density kg $m^{-3}$ | 1220 | 1290 |
| | Porosity (%) | 8.55 | 3.3 |
| Polyvinyl chloride | Density kg $m^{-3}$ | 1346 | 1378 |
| | Porosity (%) | 10.03 | 7.9 |

Table V.3: Dielectric constant and loss values of polyethylene and polyester containing $10_3$ volume percentage of WC and VT at a frequency of $10^3$ Hz

| Matrix | Property | Filler particles | |
|---|---|---|---|
| | | WC | VT |
| Polyethylene | Dielectric constant | 4.12 | 3.26 |
| | Dielectric loss x $10^{-6}$ | 650 | 290 |
| Polyester | Dielectric constant | 4.62 | 4.26 |
| | Dielectric loss x $10^{-4}$ | 1490 | 209 |

# C H A P T E R VI

## LOW TEMPERATURE MULLITE FROM SURFACE MODIFIED KAOLINITE

# CHAPTER VI

## LOW TEMPERATURE MULLITE FROM SURFACE MODIFIED KAOLINITE

### VI.1 INTRODUCTION

Mullite is the most stable crystalline compound in the $Al_2O_3$-$SiO_2$ system under normal atmospheric pressure. It has a chemical composition 3 $Al_2O_3$ . 2 $SiO_2$ and crystallizes in the orthorhombic system most commonly in the form of elongated needle shaped crystals, the exception being, when it is prepared in the absence of a liquid phase[142]. Mullite has been identified as one of the most potential refractory as well as high temperature structural material in view of its high melting point (approximately 1850°C), low thermal expansion coefficient (5.2 x $10^{-6}$ $K^{-1}$ between 20-1000°C) creep resistance, chemical inertness and good mechanical properties[143-145]. However, it is rare in nature, the most important place of occurrence being in the Isle of Mull, Scotland[142].

Mullite can primarily be prepared by mixing $Al_2O_3$ and $SiO_2$ powders in 3 : 2 stoichiometric proportions in view of the mullite composition 3 $Al_2O_3$ . 2 $SiO_2$[142-146]. The major problem of obtaining good quality mullite from basic powder mixtures is to achieve efficient mixing of $Al_2O_3$ and $SiO_2$. Good quality kaolinite and sillimanite along with fine alumina have been employed as the raw materials because of their abundant availability[147-149]. The reaction sequences in which kaolinite transforms to mullite which has got special interest in the entire field of ceramics technology, has been extensively studied by several authors[150-170]. In this Chapter formation of mullite from surface modified kaolinite is described taking into consideration the following:

(1) The first reaction occurring in the thermal transformations of kaolinite is a characteristic endothermic effect caused by the dehydroxylation of kaolinite and the formation of amorphous phase metakaolinite[103,104].

(2) The second is the exothermic reaction occurring between 950 and 1000°C. A weak diffuse XRD was obtained at this temperature.

The crystallization of $\gamma$ alumina is reported to be the cause for the exotherm at about 1000°C by several authors. Richardson and Wilde[159] in their XRD studies in many clays fired between 950 and 1000°C observed $\gamma$ alumina rather than mullite, and upto 1100°C $\gamma$ alumina persisted.

There have been reports stating the coexistence of mullite and $\gamma$ alumina phase in the temperature range 950-960°C in kaolinite and its polymorphs. According to Brindley et al[160,161], this exothermic reaction is caused by the formation of a spinel type phase of composition $Si_8 Al_{10.67} \square_{5.33} O_{32}$ rather than $\gamma$ alumina of composition $Al_8 Al_{13.} \square_{2.5} O_{32}$ with the discard of silica.

Comer[162] observed the coexistence of very strong (002) reflection of mullite and weak (440) reflection of spinel in the electron diffraction pattern of kaolinite heated to 950°C. With the rise in temperature, mullite pattern becomes more and more intense at the expense of the spinel pattern.

Nicholson and Fulrath[163] calculated the enthalpy value at the exotherm by the differential thermal calorimetry to be -9.1 K cal/mol. This is equivalent to the calculated value for crystallizing one mole

of amorphous silica to β quartz at 1000°C. Thus they attributed the exotherm at about 980°C to the crystallization of β quartz. Further, they found that the kaolinite preheated to 850°C and leached with NaOH solution failed to show a peak at 980°C because of the removal of the amorphous silica.

The above theory was contradicted by Chakraborthy and Ghosh[164]. They observed only very small amount of silica on heating kaolinite to 650-850°C and leaching with sodium hydroxide. Above 980°C, silica was in the amorphous state and hence the conversion to β quartz could not be related with the 980°C exothermic peak. Slaughter and Keller[165] observed that the development of very small mullite nuclei should preclude an exothermic peak as sharp as the one at about 1000°C.

According to Roy and Osborn[166], above the dehydroxylation temperature of kaolinite, the stable phase formed from kaolinite could be mullite and quartz only and any other peak in the temperature range 575-1000°C was unstable and transformed into the stable mullite and quartz. These authors support the mullitisation of kaolinite at the peak temperature and refutes the crystallization of $\gamma$ $Al_2O_3$.

Infrared spectral measurements of heated kaolinite[167] indicate the presence of both tetrahedral and octahedral aluminium at 980°C, supporting the $\gamma$ $Al_2O_3$. Leaching the preheated sample with sodium hydroxide removes vibrations of $SiO_4$ which indicates that the silica is either amorphous or very loosely bound and therefore not associated with a spinel lattice[167].

Leonard[168] based on RED measurements observed that cation-oxygen distances are more consistent with those predicted for $\gamma$ $Al_2O_3$ than for the spinel. Chemical shift calculations showed that silicon present

in tetrahedral spinel sites should have a shift of -79.9 ppm. Brown et al[169] could not observe such a resonance and was taken as an evidence that the cubic spinel phase did not contain detectable amounts of silicon. Comparison of the $^{27}Al$ spectra of heated kaolinite with the spectrum of $\gamma$ $Al_2O_3$ prepared from synthetic pseudoboehmite showed that although the two were not identical, the envelope of the kaolinite spectra could easily accommodate a $\gamma$ $Al_2O_3$ spectrum. Thus the NMR evidence is more consistent with $\gamma$ $Al_2O_3$ than with a silicon containing spinel. The second exothermic reaction at 1050-1100°C is thought to be the transformation of the spinel type of structure to mullite with further discard of silica. Any further reaction at higher temperature results in the continued development of mullite to the composition 3 $Al_2O_3$ . 2 $SiO_2$ and cristobalite.

In view of the higher temperature required for the mullite from clay-alumina mixtures, there have been attempts to increase the mullite content and to reduce the temperature, by the use of mineralizers. Considerable amount of work has been carried out on this aspect with contradictory results[140,151,170].

Initial particle size, surface area, and homogeneity of the starting material are some of the important factors influencing the ease of formation of mullite[142]. The strength of clay-alumina ceramics although depend on the extent of sintering at the moderate temperatures, do vary considerably at higher temperatures depending upon the extent of mullite formation.

The surface modification of kaolinite obtained by the thermal decomposition-hydration-redecomposition treatment has resulted in the formation of more reactive metakaolinite characterized by increased

surface area as mentioned in Chapter III. Also the exothermic peak at 975°C which is indicative of premullite (poorly crystalline mullite) has shifted down to a lower temperature at 940°C in the case of surface modified kaolinite (Fig.III.1). The shift in this peak showed possible increase in thermal reactivity of the surface modified kaolinite and hence indirectly indicates the possibility of formation of mullite at a lower temperature, in the case of surface modified kaolinite compared to the pure kaolinite. This probably could reduce the use of mineralizers. An attempt has been therefore made in the present investigation to study the formation characteristics of mullite from surface modified kaolinite. X-ray diffraction and microscopic observations of samples heated at different temperatures showed the extent and nature of formation of mullite. Density and dielectric properties of these compounds were found out and compared with those of unmodified kaolinite.

## VI.2 EXPERIMENTAL

### VI.2.1 Materials preparation

The details of surface modification of kaolinite used in the present investigation have been reported in Chapter III.

Pellets of 2 mm thickness and 10 mm diameter were prepared by powder pressing method using a steel die at a pressure of 3.9 $Nm^{-2}$. These pellets were sintered at different temperatures from 1050° to 1350°C in an electric furnace at a heating rate of 200°C/hr for 4 hrs.

### VI.2.2 Methods

#### VI.2.2.1 Density

Density measurements on the sintered pellets were done by the

water displacement method.

VI.2.2.2 X-ray diffraction (XRD) studies

XRD patterns of the sintered pellets were taken in Philips X-ray diffractometer model PW 1710, in the $2\theta$ range of $20-60^{\circ}$ using nickel filtered Cu-K$\alpha$ radiation at a setting of 40 KV and 20 mA.

VI.2.2.3 Dielectric measurements

The electrical properties such as dielectric constant and dielectric loss were measured on the pellets after polishing and applying room temperature silver paste for good electrical contacts using Hewlet Packard Model 4192 impedance analyser in the frequency range 10 KHz to 13 MHz.

VI.2.2.4 Scanning electron microscopy (SEM)

SEM studies of the polished pellets were conducted on a JEOL 35 SC after coating the surface with gold palladium mixture.

VI.3 RESULTS AND DISCUSSION

VI.3.1 Physical properties

The dimensional volume shrinkage and the densities of the WC and VT fired at different temperatures are given in Tables VI.1 and VI.2. It is observed that a rapid densification occurs at higher temperatures in WC compared to lower temperatures. But in the case of VT initially rapid densification occurs and after that it becomes slow at $1350^{\circ}C$. Further, the highest density observed in WC at $1350^{\circ}C$ (2880 kg $m^{-3}$) has already reached in VT at $1250^{\circ}C$.

Since the samples were made by uniaxial powder pressing method,

Table VI.1: Volume shrinkage of WC and VT fired at different temperatures

| Temperature ($^{o}C$) | $-\frac{\Delta V}{V_o}$ | |
|---|---|---|
| | WC | VT |
| 1050 | 0.091 | 0.110 |
| 1150 | 0.168 | 0.299 |
| 1250 | 0.327 | 0.459 |
| 1350 | 0.463 | 0.512 |

Table VI.2: Density data for WC and VT fired at different temperatures

| Temperature ($^{o}C$) | Density, Kg $m^{-3}$ | |
|---|---|---|
| | WC | VT |
| 1050 | 2710 | 2730 |
| 1150 | 2740 | 2790 |
| 1250 | 2800 | 2880 |
| 1350 | 2880 | 2930 |

the green as well as the sintered pellets may have certain extent of porosities. However, exact porosity measurements have not been done in the present investigation.

VI.3.2 X-ray diffraction (XRD)

The degree of crystallinity, nature of impurities and experimental conditions generally affect the intensities and positions of reflection lines. Figs. VI.1 to VI.3 give the XRD patterns for WC and VT fired at different temperatures. It can be seen that at 1050°C, WC and VT show a weak diffuse XRD pattern. But at 1150°C VT shows the peak at 4.068 A° which is identified as cristobalite. In WC, the peak is absent at 1150°C. At 1150°C VT shows almost all the peaks which are identified for mullite. Peaks corresponding to d values of 5.373 A°, 3.388 A°, 2.690 A°, 2.542 A° and 2.217 A° are identified for mullite. There is an inter-relation between the crystallization of mullite and that of cristobalite. The appearance of cristobalite starts when all the mullite phases have been crystallized[171]. As the mullite phase forms by extracting alumina from the liquid phase, it is concluded that the crystallization of cristobalite is due to devitrification of liquid phase of a high silica content. With increasing firing temperatures, appearance of cristobalite becomes more and more apparent. Similarly, the mullite formation is also increased and at most of temperatures the phases identified are mullite and cristobalite. All the mullite peaks are obtained for VT treated at 1250°C. It is interesting to note that the mullite content is approximately the same in WC heated to 1350°C and VT heated to 1250°C. It is reported that mechanically ground pyrophillite could yield mullite at a lower temperature compared to that of the unground material[172].

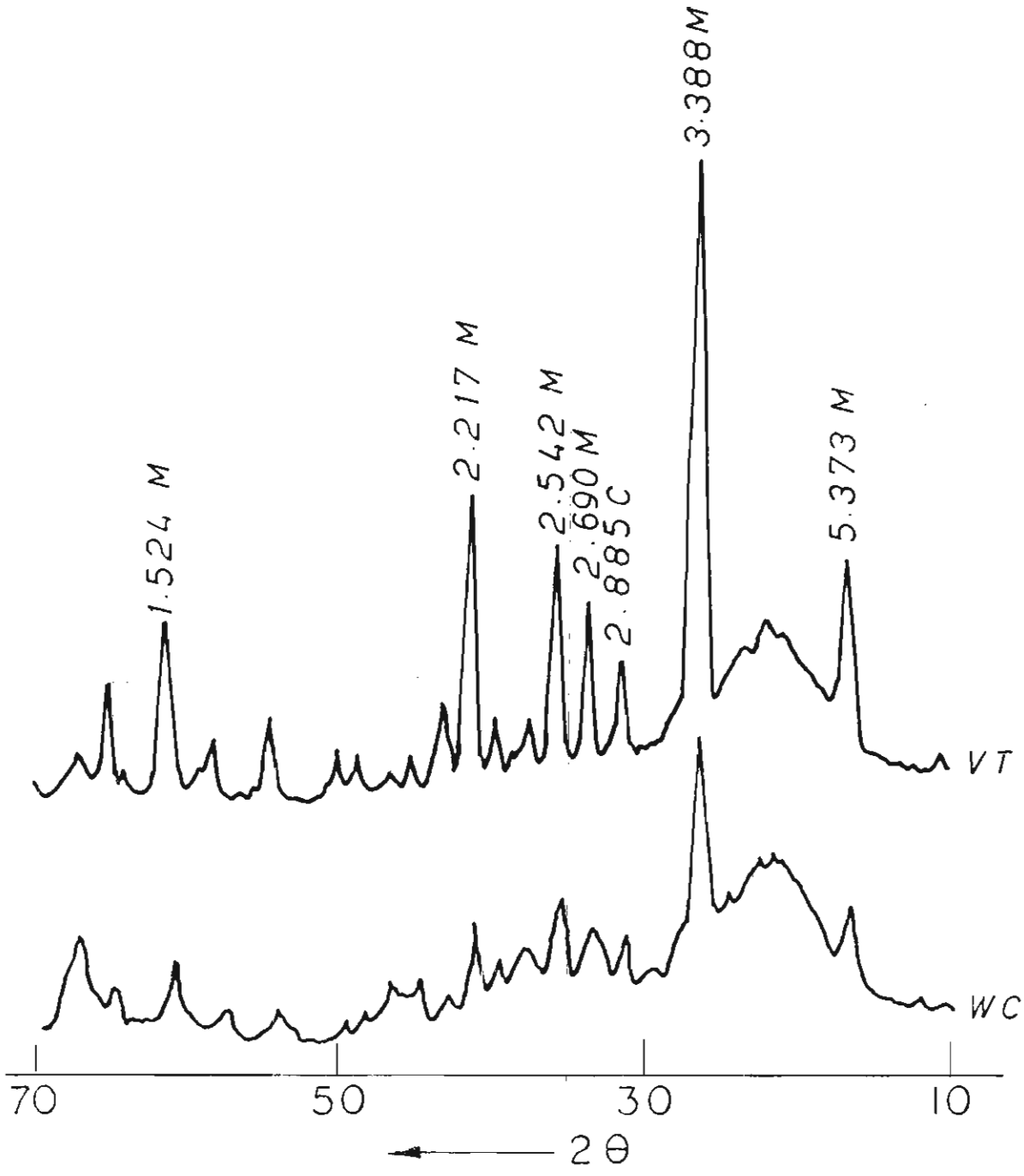


Fig. VI·1 XRD patterns for WC and VT heated at 1050° C

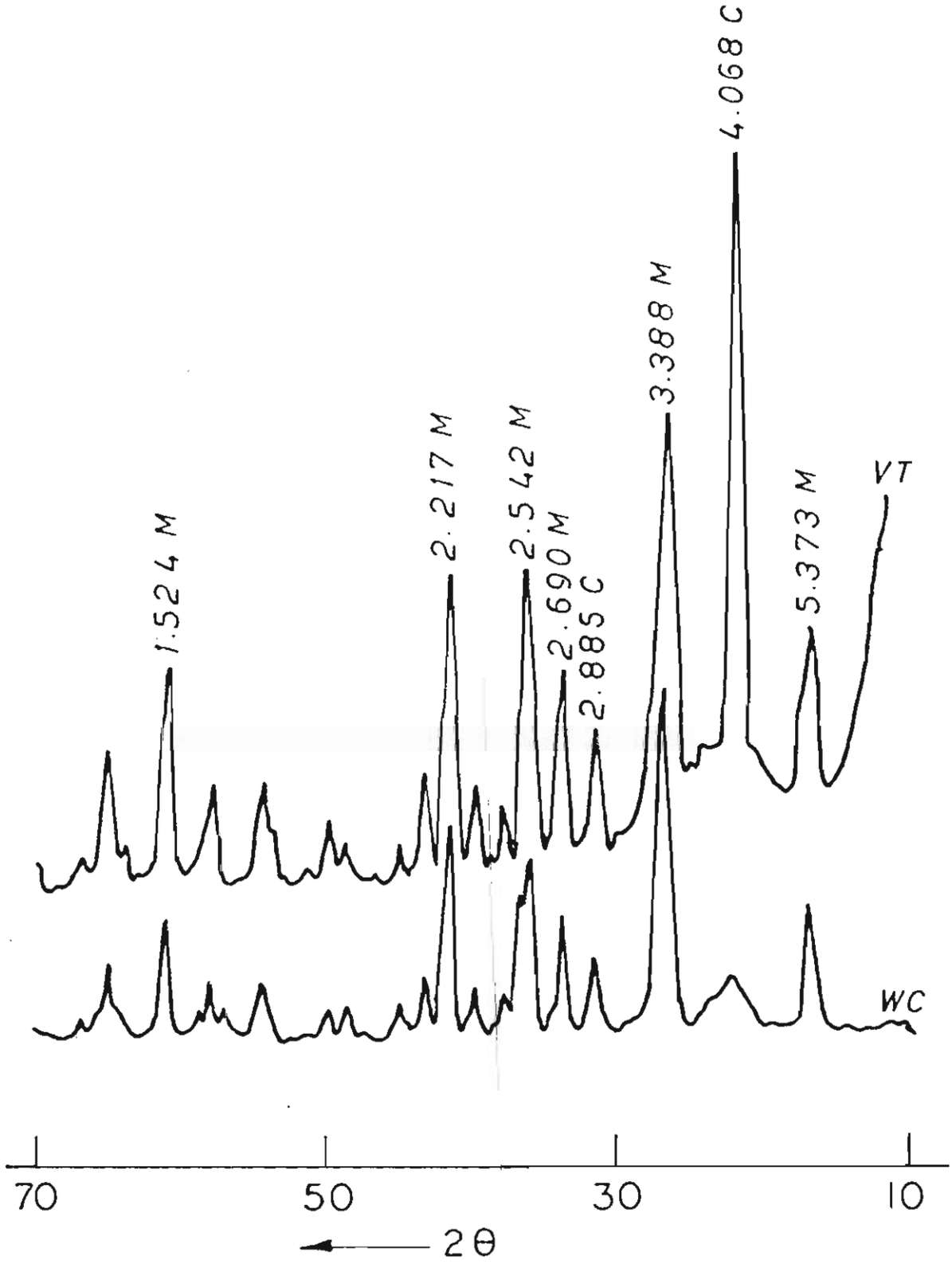


Fig. VI.2 XRD patterns for WC and VT heated at 1150°C

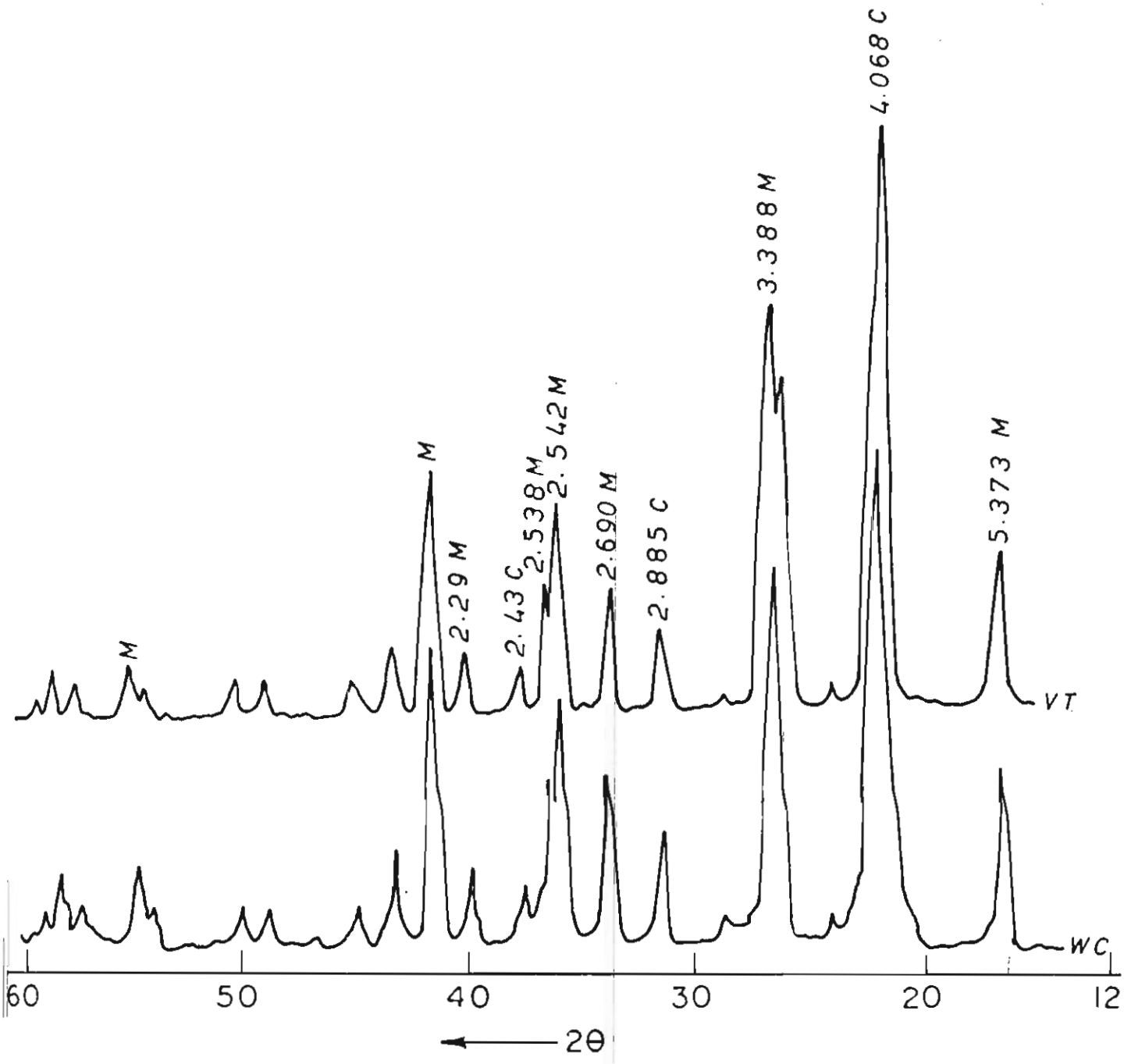


Fig. VI.3 XRD patterns for WC and VT heated at 1350° C and 1250° C

VI.3.3 Dielectric properties

Electrical properties depend mainly upon the structure of raw materials and the nature of the phase formed at higher temperatures. Figs. VI.4 and VI.5 give the k and tan $\delta$ values of WC and VT heated at different temperatures. Since the product obtained is polycrystalline, ionic contribution is greatest towards the polarisation effect, the mobility of them being increased with melt formation which in turn increases the conductivity and hence dielectric constant[173]. With increase in temperature, the extent of sintering and formation of the glassy and crystalline phases vary, the mullite formation gets enhanced. But when the shrinkage increases the percentage porosities decrease and dielectric constant will increase and so as the dissipation factor[174].

VI.3.4 Scanning electron microscopy (SEM)

The scanning electron micrographs presented in Figs. VI.6 (a-f) represent the WC and VT heated to different temperatures. Fig. VI.6a gives WC heated at 1150°C where the basic kaolinite morphology has undergone definite change. The isolated particles seem to have fused with rounded edges, similar to what has been obtained in the case of very fine intimate mixtures of $Al_2O_3$ and $SiO_2$[175]. The morphology of the VT sample heated at the same temperature has shown a greater extent of coarsening and surface reactions. Although the surface appears to be consisting of larger agglomerates there seems to be very fine particles with micropores in between. Both WC and VT get heavily consolidated as the temperature reaches 1350°C, with VT exhibiting large grain growth characteristics with inter granular porosities.

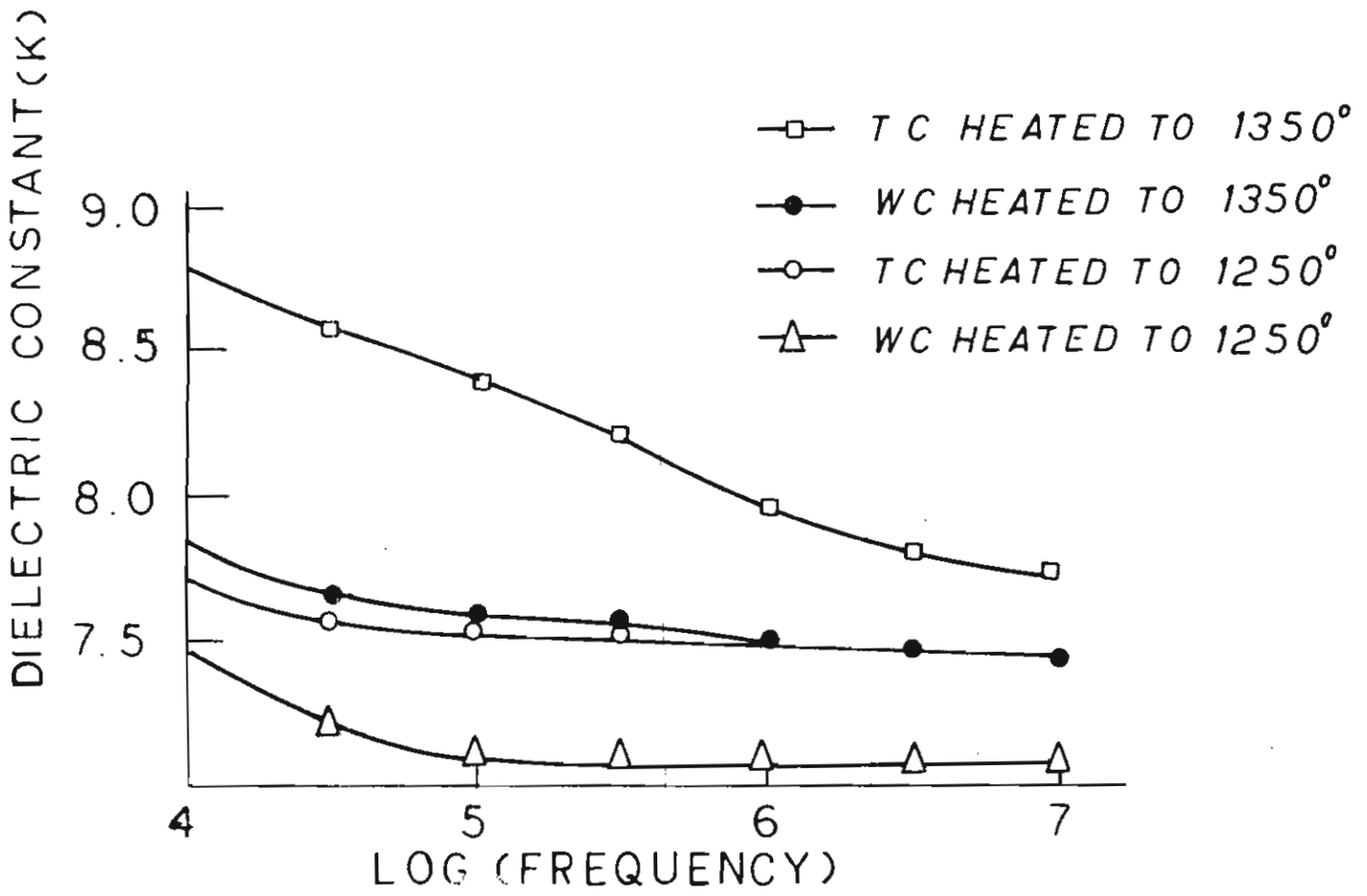


Fig. VI.4. Variation of dielectric constant with log frequency

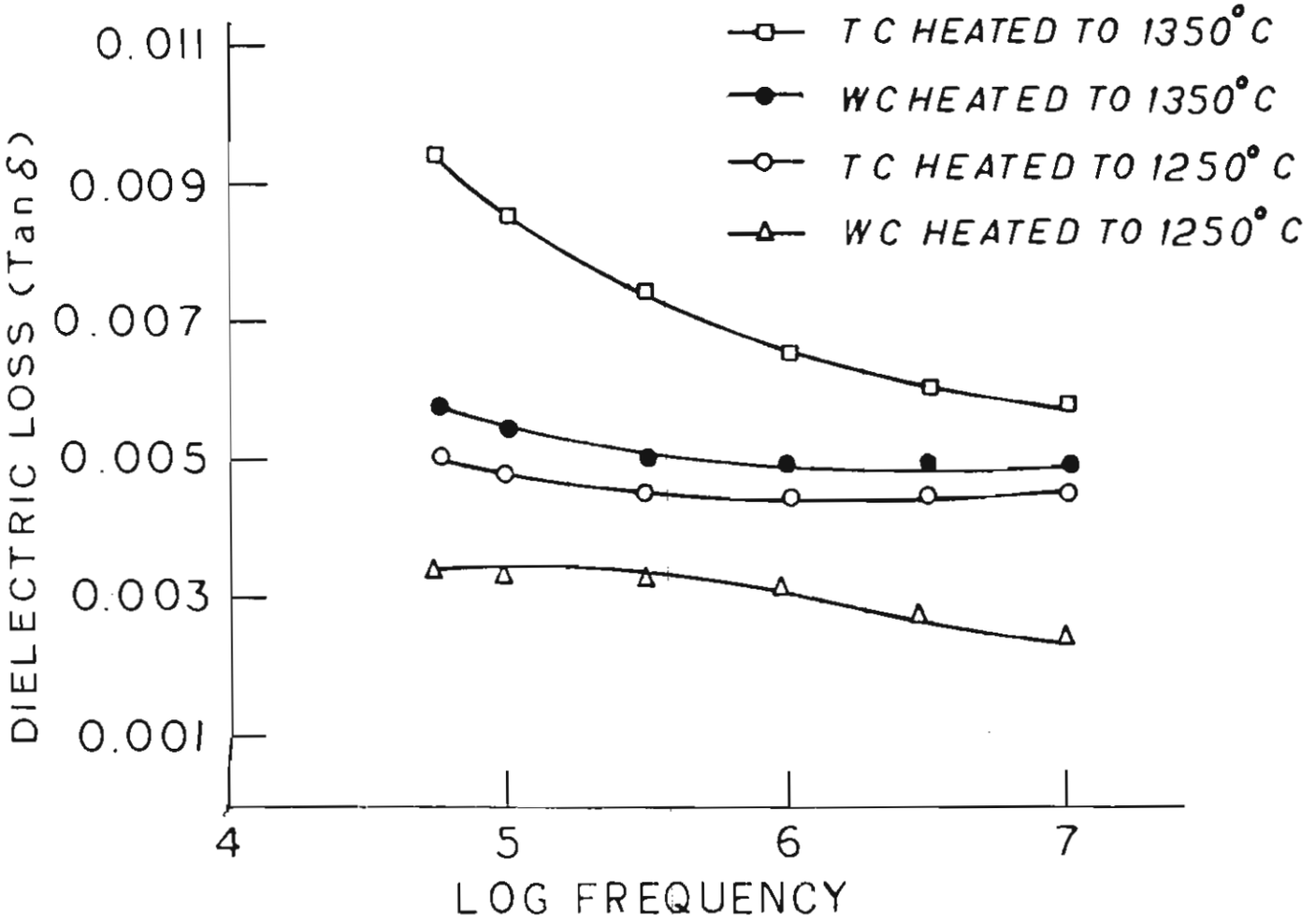


Fig. VI.5 Variation of Dielectric loss (tan δ) with Log frequency

Fig. VI.6: Scanning electron micrographs of

(a) WC heated at 1150$^{o}$C

(b) VT heated at 1150$^{o}$C

(c) WC heated at 1250$^{o}$C

(d) VT heated at 1250$^{o}$C

(e) WC heated at 1350$^{o}$C

(f) VT heated at 1350$^{o}$C

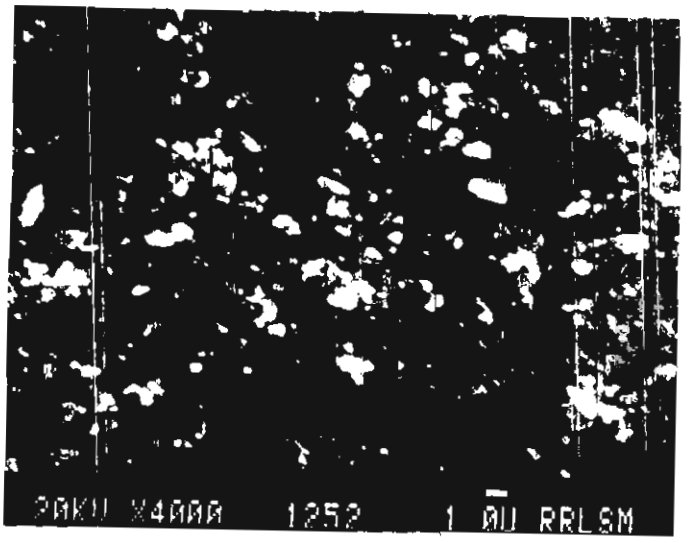


(a)

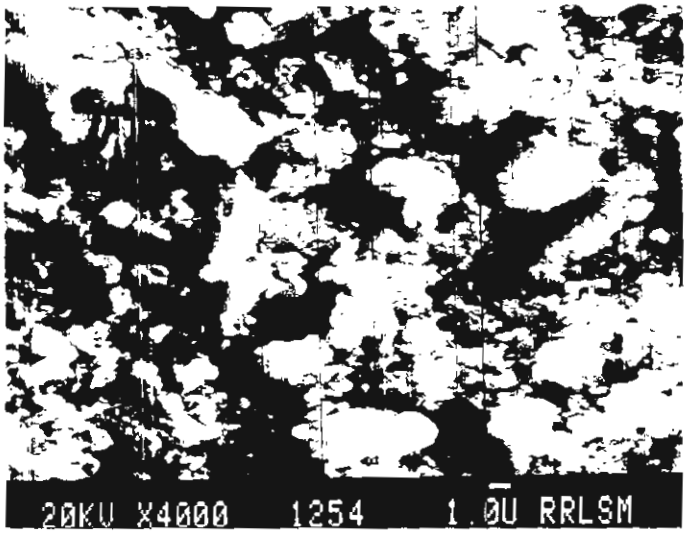


(b)

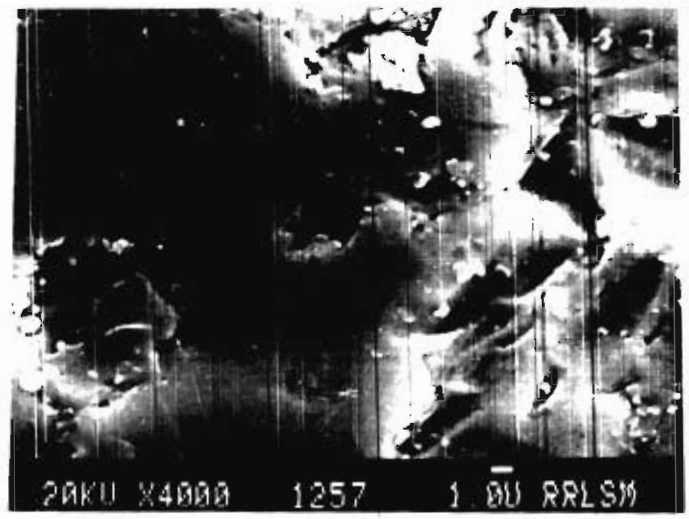


(c)

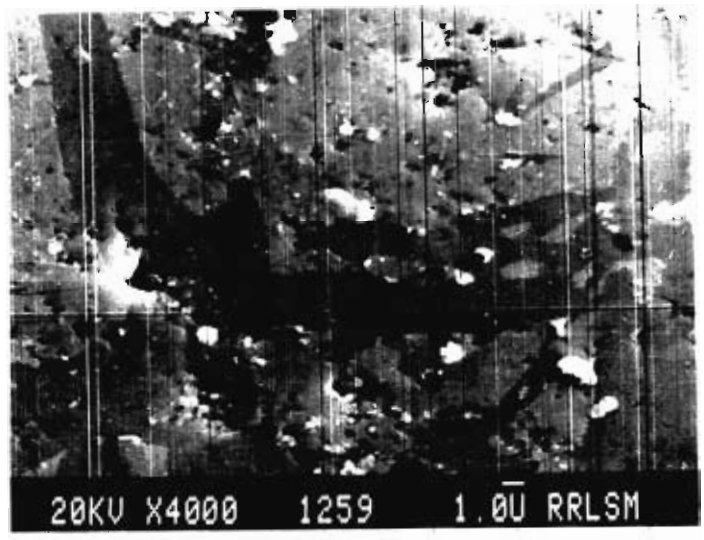


(d)

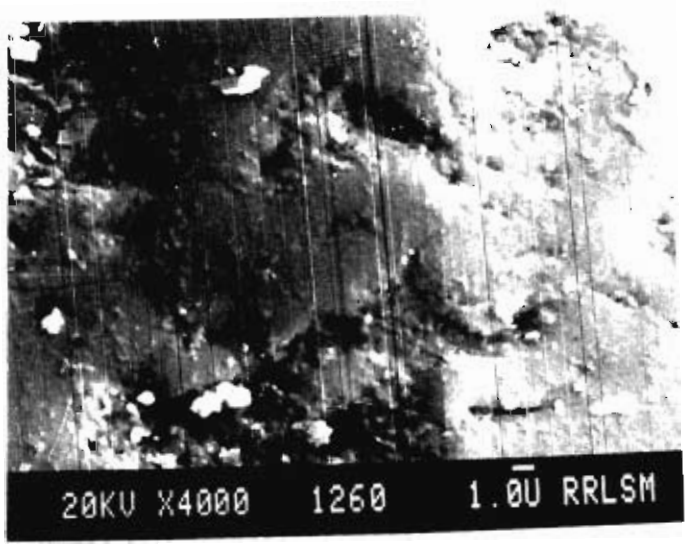


(e)

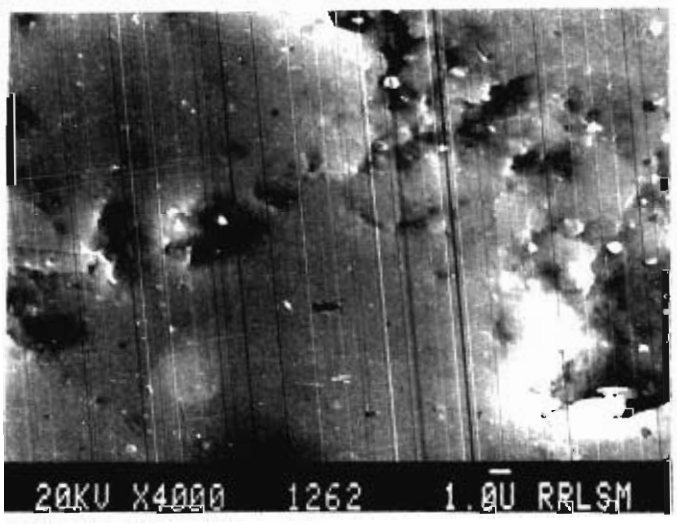


(f)

However, there are very small precipitates with rounded formation, scattered in the matrix which could be cristobalite. Needle like formations have not been observed in any case. Morphology of the WC sample heated at 1350°C follows a similar microstructure (Fig. VI.6e) although the one comparing to VT is more refined. Isolated particles of above 1 μ are also seen. The interesting observation is that a microstructure of VT heated to 1350°C was similar to that already obtained for VT at 1250°C itself (Fig. VI.6 d) indicating its enhanced reactivity. Probably this observation is complementary to the XRD data. The higher rate of increase in the density in the early stages in VT could also be an indirect indication to what has been observed in the microstructures.

## VI.4 CONCLUSIONS

1. As a result of controlled thermal modification of kaolinite it is possible to bring down the mullitisation temperature.

2. The compound formed as a result of heat treatment provides highly compact and dense sintered body resulting at relatively lower processing temperature.

# C H A P T E R VII

## CONCLUSIONS AND SUGGESTIONS FOR FURTHER WORK

# CHAPTER VII

# CONCLUSIONS AND SUGGESTIONS FOR FURTHER WORK

## VII.1 CONCLUSIONS

Kaolinite (of which India has a major deposit) is a versatile filler for polymers in view of its easy availability in pure form and due to its very fine nature. However, the surface property of kaolinite due to the OH groups imposes certain limitations for successful incorporation in polymers necessitating surface modification of the kaolinite. Thermal modification was attempted to overcome this problem and in this process, a detailed study of the thermal dehydroxylation of kaolinite achieved through a novel technique was taken up.

Thermal decomposition-hydration-redecompositon technique provided dehydroxylated kaolinite particles with increased surface area, one of the basic requirements for polymer adsorption and adhesion in particulate filled polymer composites. The effect of the surface modified kaolinite particles in three common matrices such as polyethylene, polyester and polyvinyl chloride were studied with respect to mechanical and electrical properties. The different composites were prepared by cold molding, hot injection molding and hot compression molding techniques. The following conclusion can be drawn based on the observations made on the modified kaolinite as well as on the properties of the various polymer based composites.

VII.1.1 Surface modification of kaolinite

Microstructural features of the surface modified kaolinite (VT) showed that there was a particle coarsening after surface modification. The surface area of VT is nearly double that of WC and MK. IR and XRD could not probably reveal detailed information because of the disruption of the kaolinite structure by the thermal treatments. Raman and solid state NMR spectroscopy indicated further removal of hydroxyls from metakaolinite as a result of the specific treatment. Dielectric studies showed that the specifically treated kaolinite could be a better insulator than metakaolinite and hence can be used in electrical insulators.

VII.1.2 Polymer composites

Composites were prepared using polyethylene, polyester and polyvinyl chloride as matrices. The effect of addition of surface modified and unmodified kaolinites (VT and WC) in these polymer systems on physical, mechanical and electrical properties were compared (Chapter IV). Same trend was observed in all the three systems. There was considerable increase in densities of the composites with the increase in filler content for both modified and unmodified kaolinite. Further, porosity was found to be less in the case of VT composites compared to WC in all the cases investigated. Improved mechanical properties were observed for composites prepared out of surface modified kaolinite. Compressive strength measurements on both polyester and PVC composites showed that more VT can be incorporated in both the matrices with improved strength properties.

Microstructural observations showed that the distribution of VT

is more uniform in all the cases with the lesser tendency for agglomeration compared to that of WC. Dielectric measurements on the different composite systems showed that VT composites are more insulating than WC composites.

VII.1.3 Mullite formation

Differential thermal analysis of VT indicates that the exothermic reaction assigned normally to the formation of premullite has taken place at about 35$^{o}$C lower, compared to WC and MK. Detailed investigation over temperature range 1050-1350$^{o}$C (Chapter VI) showed that the characteristic mullite phase can be obtained in VT at about 100$^{o}$C less than that from WC. Further, this reduction in temperature of mullitisation is obtaiend without the use of any mineralizers as being practised normally. However, a complete study into the kinetics of the thermal transformations of mullite was not within the scope of this investigation.

VII.2 SUGGESTIONS FOR FURTHER WORK

The following suggestions could be drawn for further work in this area in future.

1. Raman spectra has been found to be a useful tool to study the dehydroxylation reaction in kaolinite. Identification of the various peaks of kaolinite in the spectra and a quantitative estimation of the changes taking place in the thermal dechydroxylation reaction and also during the surface modification process could be worth investigating. This will open up a

new line in the thermal reactions of kaolinite from the structural point of view.

2. The present study on the kaolinite-polymer composites has shown clear indication on the improvement in properties and better compatibility of particulates to the matrix. However, the effect of processing conditions as well as the polymer interactions are not looked into. Further, the interface between the modified particles and matrices as well as the fracture mechanics of the composites are worth investigating.

3. The finding on the thermal reactions of the surface modified kaolinite seems to have a lot of significance in view of mullite which is a very demanding advanced structural ceramic material. The indication of the low temperature formation of mullite without the use of mineralizers need further work. Hence sutdy on the mullitisation reaction in surface modified kaolinite should be an ideal topic of research for the materials science point of view.

# REFERENCES

## REFERENCES


1. Broutman L.J. and Krock R.H. (1967) "Modern Composite Materials", Addision-Wesley Pub. Comp. Inc.

2. Schwartz M.M. (1983) "Composite Materials Handbook", Mc Graw Hill Inc. 23.

3. Nielsen L.E. (1966) J. Appl. Poly. Sci., 10, 97.

4. Brassell C.W. and Wishman K.B. (1974) J. Mat. Sci., 9, 307.

5. Nicolais L. (1975) Poly. Engg. Sci., 15, 137.

6. Landon G., Lewis G. and Boden G.F. (1977) J. Mat. Sci., 12, 1605.

7. Papanicolaou G.C. and Theocaris P.S. (1979) Colloid Poly. Sci., 257, 239.

8. Theocaris P.S., Papanicolaou G.C. and Papadapolulos (1981) J. Comp. Mate., 15, 41.

9. Feltham S.J., Yates B. and Martin R.J. (1982) J. Mat. Sci., 17, 2309.

10. Lange F.F. (1974) in Fracture and Fatigue (Composite Materials, Vol. 5) ed. Broutman L.J., Academic, 2.

11. Berlin A.A., Volfson S.A., Enikolopian N.S. and Negmatov (1986) "Principles of Polymer Composites", Springer-Verlag

12. Guth E. (1944) J. Appl. Phys., 16, 20.

13. Nicolais L., Guerra G., Migliaresi L. and Di Bene detto A.T. (1981) Composites, 12, 33.

14. Kadotami K., Aki E. and Watanbe T. (1981) Composites, 12, 260.

15. Kerner E.H. (1956 b) Proc. Phys. Soc. London 69 B, 808.

16. Hasselman D.P.H. (1962) J. Am. Ceram. Soc., 45, 452.

17. Hashin Z. and Shtrikman S. (1963) J. Mech. Phys. Solids, 11, 127.

18. Sata Y. and Furukawa J. (1963) Rubber Chem. Technol., 36, 1081.

19. Harvey Alter (1965) J. Appl. Poly. Sci., 9, 1525.

20. Das Roy P.K. and Phani K.K. (1987) Trans. Ind. Ceram. Soc., 46(2) 51.

21. Nielsen L.E. (1967) J. Comp. Mat., 1, 100.

22. Kenyon A.S. and Ouffey H.J. (1967) Polym. Eng. Sci., 7, 189.

23. Wambach A., Trachte K.L. and Di Benedetto A.T. (1968) J. Comp. Mater., 2, 266.

24. Nielsen L.E. and Lewis T.B (1969) J. Polym. Sci., A-27. 1705.

25. Moehlenpah A.E., Ishai O. and Di Benedetto A.T. (1970) Polym. Eng. Sci., 11, 129.

26. Lewis T.B. and Nielsen L.E. (1970) J. Appl. Polym. Sci., 14, 1449.

27. Nielsen L.E. (1974) Mechanical Properties of Polymers and Composites, Vol. 2, Chapter 7, Marcel Dekker Inc.

28. Manson J.A. and Sperling L.H. (1976) Polymer blends and composites, Plenum Press.

29. Speerschneider and Li C.H. (1962) Wear, 15, 392.

30. Anonymous (1961) Wear, 4, 419.

31. Harry S. Katz and John V. Milewski Editors (1978) Handbook of Fillers and Reinforcements for Plastics, Van Nostrand Reinhold Comp.

32. Murphy T.P. (1966) Industrial & Eng. Chem., 58, 41.

33. Dannerberg E.M. (1975) Rubber Chemistry & Tech., 48, 410.

34. Bateman L. (1963) "Physics and Chemistry of Rubber like substances" Wiley, New York, Chapters 10 & 11.

35. Harvey Alter J. (1965) Appl. Poly. Sci., 9, 1525.

36. Black A.P.,Birkner F.B. and Morgan J.J. (1965) J. Am. Water Works Assocn., 51, 1547.

37. Black A.P., Birkner F.B. and Morgan J.J. (1966) J. Colloid and Interface Science, 21, 626.

38. Theng B.K.G. (1979) Clays and Clay Minerals, 18, 357.

39. Theng B.K.G. (1979) "Formation and Properties of Clay Polymer Complexes", Elsevier Scientific Publishing Co.

40. Murray H.H. (1963) Clays and Clay Min., 10, 291.

41. Carter L.W., Hendricks J.G. and Bolley D.S. (1950) United States Patent, 2, 531, 396 (to National Lead Co.).

42. Jordan J.W. (1963) Clays and Clay Min., 10, 299.

43. Nahin P.G. (1963) Clays and Clay Minerals, 10, 257.

44. Uskov I.A. (1960 a) Vysokomolekuly arnye Soedineniya, 2, 200.

45. Walker G.F. and Garrett W.G. (1967) United States Patent, 3, 356, 611 (to Commonwealth Scientific and Industrial Research Organisation, Australia).

46. Wilcox J.R. (1961) United States Patent, 2, 982, 665 (to Minerals and Chemicals, Philipp. Corp.).

47. Helmer B.M., Prescott P.I. and Sennett P. (1976) Surface modified kaolin in plastics, 31st Annual Technical Conference, Reinforced Plastics/Composites Institute, The Society of the Plastics Industry, Inc., Section 8-G: 1-4.

48. Fujiwara S. and Sakamoto T. (1967) Japanese Patent, 76, 109, 998 (to Unitika Ltd.).

49. Ochirimi T., Matsumoto T. and Okubo M. (1976) Japanese Patent, 76, 148, 738 (to Nitto Electric Industrial Co. Ltd.).

50. Uskov I.A. and Kusnitsyna T.A. (1960) Vysokomolekulyarnye Soedineniya, 2, 728.

51. Karyin V.A. and Plate N.A. (1961) J. Polymer Sci., 52: 155.

52. Blumskein A. (1965) J. Polymer Sci., A, 3, 2653.

53. Dekking H.G.G. (1965) J. Appl. Polymer Sci., 9, 1641.

54. Dekking H.G.G. (1967) J. Appl. Polymer Sci., 11, 23.

55. Solomon D.H. and Rosser M.J. (1965) J. Appl. Polymer Sci., 9, 1261.

56. Fallick G.J., Bixler H.J., Marsella R.A., Garner F.R. and Fettes E.M. (1968) Modern Plastics, 45 No.5, 143, 144, 147, 148, 149, 209, 214.

57. Solomko V.P., Molokoyedova T.A. and Uskov I.A. (1966) Vysokomolekulyarnye Soedineniya, 8, 110.

58. Solomko V.P., Moloko Yedova T.A., Uskov I.A. and Polichkovskaya T.V. (1967) Vysokomolekulyarnye Soedineniya, 9, 40.

59. Howard E.G. Jr. (1975) Filled polyolefin compositions, German Patent, 2, 459, 118 (to Du Pont de Nemours, EI & Co.).

60. Bixler H.J. and Fallick G.J. (1969) Reinforcing filler for polymers, United States Patent, 3, 471, 439 (to Amicon Corp.).

61. Baum B.O. (1969) United States Patent, 3, 425, 980 (to Union Carbide Corp.).

62. Howard Er. Jr. (1975) German Patent, 2, 459, 118 (to Du Pont de Nemours, E.I. & Co.).

63. Nahin P.G. and Backlund P.S. (1963) United States Patent, 3, 084, 117 (to Union Oil Co. of California).

64. Nakada S. and Tagami K. (1973) Japanese Patent, 7323, 331 (to Sekisui Chemical Co. Ltd.).

65. Nahin P.G. (1965) Clays and Clay Minerals, 13, 317-330.

66. Nahin P.G. (1966) United States Patent, 3, 248, 314 (to Union Oil Co. of California).

67. Hawthorne D.G., Hodgkin J.H., Loft B.C. and Solomon D.H. (1974) J. of Macromolecular Science Chemistry, A, 8, 649-657.

68. Hawthorne D.G. and Solomon D.H. (1974) J. of Macromolecular Science Chemistry, A 8, 659-671.

69. C.A. 165440 l Selivanova A.A., Salazkin K.A., Ermolina A.V., Gorc hitsyna G.P. and Gavrilova L.D. (1970) Tr. Most. Inst. Khim. Mash.nostr., 36, 97.

70. Abramova I.M., Bunina L.V., Vasileva V.A., Zezina L.A., Kazargan L.G., Kornienko G.V. and Sergeev V.I. (1986) Plast. Massy, 4, 8, C.A. 70, 225750 K.

71. Janczak W. and Nowek E. (1986) Plaste Kautsch 33 (1) 31 CA. 104: 169438 a.

72. Opera, Clepatra, Vasiliv, Weiner and Felicia (1986) J. Appl. Polym. Sci., 31, 37, 951.

73. Cook L.E. (1966) Rubber and Plastic Age, 47, 284.

74. Kulinskii V.V. and Lapko L.P. (1985) Khim. Tekhol., 5(5) 29, CA. 73, 111111 x.

75. De Nun Zio P.J. and Held M.D. (1966) American Chemical Society, Division of Rubber Chemistry, Spring Meeting 15 pp.

76. Hermann Salmang and Marcus Francis (1961) "Ceramics - Physical and Chemical Fundamentals" Butterworths, London., Chapter II.

77. Grim R.E. (1962) "Applied Clay Mineralogy", Mc Graw Hill Book Co. Inc., New York.

78. Pauling L. (1930 b) Proc. Nat. Acad. Sci., Washington, 16, 578.

79. Brindley G.W. (Editor) (1951) X-ray identification and crystal structures of clay minerals, Chap. II, Min. Soc. London.

80. Brindley G.W. and Nakahira M. (1953) Mineralog. Mag., 31, 781.

81. Mansfield C.F. and Bailey S.W. (1972) Am. Miner. 57, 411.

82. Zvyagin B.3. (1960) Soviet Phys. Crystallogr., 5, 32.

83. Grim R.E. (1968) "Clay Mineralpgy", 57. 298.

84. Brindley G.W. and Brown G. (1980) "Crystal structures of clay minerals and their x-ray identification, Chapter I. Mineralogical Society.

85. Bradley W.F. and Grim R.E. (1951) Amer. Miner., 36, 182.

86. Roy R., Roy D.M. and Francis E.E. (1955) J. Am. Cer. Soc., 38, 198.

87. Brindley G.W. and Hunter K. (1955) Miner. Mag., 30, 574.

88. Mitra G.B. (1958) Nature, 182, 1794.

89. Brindley G.W. and Nakahira M. (1959 a) J. Am. Cer. Soc., 42, 311.

90. Stubican V. (1959) Min. Mag., 32, 38.

91. Miller J.G. (1961) J. Phys. Chem., 65, 800.

92. Sen S. (1962) Trans. Ind. Ceram. Soc., 21, 49.

93. Fripiat J.J. and Toussaint F. (1963) J. Phys. Chem., 63, 30.

94. Wolf R.G. (1963) Amer. Min., 48, 390.

95. Gastuche M.C., Toussaint F. and Fripiat J.J. (1963) Clay Min. Bull., 5, 227.

96. Toussaint F., Fripiat J.J. and Gastuche M.C. (1963) J. Phys. Chem., 67, 26.

97. Brindley G.W., Sharp J.H., Patterson J.H. and Nakabari achar B.N. (1967) Amer. Min., 52, 201.

98. Mitra G.B. and Bhattacherjee S. (1969) Amer. Min., 54 (5) 1409.

99. Mitra G.B. and Bhattacherjee S. (1969) Acta Cryst., 25 (B) 1668.

100. Mitra G.B. and Bhattacherjee S. (1970) Acta Cryst. 26 (B) 2124.

101. Mackenzie K.J.D., Brown I.W.M., Meinhold R.H. and Bowden (1985) J. Am. Ceram. Soc., 68 (5) 293.

102. Kumar S. and Sinha B.C. (1964) Trans. Ind. Ceram. Soc., 23 (4) 215.

103. I.S. Specifications for Ball Clays for Ceramic Industry, 4589-1968.

104. Bhattacherjee S. (1971) Ind. J. Pure Appl. Phys., 9, 1054.

105. Grimshaw R.W. (1971) Chemistry and Physics of clays, 4th Edn., Ernest Benn., London.

106. Todor D.N. (1976) Thermal Analysis of Minerals, Abacus, p.215.

107. Sorden J. and Eberl D.D. (1980) Clay Min., 15 (3) 317.

108. Fitzjohn and Worral W.E. (1980) Trans. Brit. Ceram. Soc., 79 (3) 74.

109. Buswell A.M. (1937) J. Am. Chem. Soc., 59, 2603.

110. Atma Ram. Bishui B.M. and Prasad J. (1960) Cent. Glass. Ceram. Res. Inst. Bull., 7 (1) 3.

111. Keelings P.S. (1963) Trans. Brit. Ceram. Soc., 62, 547.

112. Bishui B.M. and Prasad J. (1970) Cent. Glass Ceram. Res. Inst. Bull., 17 (3) 69.

113. Bharadwaj M., Bishui B.M. and Ghosh D.K. (1971) Cent. Glass Ceram. Res. Inst. Bull., 18 (3) 75.

114. Bora M.N., Hatibarua J. and Mohanty P.C. (1972) Trans. Ind. Ceram. Soc., 31 (2) 39.

115. Khosla S.M., Gupta C.S. and Bedi (1976) Cent. Glass Ceram. Res. Inst. Bull., 23 (4) 144.

116. Jha and Jai Shankar (1978) Trans. Ind. Ceram. Soc., 37, 162.

117. Singh V.B. and Joshi V.C. (1980) Trans. Ind. Ceram. Soc., 39 (1) 18.

118. Ramaswamy K. and Kamalakkannan M. (1987) Ind. J. Pure & Appl. Phy., 25, 284.

119. Miller J.G. (1961) J. Phys. Chem., 65, 800.

120. Sengupta B., De S.C. and Gupta A. (1980) Met. Min. Rev., 19 (9) 10.

121. Farmer V.C. and Russel J.D. (1964) Spectro Chim. Acta GB 20, 1149.

122. Dan T.K., Geetha Ramani, Mukundan P. and Pillai P.K. (1982) Met. & Min., 21 (4) 76.

123. Rouxhet P.G., Samudacheata N., Jacobs H. and Anton O. (1977) Clay Min., 12, 171.

124. Mukherjee P.S., De A.K. and Bhattacherjee S. (1978) J. Mat. Sci. Let., 13, 1824.

125. Lokanatha S. and Bhattacherjee S. (1984) J. Mat. Sci. Lett., 3, 299.

126. Lokanatha S. and Bhattacherjee S. (1984) Ind. J. Pure & Appl. Phys., 22, 719.

127. Lokanatha S. and Bhattacherjee S. (1986) Trans. Ind. Ceram. Soc., 45 (2) 41.

128. Lokanatha S. and Bhattacherjee S. (1986) Ind. J. Pure & Appl. Phys., 24, 152.

129. Petro N.S.H., Mourad W.E. and Grigis B.S. (1981) Surf. Technol., 13, 189.

130. Girgis B.S. and Girgis L.S. (1969) J. Appl. Chem., 19, 292.

131. Girgis B.S. (1975) J. Br. Ceram. Soc., 74 (4) 135.

132. Wiewiora A., Wieckowski T. and Sokolowska A. (1979) Arc. Min. XXXV, z. 1, 5.

133. Johnston C.T., Sposito G. and Birge R.R. (1985) Clays & Clay Min., 33 (6) 483.

134. Smith J.V. and Blackwell C.S. (1983) Nature, 303, 223.

135. Barron P.F., Frost R.L., Skjemstad J.O. and Koppi A.J. (1983) Nature, 302, 49.

136. Mackenzie K.J.D., Brown I.W.M., Meinhold R.H. and Bowden (1985) J. Am. Ceram. Soc., 68 (5) 266.

137. Murthy N.S., Kotliar A.M., Sibilia J.P. and Sack S.W. (1986) J. Appl. Poly. Sci., 31, 2569.

138. Rybnikar F.J. (1981) J. Macromol. Sci. Phys., B 19, 1.

139. Badran B.M., Galeski A. and Kryszewski (1982) J. Appl. Polym. Sci. 27, 3669.

140. Clerico M. and Patierno V. (1979) Wear, 53, 279.

141. Burns R. (1982) "Polyester Molding Compounds", Marcel Dekker Inc.

142. Davis R.F. and Pask J.A. (1971) Mullite in high temperature oxides Part IV, Chapter 3, Editor Alper A.M., Academic

143. Reynen P. and Faizullah M. (1979) Sintering of mullite in Sintering and Developments, Editor Ristic N.M., Elsevier

144. Lessing P.A., Gordon R.S. and Mazdiyasni K.S. (1975) J. Am. Ceram. Soc., 58 (3-4) 149.

145. Qi Jing Huan, Jia-Qi Tan and Zhung-Guo Jin (1986) J. Am. Ceram. Soc., 69 (3) 265.

146. Okada K., Hoshi Y. and Otsuka N. (1986) J. Mat. Sci. Lett., 5, 135.

147. Banerjee G., Banerjee S.P. and Roy A.K. (1985) High alumina bricks from sillimanite beach sand, Proc. of the Int. Sem. on Refractories, Jamshedpur, 183.

148. Das Gupta A., Malaviya S.K., Sen P.C., Mitra B.K. and Rao M.R.K. (1986) Development of refractories from sillimanite beach sand, Proc. of the Int. Seminar on Refractories, Jamshedpur, 209.

149. Ismailov (1981) Thermodynamic analysis of the formation of mullite, Steklokeram, 1, 23.

150. Teresa N. Campos and Helena de Souza Santoz (1976) J. Am. Ceram. Soc., 57 (7-8) 357.

151. Kulkarni A.K., Das A. and Rao S.V.K. (1978) Trans. Ind. Ceram. Soc., 37 (6) 215.

152. Das P., Kulkarni A.K. and Murthy V.K. (1970) Development of mullite ware, Trans. Ind. Ceram. Soc., 31 (2) 46.

153. Jonson B.L. and Cutler I.B., Use of phase diagrams in the sintering of ceramics and metals in 'Phase diagrams materials science and technology', Vol.II Editor Alper A.M., Academic Press, New York.

154. Ford W.F. The effect of heat on ceramics, Institute of Ceramics Text Book Series, Maclaren and Sons Ltd., London, 120.

155. Searles A.B. and Grimshaw R.W. (1959) The chemistry and physics of clays and other ceramic materials, Third Edition, Ernest Benn Ltd., London.

156. Aggarwal P.S. (1975) Glass & Ceramics Bulletin, 22 (1) 19.

157. Jay A.H. (1939) Trans. Brit. Ceram. Soc., 38, 455.

158. Colegrave E.B. and Rigby G.R. (1952) Trans. Brit. Ceram. Soc., 51 (6) 355.

159. Richardson H.M. and Wilde F.G. (1952) Trans. Brit. Ceram. Soc., 51 (7) 387.

160. Brindley G.W. and Nakahira M. (1958) Nature, 181.

161. Brindley G.W. and Mackinstry H.A. (1961) J. Am. Ceram. Soc., 44, 506.

162. Comer J.J. (1961) J. Am. Ceram. Soc., 44 (1) 561.

163. Nicholson P.S. and Fulrath R.M. (1970) J. Am. Ceram. Soc., 53 (5) 237.

164. Chakraborty A.K. and Ghosh D.K. (1978) J. Am. Ceram. Soc., 61, 170.

165. Slaughter M. and Keller W.B. (1959) Amer. Ceram. Soc. Bull., 58 (12) 703.

166. Roy R. and Osborn E.F. (1954) Amer. Mineral, 39 (11/12) 853.

167. Percival H.J., Duncan J.F. and Foster P.K. (1974) J. Am. Ceram. Soc., 57 (2) 57.

168. Leonard A.J. (1977) J. Am. Ceram. Soc., 60 (1-2) 37.

169. Brown I.W.M., Mackenzie K.J.D., Bowden M.E. and Meinhold R.H. (1985) J. Am. Ceram. Soc., 68 (6) 298.

170. Chaudhuri S.P. (1969) Trans. Ind. Ceram. Soc., 28 (1) 24

171. Anseau M.R., Delette R.M. and Cambier F. (1981) Trans. J. Br. Ceram. Soc., 80, 142.

172. Pedro J. Sanchez, Soto Jose L. and Peres Rodriguez (1989) J. Am. Ceram. Soc., 72 (1),154.

173. Kittel C. (1985) "Introduction to Solid State Physics", Wiley Eastern Limited.

174. Khosla S.N. and Bedi R.K. (1980) CGCRI Bulletin, 27 (1-2) 1.

175. Suchitra Sen and Thiagarajan S. (1988) Ceramics International, 14 (2) 77.